Transverse expansion of muscle fascicles during dynamic tasks: experimental and modelling approaches to study human gastrocnemii

by

Avleen Randhawa

M.Sc., Simon Fraser University, 2012

B.Phty., Punjabi University, 2008

Thesis Submitted in Partial Fulfillment of the
Requirements for the Degree of
Doctor of Philosophy

in the
Department of Biomedical Physiology and Kinesiology
Faculty of Science

SIMON FRASER UNIVERSITY

Fall 2018

Approval

Name:	**Avleen Randhawa**
Degree:	**Doctor of Philosophy (Biomedical Physiology and Kinesiology)**
Title:	**Transverse expansion of muscle fascicles during dynamic tasks: experimental and modelling approaches to study human gastrocnemii**
Examining Committee:	**Chair:**
	James Wakeling Senior Supervisor Professor
	Dawn Mackey Supervisor Associate Professor
	Dan Marigold Internal Examiner Associate Professor Biomedical Physiology and Kinesiology
	Tobias Siebert External Examiner Professor University of Stuttgart Institute of Sport and Motion Science
Date Defended/Approved:	26 October 2019

Ethics Statement

The author, whose name appears on the title page of this work, has obtained, for the research described in this work, either:

a. human research ethics approval from the Simon Fraser University Office of Research Ethics

or

b. advance approval of the animal care protocol from the University Animal Care Committee of Simon Fraser University

or has conducted the research

c. as a co-investigator, collaborator, or research assistant in a research project approved in advance.

A copy of the approval letter has been filed with the Theses Office of the University Library at the time of submission of this thesis or project.

The original application for approval and letter of approval are filed with the relevant offices. Inquiries may be directed to those authorities.

Simon Fraser University Library
Burnaby, British Columbia, Canada

Update Spring 2016

Abstract

Force generation is influenced by transverse shape changes of a muscle. Recent studies suggest that muscle fascicles may bulge in an anisotropic manner, and this may affect the relation between internal architecture and muscle deformations; however, to date fascicle bulging has not been quantified during active contractions. Understanding the nature and extent of the transverse deformations is necessary to explore the mechanisms driving the changes in internal geometry of whole muscle during contraction. The goal of this thesis is to quantify transverse deformations in muscles and fascicles using novel modelling and experimental techniques. The first study tested the accuracy with which 1D, 2D or 3D structural models of muscle could predict the pennation and muscle thickness for the medial gastrocnemius (MG) and lateral gastrocnemius (LG) in man during ankle plantarflexions. The second study acquired images from the MG and LG during cyclic contractions, and the transverse fascicle strains were calculated from their wavelengths within B-mode ultrasound images. For the third study, fascicle deformations were measured from two orthogonal ultrasound scans to provide 3D information of muscle geometry for the MG and LG. The results from the modelling study showed that a 1D model established a good relation between fascicle length and pennation; however, 3D models are necessary to understand the mechanisms underlying 3D structural changes. The second study found increases in the transverse fascicle strain while the longitudinal fascicle length decreased, however, the extent of these strains was smaller than expected. In the third study, transverse deformations in the MG were similar for the two transverse directions. However, the data for the LG confirm that transverse anisotropy in strain can occur in the muscle fascicles: as the LG fascicle length shortened, the fascicles bulged transversally in one direction while thinned in the other orthogonal direction. These results highlight that muscle fascicles do not bulge uniformly during contraction, and the implications for this behaviour on muscle function remain largely unexplored. This thesis provides a novel 3D perspective to enhance our understanding of the deformations of muscle fascicles during contraction, which in turn affect contractile performance and muscle function.

Keywords: B-mode ultrasound; muscle models; gastrocnemii; transverse deformation; plantarflexion; belly

Acknowledgements

I owe many thanks to a lot of people who have helped me during this incredible journey of completing my PhD thesis.

First, I would like to thank my incredible supervisor, Dr James Wakeling. His supervision, mentorship, encouragement and patience has been extremely helpful to me in successfully completing this research. Not only have I been truly inspired by his dedication towards research and his students, I have acquired valuable life skills from him over the many years of being a member of his lab. James, I am especially grateful to you for always believing in me!

I must thank my brilliant co-supervisor, Dr Dawn Mackey, for her constant motivation and guidance on my thesis work over the years. I am incredibly thankful to her for challenging me through insightful questions and her valuable feedback that helped me widen my research perspectives.

A special thanks to my current and former lab mates and colleagues who shared their knowledge, engaged in intriguing discussions, and created a positive and supportive lab environment.

I would like to thank my family for their love, support and encouragement over the course of my PhD research.

A very special thanks to my yellow lab (Don) who brightened my days and was an energetic companion during my thesis writing process.

Most importantly, to Jas, no words can express my gratitude for your presence in my life. Finishing this thesis is a beginning of something new, not only for me, but for us. You have been such a dedicated and motivating partner during this journey and for that I am forever grateful.

Table of Contents

List of Tables

List of Figures

List of Symbols

Symbol	Definition
1D	One-dimensional
2D	Two -dimensional
3D	Three-dimensional
β	Pennation
β_0	Initial pennation
β_1	Current pennation
B-mode	Brightness mode
B_p	Pixel brightness
c_1, a_1, a_2, o_1, o_2	Coefficients for Fourier series
d	Depth of the muscle belly
DT	Diffusion-tensor
ε_f	Fascicle strain
F_f	Fascicle force
F_t	Tendon force
k	Aponeurosis compliance
L_{apo}	Aponeurosis length
L_b	Belly length
$\hat{L}_b$	Normalized belly length
L_f	Fascicle length
$\hat{L}_f$	Normalized fascicle length
L_{fd}	Fascicle depth
L_{fd}	Fascicle width
LG	Lateral gastrocnemius
L_y	Belly thickness
m	Moment of frequency
MG	Medial gastrocnemius
MRI	Magnetic resonance imaging
n	Shape parameter
P	Position
PCSA	Physiological cross-sectional area
r^2	Coefficient of determination
RMS	Root-mean-square
T	Torque
u, v	Spatial frequencies
u', v'	Moment of frequency
ν	Poisson ratio
ω	Angle in contraction cycle
X, Y, Z	Coordinate system for muscle belly
x, y, z	Coordinate system for muscle fascicle
λ_f	Transverse wavelength
λ_u, λ_v	Wavelengths in x- and y- directions respectively

θ_d	Fascicle inclination determined by manual digitization
θ_F	Inclination angle determined from the discrete Fourier transform

Published Studies from this Thesis

Chapter 2	Randhawa, A., & Wakeling, J. M. (2015). Multidimensional models for predicting muscle structure and fascicle pennation. *Journal of Theoretical Biology*, 382, 57-63.
Chapter 3	Wakeling, J. M., & Randhawa, A. (2014). Transverse strains in muscle fascicles during voluntary contraction: a 2D frequency decomposition of B-mode ultrasound images. *International Journal of Biomedical Imaging*, Volume 2014, Article ID 352910, 9 pages http://dx.doi.org/10.1155/2014/352910.
Chapter 4	Randhawa, A., & Wakeling, J. M. (2018). Transverse anisotropy in the deformation of the muscle during dynamic contractions. *Journal of Experimental Biology*, jeb-175794.

Chapter 1.

Introduction

Skeletal muscles perform various mechanical roles by shortening and generating force, thus facilitating movement, which is essential for the existence of human life. Muscle structure is made up of muscle fascicles (bundles of fibres) that are primary force generators in the musculoskeletal system and typically described by parameters such as fascicle lengths, pennation angles and transverse deformation of the muscle belly (Azizi et al., 2008; Azizi and Roberts, 2009; Rahemi et al., 2014; Fukunaga et al., 1997; Kawakami et al., 1998; Narici et al., 1996). Through the actin-myosin interactions within muscle fibres (Williams et al., 2013; Daniel et al., 2013), fascicles can change length and produce force to allow for locomotion, mobility and postural control (Gans, 1982; Gans & De Vree, 1987; Zajac, 1989; Maganaris et al., 2003; Maganaris et al., 1998; Manal et al., 2006). To perform these diverse roles, muscles come in a range of shapes and sizes (Wakeling et al., 2011; Randhawa et al., 2013; Aziz et al., 2008; Maganaris et al., 1998) thus making it difficult to determine dynamic muscle behavior. The change in length of fascicles affects pennation angle and changes the transverse deformation of fascicles and belly (Siebert et al., 2017; Siebert et al., 2014; Wakeling et al., 2011; Kawakami et al., 1998). This changes the speed of fascicle shortening, which in turn affects the force output of a muscle (Brainerd & Azizi, 2005; Azizi et al., 2008). Therefore, the internal muscle structure and transverse deformation of muscle belly is directly linked to muscle function; however, we know very little about dynamic muscle behavior during active tasks. To expand our knowledge of how muscles function, scientists have studied various aspects of muscle structure and its mechanical properties. These studies have been focused on isolated muscles, fixed-length contractions or unidimensional muscle models (Böl et al., 2013; Stark and Schilling, 2010). While these studies have provided valuable insight into muscle structure, muscle as sheets of fascicles surrounded by other muscles, blood vessels and bones is a complex 3D (three-dimensional) entity and operates differently in 3D space (Rahemi et al., 2014; Azizi et al., 2008; Azizi and Roberts, 2009). Despite the availability of sophisticated imaging devices (such as Magnetic Resonance Imaging, MRI, and ultrasound), we currently lack a complete picture of the internal geometrical deformations, and how these are utilized to perform dynamic tasks in humans. Since

muscle structure influences muscle function, a detailed three-dimensional (3D) analysis of muscle and fascicle structure during dynamic tasks will be significant. We can quantify the 3D changes occurring within a muscle and enhance our understanding of the underlying mechanisms that have functional implications. Therefore, the central theme of this thesis is to quantify transverse expansion of muscle belly and fascicles during active contractions in humans by combining ultrasound imaging and motion tracking system, and utilizing muscle models and experimental techniques.

In this chapter I will review the structural and functional properties of skeletal muscles and describe the factors that influence these properties. I will also discuss modelling approaches and how they can predict muscle parameters, and the tools and techniques used to quantify muscle structure and function in humans and other animals. Lastly, I will provide a logical framework to test hypotheses about transverse deformation of muscle fascicles and belly during dynamic tasks.

1.1. Skeletal muscle structure and mechanics (Figure 1-1)

Muscle bellies contain fibre bundles called fascicles that are oriented at a range of angles to the line of action of the muscles and run between sheets of connective tissue that form the aponeuroses (Rahemi et al., 2014; Wakeling et al., 2011; Randhawa et al., 2013; Azizi et al., 2008; Maganaris et al., 1998). Fascicles came into picture in early 20th century when muscle force, mechanical work and power output were linked to the changes in fascicle (or fibre) length thus defining the task-specific nature of muscle fascicles (Roberts, 1997; Rome, 1988; Gordon et al., 1966; Hill, 1938). Scientists have extensively explored the fascicle microstructure which is made up of sarcomeres arranged in series and packed within fibres that are bundled in parallel to form a fascicle (Winter et al 2011; Burkholder and Lieber, 2001; Gordon et al., 1966). The sarcomeres contain actin and myosin filaments that slide past each other (Gordon et al., 1966). When oriented at an oblique angle (called pennation angle) to the line of action of the muscle, fascicles can rotate to higher angles during muscle contraction (Randhawa et al., 2013; Azizi et al., 2008; Fukunaga et al., 1997; Kawakami et al., 1998). Muscles with fascicles oriented at a pennation angle greater than zero are called pennate muscles and exhibit a range of dynamic structural changes with changes in muscle length (Alexander, 1969). Being pennate allows for more fascicles to be packed within a given volume of muscle and allows greater force generation owing to the angular arrangement of fascicles (Narici et al., 1992;

Fukunaga et al., 1996; Maganaris et al., 2001), and increased physiological cross-sectional area (PCSA). The dynamic behaviour exhibited by contracting muscles is thus a complex and multifactorial phenomenon.

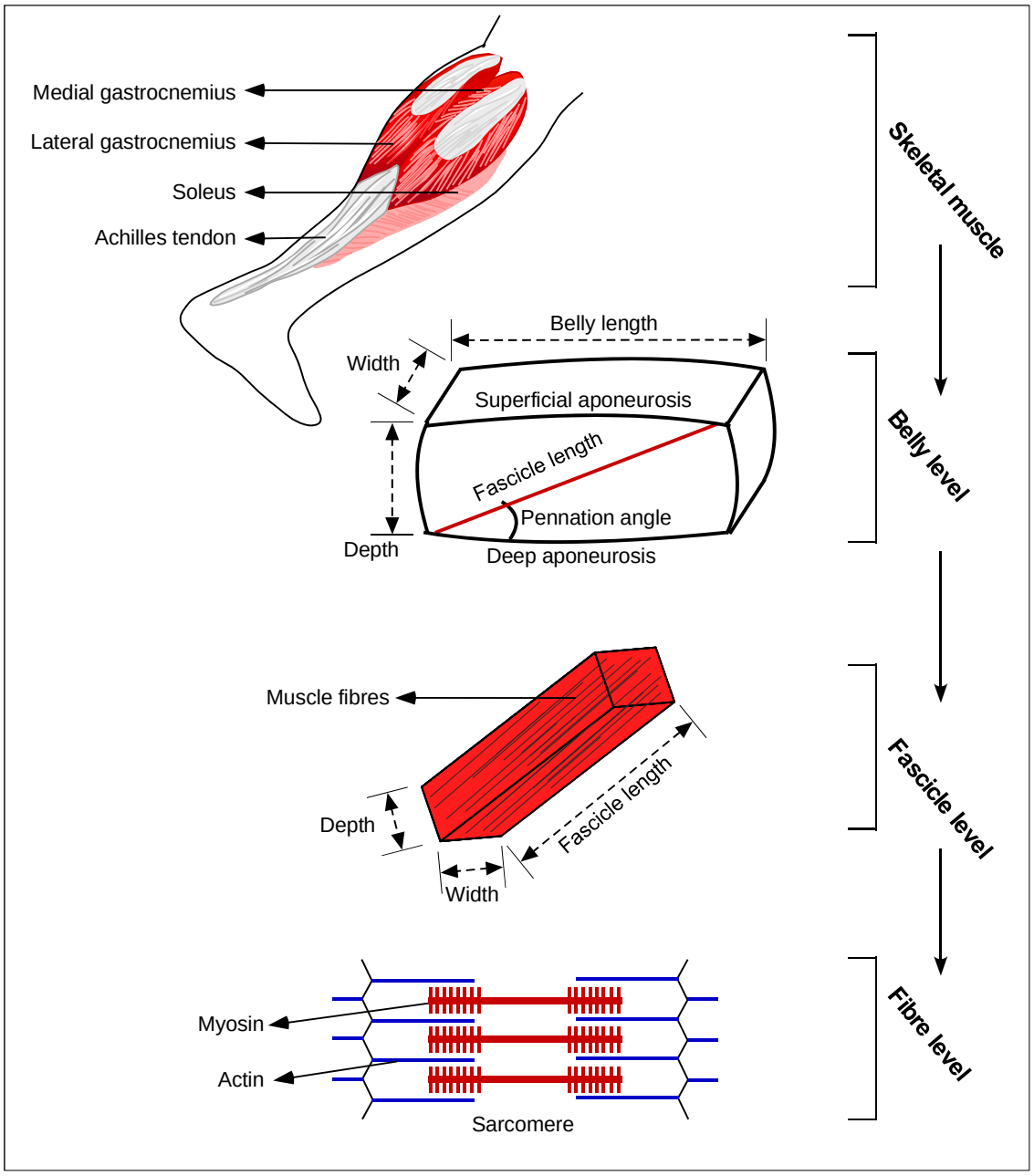

Figure 1-1. Structural organization of skeletal muscle.

The calf compartment consists of the triceps surae muscle complex that includes the medial gastrocnemius, lateral gastrocnemius and the soleus, which insert in the common Achilles tendon. Skeletal muscle structure is shown in a hierarchical manner from belly level to fascicle level to fibre level.

Muscles are nearly incompressible structures (Baskin and Paolini, 1967), and so their fascicles can change shape to ensure they still pack together in close proximity within the belly during contraction (Alexander, 1969). When pennate fascicles shorten and rotate, a component of their force acts to draw the two sheets of aponeuroses together and tends to decrease in belly thickness in the transverse direction (Rahemi et al., 2014; Zuurbier and Huijing, 1992). However, fascicles are also nearly isovolumetric structures and tend to expand during shortening leading to a contrasting phenomena of increased aponeurosis separation leading to the muscle belly bulging out transversely and the belly getting thicker (Wakeling et al., 2011). Therefore, the resultant change in transverse belly deformation is influenced by the balance of these changes and is additionally affected by the properties of the extracellular matrix and surrounding connective tissues. In relation to the muscle belly, muscle fascicles shorten at a lower velocity in a process known as muscle belly gearing (Azizi et al., 2008), that tends to enhance force in a contracting muscle (Azizi and Roberts, 2014). It has been suggested that the belly gearing within a muscle shows variability as the load and stretch of the connective tissues such as aponeurosis changes (Azizi et al., 2008). Muscle fascicles that are oriented at a range of pennation angles for a given fascicle length allow for the belly gearing to vary depending on the mechanical demands of contraction, thus influencing force generation in an activity dependent manner (Azizi et al., 2008; Wakeling et al., 2011). Currently we lack a clear understanding of how the dynamic changes in fascicle geometry, belly gearing and forces produced by our muscles relate to the transverse fascicle and belly dimensions. Understanding how various components of muscle structure change shape and interact during contraction will inform how structural phenomena influence muscle function.

Muscle function is tightly linked to the arrangement of active and passive muscle components (Epstein and Herzog, 1998). In its hierarchical structure, muscle contains myofibrils, fibres and fascicles that are surrounded by connective tissue matrices with variant elastic properties (Gordon et al., 1966; Williams and Goldspink, 1984). The flow of elastic strain energy through these structures, the arrangement of these structures and their properties can provide important information regarding the mechanical role of muscles (Ker, 1981; Matson et al., 2012; Fukashiro et al., 1995a). For example, the stiffness and stretch of aponeurosis influences the change in pennation during contraction and the magnitude of the whole muscle force (Rahemi et al., 2014; Fukashiro et al., 1995b). In fact, the mechanical stability of the muscle belly is enhanced as the internal

pressure developed by the aponeuroses is balanced by the pressure developed due to fascicle curvature during contraction (Namburete and Wakeling, 2012; Muramatsu et al., 2002a; Muramatsu et al., 2002b; Van Leeuwen and Spoor, 1992). The curvature of fascicles shows regional variations with varying fascicle pennation angles and orientations (Rana et al., 2013; Stark and Schilling, 2010), intramuscular pressures (Sejersted et al., 1984; Otten, 1988) and aponeurosis strains (Kinugasa et al., 2008). While muscle force is important, it is not as simple - various geometric combinations of fascicle length, pennation angle, belly thickness and surrounding connective tissues can generate different force output. However, to date, the functional implications of in vivo shape changes during active contraction of skeletal muscle remain largely unexplored.

In addition to the conventional thought that force is transmitted via the muscle tendon junction, a contracting muscle interacts with adjacent muscles and surrounding tissues via the myofascial connections between muscles (Huijing et al., 1998) and exerts pressure on surrounding tissues due to their tendency to bulge. These additional connective tissue pathways for force transmission have been observed in animals (Huijing et al., 1998) and humans (Riewald et al., 1996). For instance, the aponeuroses of human soleus and gastrocnemii muscles may show decreased relative displacement of soleus and lateral gastrocnemius (LG) during knee flexion as the connective tissue linking the aponeuroses may transmit force between the two muscles (Finni et al., 2017; Bojsen-Møller et al., 2010; Kinugasa et al., 2013; Hodgson et al., 2006). Additionally, longitudinal forces developed by a muscle belly can be substantially decreased by a transverse load acting on the muscle as adjacent muscle bellies expand or when external forces are applied to the muscle belly (Siebert et al., 2017; 2014). Therefore, understanding how muscles expand and impinge on each other is important to understanding muscle force development and function.

In order to nearly maintain volume during muscle shortening, a multilevel change in transverse deformation occurs within the muscle - the muscle belly, fascicles, fibres and the myofilament lattice tend to expand transversely or radially (Baskin and Paolini, 1967; Smith et al., 2011; Huxley, 1969; Williams et al., 2013; Daniel et al., 2013). Scientists have observed dorso-ventral and medio-lateral expansions during muscle shortening in axial muscle of salamanders (Azizi et al., 2002). However, the turkey LG muscle predicted contrasting changes in transverse deformation as it expands in one transverse direction and decreases in another transverse direction during low force contractions (Azizi et al.,

2008). Studies involving human participants have found that the gastrocnemii muscles show transverse deformation during isometric and dynamic contractions (Maganaris et al., 1998; Randhawa et al., 2013). However, despite the anatomical and functional similarities between the medial gastrocnemius (MG) and the LG, their bellies show contrasting changes in transverse deformation of the muscle belly during contraction (Maganaris et al., 1998; Randhawa et al., 2013; Randhawa and Wakeling, 2013). The belly of the MG thins as it shortens; while the LG increases in thickness during plantarflexion (Randhawa et al., 2013). In order to conserve volume, a muscle belly that shortens in length should typically expand transversely (Zajac, 1989; Millard et al., 2013; Abbott and Baskin, 1962; Baskin and Paolini, 1967). Therefore, the MG muscle belly must expand in the direction orthogonal to length and thickness if the belly shortens and decreases in thickness. Recently, a modelling study predicted asymmetric transverse belly deformations and showed that such asymmetries at the muscle belly level may be associated with asymmetries in the transverse deformations of its constituent fascicles (Rahemi et al., 2015). However, to date there are no data to describe asymmetries in fascicle deformation during active dynamic muscle contractions.

The two gastrocnemii muscles, the MG and LG, in the lower leg are pennate biarticular muscles. These muscles insert into the Achilles tendon and are dominant power generators in the lower limb that extend the ankle joint and generate knee flexion moments (Farris and Sawicki, 2012). These muscle-tendon units propel the body during walking (Neptune et al., 2001), produce high ankle moments to push the body upwards during stair-climbing (Radtka et al., 2006) and act like a spring by storing and releasing elastic energy during running (Winters, 1987). The structure of the two gastrocnemii muscles are comprised of short pennate fascicles that have the ability to rotate during contraction (Fukunaga et al., 1997; Kawakami et al., 1998; Azizi et al., 2008; Randhawa et al., 2013). Due to the importance of their role in locomotion, the two gastrocnemii have been the muscle of choice to investigate dynamic muscle behaviour in various human and non-human species for experimental and modelling studies (Lichtwark et al., 2007; Roberts et al., 1997; Biewener, 1998; Daley and Biewener, 2003; Fukunaga et al., 2001). In addition to the large body of research on the gastrocnemii muscles, their superficial location and relatively higher pennation angles makes them ideal for imaging and quantitative analysis.

1.2. Physiological characteristics of skeletal muscles

Research on muscles has progressed from relatively straightforward cadaveric illustrations to considering muscle as a sophisticated actuator performing highly intricate tasks (Siebert et al., 2017; Zajac et al., 2002). The 20th century witnessed work of several muscle pioneers who defined various facets of muscle functioning such as joint torque, power output, shortening velocity of fibres and whole muscle, and the relationships of these parameters with each other (for review see Kwah et al., 2013; Herzog, 2017). The historical inverse relationship of muscle force and shortening velocity during a muscle contraction was described by A.V. Hill (1938), which can be explained as: the velocity of muscle shortening depends on the force resisting the muscle and there is a maximum shortening velocity that the muscle attains (Vmax), following which no force generation is possible in the muscle (Hill, 1970). Shortening velocity is a feature of the whole muscle length change or fibre excursions; therefore, it is different for different muscles and for varied fibre lengths (Azizi et al., 2008). In real-life activities, muscles can generate shortening velocities that allow optimal force generation and energy expenditure (Huxley, 1964; Hill, 1964; Wakeling and Johnston, 1998). A parabolic relationship of sarcomere length and tension (force) in single intact frog muscle fibre was described during isometric contraction (Gordon et al., 1966) and a plateau region was observed indicating optimal actin and myosin overlap to allow for maximum force generation. This property of the muscle can be scaled up to the fascicle level where plateau regions are represented by optimal fascicle length (Herzog et al., 1992; Zajac, 1989). However, when this relationship is scaled to whole muscle level, it becomes crucial to account for the properties of passive and active internal muscle structures, tendons, related connective tissues (Zajac, 1989) and the fascicle arrangement within a muscle.

An intra-sarcomeric protein called titin is a passively extensible structure that has been associated with the passive force-length properties of muscles (Nishikawa et al., 2018) and results in a resistance to stretch at longer sarcomere lengths. Additionally, the mechanical properties of titin change when the muscle is activated, resulting in it developing higher forces if the muscle is stretched when it is active (Herzog et al., 2012). Passive force generation is critical to prevent unstable behaviour leading to sarcomere and muscle damage when muscles are excessively stretched (Heidlauf et al., 2017; Herzog et al., 2012). The passive force-length properties are not consistent across the

length of the muscle and vary with varied muscle geometry, thus influencing sarcomere length and interaction of titin with the contractile myofilaments (Heidlauf et al., 2017; Azizi and Roberts 2010). Since muscles are complex three-dimensional structures, it is important to explore how muscle level geometrical changes are associated with passive intra-sarcomeric structures such as titin, and implement the properties of such passive structures in muscle models. Forces from the surrounding tissues also transmit to acting muscles causing compression (Huijing et al., 1998; Maas et al., 2001) and this may also alter the fascicle arrangement and force. A study on rat MG muscle showed that when the muscle was loaded transversely with a plunger, the rate of force development in the longitudinal direction was reduced by 25% and maximum isometric force was reduced by 5% (Siebert et al., 2014). This study demonstrates the effect of transverse muscle loading on longitudinal force (Siebert et al., 2014). However, it is not clear how the transverse changes in fascicles influence the transverse belly expansions.

During daily activities, our muscles play various mechanical roles: motors, brakes, springs, struts and gears (Dickinson, 2000; Azizi et al., 2008; Wakeling et al., 2011). Interestingly, the two ankle extensors perform these functions by acquiring contrasting geometrical strategies: the LG bulges (increases in thickness) when it contracts whereas MG thins transversally during isokinetic contractions in healthy muscles (Randhawa et al., 2012), in muscles with sarcopenia (Randhawa and Wakeling, 2013), and in individuals with locomotor disorders when they performed isometric contractions (Koryak, 2008). Transverse deformation of a muscle belly is sensitive to force levels within the muscle as observed during experimental (Maganaris et al., 1998; Wakeling et al., 2011) and modelling investigations (Azizi et al, 2008; van Leeuwen and Spoor, 1992). Several 2D studies have shown that the MG muscle in humans does not bulge or significantly decrease in thickness during contraction (Narici et al.,1996; Azizi et al., 2008; Wakeling et al., 2011; Randhawa et al., 2012; Randhawa and Wakeling, 2013). However, a significant increase in the belly thickness of LG has been observed during isometric contractions (Maganaris et al., 1998), isotonic contractions (Azizi et al., 2008; Randhawa et al., 2012) and during cycling (Wakeling et al., 2011) in humans. Within a muscle belly, transverse deformations can occur in three main ways: (1) by changing the distance between the two sheets of aponeuroses (Kawakami et al., 1998; Wakeling et al., 2011), or (2) by changing the distance between muscle boundaries in a transverse direction that is parallel to the sheets of aponeuroses, or (3) by balancing the effects of the two ways mentioned above

since the connective tissues such as the aponeuroses and tendon may constrain the exact direction of transverse deformation. To account for the transverse deformation of muscle belly in the directions stated previously, a three-dimensional view of muscle structure during active dynamic tasks is warranted.

Longitudinal changes in fascicles influence the geometrical changes of the muscle belly. The fascicle length decreases as it contracts; however, there is an increase in its diameter. This results in a greater cross sectional area (CSA) of muscle fascicles and thus the muscle PCSA (sum of the CSAs of all the fascicles in a muscle: Lieber and Friden, 2000). In order to conserve volume (Baskin and Paolini, 1967), the thickness of muscle belly changes (Azizi et al., 2008; Maganaris et al., 1998; Wakeling et al., 2011). A greater fascicle excursion allows for the muscle belly to shorten and generate force (Lieber and Ward, 2011; Azizi et al., 2008). Transverse changes in isolated rat muscle have been recently studied to demonstrate the effects of transverse muscle loading on longitudinal force (Siebert et al., 2014). However, it is not clear how the transverse changes in fascicles influence the transverse belly expansions.

In conjunction with a dramatic change in pennation angle during muscle contraction, the change in transverse deformation of a muscle belly can decouple the force-velocity characteristics of the belly from those of the muscle fascicles (Azizi and Brainerd, 2007). Thus, the change in transverse deformation of the muscle belly has been suggested to play a functional role in adjusting the velocities at which fascicles shorten, and thus influence the prediction of in vivo muscle force (Azizi et al., 2008). In addition to force, the structural properties of skeletal muscles are also sensitive to varying activation levels (Holt et al., 2014; Josephson and Edman, 1988; Rassier et al., 1999; Rack and Westbury, 1969) that may change fascicle velocity thus allowing it to maximize performance during locomotion (Holt and Azizi, 2016). Change in muscle belly thickness may also influence longitudinal tendon strains as suggested by Farris and colleagues (2013). They found that as the bellies of triceps surae muscles thicken during fixed-position contractions, a 5% transverse strain develops in the proximal end of Achilles tendon compared to a longitudinal strain of 5% at the distal end. Additionally, the tendon and aponeurosis exhibit different strains during dynamic contractions (Fukashiro et al., 1995b), and the internal work required to effectively transmit force by stretching these connective tissues likely relates the dynamic muscle structure to the elastic properties of surrounding connective tissues (Holt and Azizi, 2014). However, major contributions to the

field of muscle mechanics largely come from studies that conducted 1D or 2D analysis of muscle structure during fixed length contractions or from muscle models assuming constant thickness, area and volume.

1.3. Multidimensional considerations of skeletal muscles

Muscle models are a representation of muscles providing information regarding muscle function within the musculoskeletal system and thus have been essential to biomechanical analyses (Lieber et al., 2017; Dick et al., 2017; Wakeling et al., 2012). Not only have muscle models provided essential quantitative information on how muscle structure and function interact to generate movement (Rahemi et al., 2014; Lieber et al., 2017), muscle models have enabled us to explore cause-and-effect relationships that we are unable to simulate experimentally or could not test in humans (Siebert et al., 2017; Dick et al., 2017). We can expand the applicability of muscle models by adding more parameters such as changes in muscle structure (Dick et al., 2017; Rahemi et al., 2014; Randhawa et al., 2013), fibre-types (Sandercock and Heckman, 1997; Wakeling et al., 2012; Lee et al., 2013) and motor-unit recruitment (Zajac, 1989; Delp et al., 2007; Millard et al., 2013). However, this makes a muscle model structurally complex. Hill-type muscle models have been extensively used to describe the mechanical behavior of muscles (Hill, 1938), but the information these models provide regarding the mechanism of muscle contraction is limited (Herzog, 2017). Over the past decades, scientists have developed and tested the robustness of musculoskeletal models in many research realms ranging from healthy to pathological conditions (Rajagopal et al., 2016; Hamner et al., 2010; Peterson et al., 2010; Arnold et al., 2013), and with a further increase in computational power, muscle models will allow for higher levels of detail, thus widening their application.

Multidimensional muscle models have been in place to investigate various dynamic muscle properties including fascicle orientations (Agur et al., 2003; Rana et al., 2012), fascicle curvatures (Van Leeuwen and Spoor, 1992), force transmission (Yucesoy et al., 2002) and intramuscular pressures (Jenkyn et al., 2002). Muscle structure can be represented by a simple 1D model with series of line segments and predict muscle behaviour of an isolated muscle (Delp et al., 1990; Hoy et al., 1990). Since 1D models do not represent the changes in a muscle's shape due to surrounding connective tissues, adjacent muscles and underlying bones (Randhawa et al., 2013; Blemker and Delp, 2005), the information we receive from these models cannot be fully applied to real life as muscles

operate in three dimensions. The 2D and 3D represent muscles as a relatively more complex system with additional input parameters thus improving the accuracy of predicting muscle behaviour. However, all models may have limitations due to the assumptions we make when building these models.

A common assumption is that the whole muscle maintains constant volume during contraction in a manner consistent with its constituent fibres (Baskin and Paolini, 1967). This condition is misinterpreted by 1D and 2D pennate muscle models in different ways as they are unable to conserve volume: 1D models of pennate muscles assume constant muscle thickness, which is the gap between the bounding sheets of aponeurosis (Alexander and Vernon, 1975; Zajac, 1989; Delp and Loan, 1995; Maganaris et al., 1998; van den Bogert et al., 2011) whereas 2D models can assume a constant area in the fascicle plane (Zuurbier and Huijing, 1992; Epstein and Herzog, 1998; van Leeuwen, 1992; Randhawa et al., 2012). However, a 2D panel model of pennate muscle with constant area must decrease in thickness when a compliant aponeurosis is included within the model as the aponeurosis will increase in length during contraction (Randhawa et al., 2013; Lieber et al., 2017). When 3D muscle geometry is accounted for in models, they allow muscle belly to change shape transversely as well as in length (Siebert et al., 2017). Studies in the past have shown that 3D models of isolated rat MG show changes in transverse deformation of muscle belly during isometric contractions (Siebert et al., 2012) and 3D fascicle and muscle deformations occur in the rabbit soleus for multiple contracting conditions (Böl et al., 2013). However, the data available on the 3D changes occurring within muscles in man during active dynamic tasks that would allow for detailed 3D models to be validated for human muscle contractions are relatively lacking.

Changes in transverse belly deformation are important to study as they can influence both fascicle strains (Azizi and Deslaurens, 2014) and tendon strains (Farris et al., 2013) and the resultant forces generated by the muscle. While each model accurately predicts the desired parameter; many models simplify the geometrical representation of muscle by assuming constant thickness (Zajac, 1989; Delp et al., 2007; van den Bogert et al., 2011; Millard et al., 2013; Rajagopal et al., 2016; Randhawa and Wakeling, 2015). Such models may allow for a straightforward prediction of fascicle pennation given a fascicle length; however, we cannot investigate the mechanisms by which shape changes influence muscle mechanics and the internal structure of muscles. Recently, imaging studies have reported that the change in transverse deformation of muscles can vary in a

complex and muscle-specific manner, and can vary for both isometric (Maganaris et al., 1998) and dynamic (Wakeling et al., 2011; Randhawa et al., 2013; Azizi et al., 2008) contractions. In a previous 2D study, a constant panel area model was used to study fascicle structure in the MG muscle of the rat (Zuurbier and Huijing, 1992) and the relation between fascicle length, pennation and aponeurosis stretch was predicted, however, the scientists later reported that the panel area decreased during muscle shortening, and was balanced by an increase in the transverse deformation of the fascicle (by increasing cross-sectional area) (Zuurbier and Huijing, 1993). While these findings show interesting results, they are insufficient to explain the contrasting change in transverse deformation that occurs in the LG and MG in humans (Randhawa et al., 2013).

Some studies have implemented a constant area assumption into a 2D muscle model (Randhawa et al., 2013; Zuurbier and Huijing, 1992; Epstein and Herzog, 1998; van Leeuwen, 1992), and other studies have assumed nearly incompressible volumes when investigating 3D properties (Otten and Hulliger, 1995; Azizi et al., 2002; Oomens et al.,2003; Blemker et al., 2005). However, the action of muscle contraction can cause variable amount of blood that may pool and be pumped out from the muscle, thus allowing the whole muscle to change volume to a greater extent than in the fibres (Sheriff and Bibber, 1998). Dynamic shape changes and mechanical output of a contracting muscle can be influenced by structural and material properties of connective tissue (Azizi et al., 2002). Additionally, changes in fascicle length, pennation, muscle thickness (Wakeling et al., 2013) and muscle force (Siebert et al., 2014) were observed when external pressure was experimentally increased on a muscle. These dynamic shape changes can be important in adjusting the muscle fascicle shortening velocity (Azizi et al., 2008). As a muscle contracts, the fascicles rotate and their shortening velocity is decoupled from the shortening velocity of the muscle belly (Azizi and Brainerd, 2007; Azizi et al., 2008; Wakeling et al., 2011). Since gearing is sensitive to the speed and force of contraction, and thus can vary, muscle models should be able to predict this variability when predicting muscle force (Azizi et al., 2008; Wakeling et al., 2011). However, traditional muscle modelling studies did not implement shape changes and variable gearing into the muscle models, and thus underestimated the muscle force for certain mechanical tasks (Epstein et al., 2006; Herzog, 2017). Forces generated by skeletal muscles and the accuracy by which these forces are predicted in muscle models are essential to enhance clinical decision-making for musculoskeletal and neurological conditions.

The validity of traditional 1D muscle models has been questioned in the past (Herbert and Gandevia, 1995), but it is possible that these models may be sufficiently competent in predicting in vivo muscle forces during specific submaximal tasks (Randhawa et al., 2013). The expanding pool of data, development of sophisticated methods and understanding of structure-function relationships has enabled us to model muscle geometry by giving specific inputs and constraints to drive the models (Rahemi et al., 2014, Böl et al., 2013, Siebert et al., 2012). The models can predict a range of parameters from overall changes of the muscle-tendon unit length and force (Delp et al., 2007; Rahemi et al., 2014) to intricate structural features within the muscle belly (Böl et al., 2013; Randhawa et al., 2013); however, 3D changes in fascicle thickness during dynamic contractions have never been explored in humans before. It is important to study the 3D changes in muscles, which can enable more accurate assessment of the contraction behavior of muscles and biomechanical factors at the muscle level that contribute to diseases in humans and help plan efficient rehabilitation programs (Lieber et al., 2017). We need to develop a 3D model of the muscle structure that could predict changes in muscle thickness, and to evaluate the accuracy with which existing 1D, 2D and this new 3D muscle model predicts fascicle pennations, and changes in thickness in the two gastrocnemii. A 3D model that accommodates both increases and decreases in thickness could possibly provide the best predictions of structure.

1.4. Techniques for *in vivo* assessment of 3D muscle behaviour

Direct assessments of 3D passive muscle structure can be obtained from cadaveric muscles (Haughton, 1873; Benninghoff and Rollhauser, 1952; Huijing, 1985), and when used in conjunction with muscle modelling, they can predict dynamic shape changes of a muscle. The cadaveric studies have been used to measure muscle belly length, fascicle lengths and pennation angles in 2D (Wickiewicz et al., 1983; Friederich and Brand, 1990) and to obtain 3D information of muscle structure (Agur et al., 2003). Compared to cadaveric muscle, the muscle structure of an active muscle has greater pennation angles, smaller fascicle lengths, and altered muscle-tendon properties (Li et al., 2009; Martin et al., 2001). Additionally, isolated muscle fibres may not be ideal to predict whole muscle behaviour as the properties of aponeurosis, tendinous connective tissues that these fibres anchor to, cannot be fully accounted for (Zuurbier and Huijing, 1992). To

understand muscle function and conduct quantitative analysis of muscle structure during active dynamic tasks, we require techniques to study in vivo muscle behaviour. In order to find structure-function associations of muscles during locomotion and clinical gait analysis, we require techniques to quantify behaviour of muscles within intact bodies, surrounded by tissues such as other muscles and bones (Maas et al., 2001).

Recent developments in muscle imaging have allowed the dynamic muscle properties of muscle and its components to be determined. Using diffusion-tensor (DT) MRI, scientists have extracted information regarding the length and orientation of muscle fascicles (Damon et al., 2002; Heemskerk et al., 2009; Kan et al., 2008; Lansdown et al., 2007; Levin et al., 2011). MRI studies have provided estimation of fascicle trajectories through 3D imaging of the muscle belly (Blemker and Delp, 2005; Heemskerk et al., 2009; Wokke et al., 2014; Mercuri et al., 2005). However, MRI imaging is largely limited to passive tissues due to long scan times, or it requires prolonged low-level isometric contractions for image acquisition. Additionally, the long scan durations used in DT-MRI studies make this technique sensitive to involuntary soft tissue motion that may occur during scanning (Bishop et al., 2009). Furthermore, information regarding fascicle shape and dynamic changes cannot be quantified using MRI as these intricate structures are barely visible during scanning (Bolsterlee et al., 2013).

Brightness mode (B-mode) ultrasound provides a more rapid imaging of muscle structure, and with this imaging tool we can track dynamic muscle contractions (Cronin and Lichtwark, 2013), quantify muscle structural properties (Maganaris and Paul, 2000; Rana et al., 2013) and observe structural changes due to an underlying muscle pathology (Narici et al., 2003; Morse et al., 2005). The earliest ultrasound studies showed in vivo changes in fascicle length and pennation (Narici, 1999; Kawakami et al., 1993; Kuno and Fukunaga, 1995) however recently, a range of automated approaches have been used to quantify intricate muscle features such as fascicle curvatures (Rana et al., 2009), details on 3D muscle properties (Barber et al., 2009; Kurihara et al., 2005; Malaiya et al., 2007; Fry et al., 2004; Hiblar et al., 2003), and muscle volume (Barber et al., 2009). Since ultrasound provides information regarding the structural anatomy of underlying muscle tissue, the most accurate estimates of fascicle lengths can be obtained when the ultrasound image plane is aligned with the plane in which fascicles are orientated (Benard et al., 2009; Klimstra et al., 2007). Also, due to the 2D nature of ultrasound imaging, a

single probe cannot simultaneously acquire out-of-plane motion of muscle belly (eg. change in transverse deformation out of the plane).

2D ultrasound imaging can be combined with 3D motion capture markers, and thus 2D images from the ultrasound can be projected in 3D space and we can quantify muscle as a 3D entity (Rana and Wakeling, 2011; Barber et al., 2009; Malaiya et al., 2007). Since muscle fascicles appear as nearly parallel, repeating bands within B-mode ultrasound images, we can potentially extract information on the spatial frequencies of the fascicular structure within the muscle belly, and relate this information to the fascicle size, shape and orientations during muscle contraction. Together with a high temporal resolution (Cronin and Lichtwark, 2013; Narici et al., 1996; Fukashiro et al., 1995b), ability to track the ultrasound probe in 3D (Prager et al., 1998; Rana and Wakeling, 2011), and using image processing techniques, we can capture changes in transverse deformation in the muscle belly and fascicles using two ultrasound probes or dual-probe imaging. Unlike the 3D ultrasound probe that acquires data sequentially in 3D space by moving its scanning direction through time (Lindop et al., 2006; Lopata et al., 2010; Lopata et al., 2007), the dual-probe technique can employ two probes that scan a common region of the muscle from two orthogonal directions and acquire data simultaneously from the given directions. This dual-probe imaging and processing approach may provide a successful experimental framework for quantifying dynamic structural changes in a 3D perspective, however; this approach has not yet been used to obtain 3D information of muscle belly and fascicles. This approach will enhance our understanding of how whole muscle shape changes interact with the fascicle deformations and geometry, using 3D information of the deformations and a 3D mechanistic framework to describe the system.

1.5. Rationale and specific aims of this thesis

The overarching goal of my thesis was to implement modelling and experimental techniques to quantify changes in the transverse deformation of muscle belly and fascicles during active dynamic tasks, and to investigate if asymmetries in the transverse deformations of muscle fascicles occur during active contractions of two pennate muscles – the LG and the MG. I used advanced structural muscle models, B-mode ultrasound imaging and sophisticated image processing techniques to predict and measure 3D deformations of muscle belly and fascicle during active plantarflexion contractions.

I quantified the 3D structure of the two gastrocnemii muscles during a range of dynamic tasks including changes in muscle belly and fascicle transverse deformations. Based on the findings, I drew relations of these features with each other as well as with the functional output of the given tasks. This fundamental research has identified some of the connective links between 3D muscle structure and dynamic muscle function in humans. This research will help us understand how longitudinal belly and fascicle strains link to transverse fascicle and belly changes, and how the dynamic 3D muscle structure is linked to force output and muscle function.

The specific aims of this thesis were:

Aim 1 (Chapter 2): I aimed to predict transverse deformations in muscles and highlight the importance of 3D changes in dynamic muscle structure by comparing existing 1D and 2D muscle models with a new 3D model that allows for transverse deformations to occur in all orthogonal directions.

Aim 2 (Chapter 3): I aimed to develop image processing techniques to quantify changes in transverse fascicle deformations of the two gastrocnemii muscles as viewed in 2D ultrasound images and investigate the relationship of geometrical changes in fascicles to overall muscle structure.

Aim 3 (Chapter 4): I aimed to use a dual-probe ultrasound technique to measure and compare in vivo changes in transverse deformation of muscle belly and fascicles in 3D, and determine whether such transverse deformations were asymmetrical in their orthogonal directions.

The change in transverse deformation in muscle belly and fascicles can occur in various directions perpendicular to the longitudinal axis of the muscle belly and fascicles, respectively. Chapter 2 describes this transverse deformation in two directions - depth-wise and width-wise. The change in thickness of the belly in the depth-wise direction occurs between the two sheets of aponeurosis. The change in thickness of the belly in the width-wise occurs in the direction perpendicular to the depth-wise direction and perpendicular to the longitudinal axis of the muscle. Chapter 3 describes transverse changes in the muscle fascicles occurring in the depth-wise direction. Chapter 4 describes transverse deformations of muscle belly in X and Y directions, and transverse deformations of muscle fascicles in x and y directions, and these directions may not be

similar to the depth-wise and width-wise directions in Chapter 2. These directions depend in part on the ultrasound scanning directions, and due to the dual-probe technique used, these directions are not constrained to the depths and widths of Chapters 2 and 3.

Chapter 2.

Multidimensional models for predicting muscle structure and fascicle pennation

This paper was published as Randhawa, A., & Wakeling, J. M. (2015). Multidimensional models for predicting muscle structure and fascicle pennation. *Journal of Theoretical Biology*, 382, 57-63.

Author contributions: A.R. and J.M.W. conceived and designed the study. A.R. collected and analyzed the experimental data. Both A.R. and J.M.W. interpreted the results of experiments, analyzed the models, and drafted the manuscript. Both authors approved the final version for publication.

2.1. Introduction

The volume of muscle fibres remains nearly constant during contraction (Baskin and Paolini, 1967), and thus a commonly stated assumption in muscle models is to keep volume constant. However, in reality, 1D and 2D models are unable to conserve volume, but interpret this condition in different ways: 1D models of pennate muscle assume constant muscle depth, which is the distance between the bounding sheets of aponeurosis (Alexander and Vernon, 1975; Zajac, 1989; Delp and Loan, 1995; Maganaris et al., 1998; van den Bogert et al., 2011) whereas 2D models can assume a constant area in the mid-longitudinal (or fascicle) plane (Zuurbier and Huijing, 1992; Epstein and Herzog, 1998; van Leeuwen, 1992; Randhawa et al., 2012). A 2D panel model of pennate muscle with constant area but an inextensible aponeurosis will maintain a constant depth during contraction. However, when aponeurosis compliance (and thus muscle force) is included in 2D models the muscle must decrease in depth to balance increases in aponeurosis length. 3D models allow changes in dimension of the muscle belly in all directions of length, width and depth. Previously, 3D modelling of isolated rat medial gastrocnemius undergoing isometric contractions have shown changes to the depth and width of the muscle belly (Siebert et al., 2012) and 3D fascicle and muscle deformations in the rabbit soleus for multiple contracting conditions (Bol et al., 2013). However, there are relatively

little data available on the 3D changes in the dynamic structure of muscles in man that would allow detailed 3D models to be validated for human muscle contractions.

Early considerations of pennate muscle structure assumed a constant distance between aponeuroses during contraction as an approximation to the constant volume assumption (Benninghoff and Rollhäuser, 1952; Alexander, 1968; Alexander and Vernon, 1975; Hatze, 1978), and this simplification is still widely used in musculoskeletal models of movement (Zajac, 1989; Delp and Loan, 1995; van den Bogert et al., 2011). However, when muscles contract they can change in width or depth, and some studies have questioned the constant-depth assumption (Zuurbier and Huijing, 1992, 1993; Herbert and Gandevia, 1995). Measurements on the axial muscle of salamanders showed increases in dorso-ventral depth as the longitudinal length decreased (Azizi et al., 2002), and recent studies have shown that the muscle depth can change during contraction for pennate muscles during both isometric (Maganaris et al., 1998) and dynamic tasks (Azizi et al. 2008; Wakeling et al., 2011; Randhawa et al., 2012). It is therefore possible that 1D models, which make assumptions of constant depth, do not recreate the internal structure of muscles adequately (Zuurbier and Huijing, 1992, 1993). Furthermore, opposing changes in depth can occur for the medial and lateral gastrocnemii during ankle plantarflexions (Randhawa et al., 2012) and so 2D models that can only account for decreases in depth as the aponeurosis is loaded may also be insufficient. It has been suggested that the structural and material properties of connective tissue affect the bulging and mechanical output of muscle during contraction (Azizi et al., 2002), and, indeed, experimentally increasing the external pressure on a muscle caused changes in fascicle length, pennation, muscle depth (Wakeling et al., 2013) and muscle force (Siebert et al., 2014) during contraction. It is thus possible that differences in the modes of bulging of muscles may result from differences in their internal and surrounding connective tissues, and that these can be explained by 3D models of muscle structure.

Previous studies of the fascicle structure in the medial gastrocnemius muscle of the rat (Zuurbier and Huijing, 1992) initially assumed a constant panel area when relating fascicle length, pennation and aponeurosis stretch, but later reported that the panel area decreased during muscle shortening, and suggested that this was consistent with the fascicle cross-sectional area increasing equally in width and depth (Zuurbier and Huijing, 1993). However, these findings are insufficient to explain the contrasting bulging that occurs in the lateral and medial gastrocnemius in man (Randhawa et al., 2012). The

purpose of this study was to develop a 3D model of the muscle structure that could predict the opposing bulging characteristics of the bulging between the medial and lateral gastrocnemis in man, and to evaluate the accuracy with which 1D, 2D and this 3D muscle model could predict fascicle pennations, and changes in depth in the gastrocnemii during ankle plantarflexions in man. It was expected that the 3D model that could accommodate both increases and decreases in muscle depth would provide the best predictions of structure.

2.2. Methods

2.2.1. 1D Constant depth model (Figure 2-1 (A))

The 1D muscle model is based on a commonly used model (Zajac, 1989) and is considered as a contractile element in series with an elastic tendon. The contractile element is represented by a muscle fascicle with length L_f at a pennation angle β to the tendon. The depth of the muscle belly, *d*, is kept constant, where:

$$L_f \sin\beta = d, \qquad \text{equation 1}$$

For all models in this paper, length can be represented in a normalized form:

$$\hat{L}_f = \frac{L_{f1}}{L_{f0}}, \qquad \text{equation 2}$$

where the “hat” symbol denotes that a variable’s current state (subscript 1) is normalized by its initial value (subscript 0).

As the depth is assumed to be constant:

$$L_{f0}\sin\beta_0 = L_{f1}\sin\beta_1, \quad \text{or} \quad \sin\beta_0 = \hat{L}_f \sin\beta_1, \qquad \text{equation 3}$$

This model therefore predicts that the current pennation β_1 is entirely dependent on the initial pennation β_0 and the normalized fascicle length $\hat{L}_f$ of the muscle fascicle, and that there is a unique β_1 for each corresponding fascicle length.

2.2.2. Constant panel area models

Some models consider the muscle to be a 2D panel, and have assumed that the area within the panel remains constant. This type of model can be considered from two approaches: (A) the first approach is to directly model the panel that represents the whole muscle belly (van Leeuwen, 1992), and (B) the second approach is to model the individual muscle fascicles as panels. In the following 2D models in this paper the muscle fascicles originate and insert onto sheets of aponeurosis. The aponeuroses are parallel to each other and in line with the tendon.

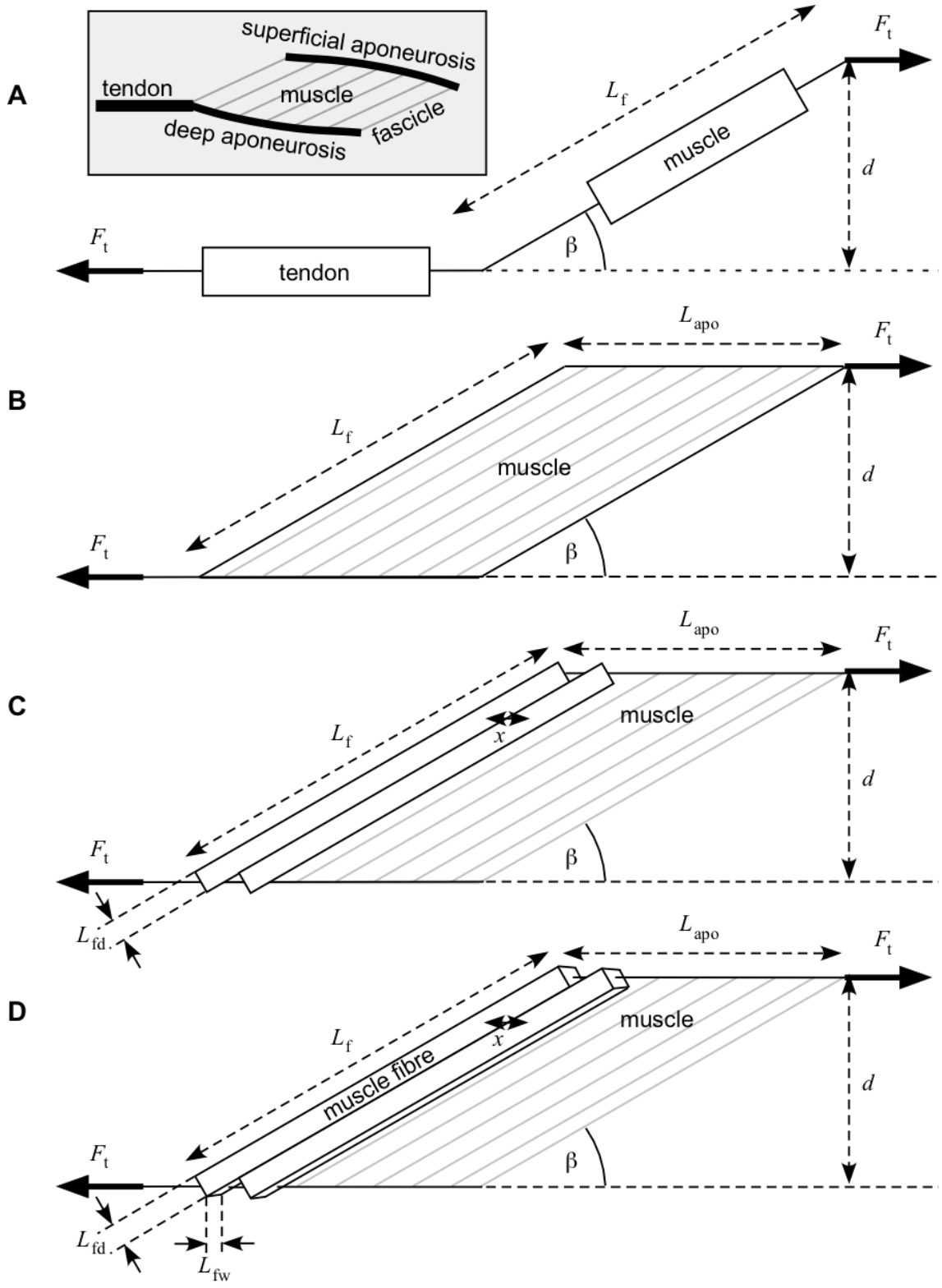

Figure 2-1. Graphical representation of the 1D (A), 2D (B and C) and 3D (D) models of muscle structure.

2D Panel model for muscle belly (Figure 2-1 (B))

The 2D model derivation begins with the same initial parameters from the 1D model, and so equation 1 is repeated as equation 4. As with the constant depth model, we can consider:

$$L_f \sin\beta = d, \qquad \text{equation 4}$$

The area within the panel remains the same throughout the contraction and so:

$$L_{f1} \sin\beta_1 L_{apo1} = L_{f0} \sin\beta_0 L_{apo0}, \quad \text{or} \quad \sin\beta_0 = \hat{L}_f \sin\beta_1 \hat{L}_{apo} \qquad \text{equation 5}$$

The tendon force F_t is a component of the fascicle force F_f that acts along the aponeurosis. The F_t was calculated by normalizing ankle plantarflexion torque to the maximum isometric plantarflexion torque for each subject (assuming the moment arm remained constant).:

$$F_t = F_f \cos\beta, \qquad \text{equation 6}$$

The aponeurosis has a compliance k, and stretches in proportion to F_t. Therefore the normalized aponeurosis length $\hat{L}_{apo}$ is given by:

$$\hat{L}_{apo} = 1 + kF_{f1} \cos\beta_1, \qquad \text{equation 7}$$

Solving equations 5 and 7 together gives:

$$\sin\beta_0 = \hat{L}_f \sin\beta_1 (1 + kF_f \cos\beta_1), \qquad \text{equation 8}$$

2D Panel model for muscle fascicles (Figure 2-1 (C))

The constant area model can also be considered from the perspective of the individual muscle fascicles. The fascicles have length L_f, and depth L_{fd} (in the "fascicle plane" which is the plane of Figure 2-1), and it is assumed that their panel area $L_f \times L_{fd}$ remains constant during contraction.

As the fascicle length decreases, the fascicle depth would need to increase to maintain constant panel area:

$$L_{f0}L_{fd0} = L_{f1}L_{fd}, \qquad \text{or} \qquad \hat{L}_f = \frac{1}{\hat{L}_{fd}}, \qquad \text{equation 9}$$

and this would increase the distance *x* that is in the direction of the main muscle axis and parallel to the aponeuroses.

$$\hat{x} = \hat{L}_{fd}\frac{\sin\beta_0}{\sin\beta_1}, \qquad \text{equation 10}$$

Elongation in $\hat{x}$ would be matched by elongation in $\hat{L}_{apo}$, and so:

$$\hat{x} = \hat{L}_{apo} = 1 + kF_f\cos\beta_1, \qquad \text{equation 11}$$

It is assumed that adjacent fascicles touch each other and cannot overlap. During fascicle shortening the spaces taken up by the fascicles can be balanced if either the pennation β increases, or the distance *x* increases. Solving equations 10, and 11 together gives:

$$\hat{L}_{fd}\frac{\sin\beta_0}{\sin\beta_1} = 1 + kF_f\cos\beta_1, \qquad \text{equation 12}$$

and finally solving 9 and 12 together gives

$$\sin\beta_0 = \hat{L}_f\sin\beta_1(1 + kF_f\cos\beta_1), \qquad \text{equation 13}$$

This equation is the same as equation 8, and shows that the same relation between fascicle length and pennation can be calculated from either approach of assuming a constant panel area for the muscle belly, or a constant panel area of the constituent muscle fascicles. These panel models predict that the current pennation β_1 depends on the initial pennation β_0 and the normalized muscle length $\hat{L}_f$. Note that these 2D models allow for different pennation angles for a given fascicle length (if the product of aponeurosis compliance and muscle fascicle force changes). This can happen as the fascicles generate more force, leading to a greater aponeurosis stretch, thinner depth and lower fascicle pennation. If the aponeurosis is considered as inextensible (*k*=0) then these panel models (equations 8 and 13) reduce to become the same as the constant depth model.

2.2.3. 3D Constant volume model (Figure 2-1 (D))

The third dimension can be modelled by including a width L_{fw} to the muscle fascicles. In order to conserve volume in the fascicles as they change length, the following relation must be true:

$$\hat{L}_f \hat{L}_{fd} \hat{L}_{fw} = 1, \qquad \text{equation 14}$$

Decreases in muscle fascicle length must be matched by increases to the cross-sectional areas of the fascicles, and thus the muscle fascicle depth L_{fd} is related to the muscle fascicle width L_{fw} by the shape parameter, n, where:

$$\hat{L}_{fd}^{\,n} = \hat{L}_{fw}^{\,(1-n)}, \quad \text{or} \quad \hat{L}_{fw} = \hat{L}_{fd}^{\,(\frac{n}{1-n})}, \qquad \text{equation 15}$$

Equating equations 14 and 15 gives:

$$\hat{L}_f \hat{L}_{fd}^{\,(1+\frac{n}{1-n})} = 1, \quad \text{or} \quad \hat{L}_{fd} = \hat{L}_f^{\,(n-1)}, \qquad \text{equation 16}$$

Similar to the constant panel area case, the distance x that the fascicle cross-sections occupy in the main direction of the muscle is given by:

$$\hat{x} = \hat{L}_{fd} \frac{\sin\beta_0}{\sin\beta_1}, \qquad \text{equation 17}$$

and similarly, expansion in x is related to extension of the aponeurosis:

$$\hat{x} = \hat{L}_{apo} = 1 + kF_f \cos\beta_1, \qquad \text{equation 18}$$

Combining equations 16, 17, and 18 together yield:

$$\sin\beta_0 = \hat{L}_f^{\,(1-n)} \sin\beta_1 (1 + kF_f \cos\beta_1), \qquad \text{equation 19}$$

This equation takes a very similar form to the constant panel area expression (equations 8 and 13), with the addition of the shape factor n. Note that if n=0.5 then $\hat{L}_{fd} = \hat{L}_{fw}$ and so the fascicle would expand equally in depth and width as it shortens. By

contrast, if n=0 then $\hat{L}_{\mathrm{fw}} = 1$ and so the muscle fascicle width remains constant during shortening, and equation 19 reduces to become the same as the constant panel area models (equations 8 and 13). If a further inextensible constraint (k=0) is placed on the aponeurosis, in addition to n=0, then the constant volume model in equation 19 reduces to become the same as the constant depth model (equation 3).

2.2.4. Model validation (Figure 2-2)

The models were validated against structural data from the lateral (LG) and medial (MG) gastrocnemius. Fascicle length, L_f, pennation angle, β, and muscle depth, d, were quantified from B-mode ultrasound images of the lateral and medial gastrocnemii of maximal-effort isokinetic plantarflexion contractions and submaximal effort isotonic contractions for 10 male subjects (age 27.4 $\pm$ 4.8 years; height 177.6 $\pm$ 4.1 cm, body mass 81.5 $\pm$ 10.4 kg; mean $\pm$ SD). Subjects performed plantarflexions on a dynamometer (System 3, Biodex, New York, USA) with their knee held at 135 ° at ankle velocities of 45, 210, 360, 500 °/s, and six trials were performed for each speed. For the isotonic trials, they performed 8 cyclic ankle plantarflexions at 0.4, 1.0 or 1.2 Hz and at a torque of 60, 25 or 5 N m. The ankle plantarflexion torque was measured during each contraction and normalized to the maximum isometric force for each subject to give the normalized tendon force F_t (assuming the moment arm remained constant). The mean change in ankle angle during plantarflexion contractions was 13.5 $\pm$ 4.4 °.

Ultrasound probes were placed on the bellies of MG and LG, carefully aligned to the fascicle planes and secured to the leg. The bellies were imaged simultaneously using two 128-element (60mm width) linear array B-mode ultrasound probes (Echoblaster 128, Telemed, Lithuania), scanning at 40 Hz each. The ultrasound data were synchronized to the position and torque data from dynamometer for analysis.

The 1D, 2D and 3D models were tested against the measured data (equations 3, 13 and 19, respectively). The models were driven by the time-varying L_f that was measured. The parameter k was optimized for the 2D model to minimize the sum of squares for the difference between the measured and predicted β for each contraction for each subject. The parameters n and k were optimized for the 3D model to minimize the weighted sum of the sum of square differences between the measured and predicted β

and the measured and predicted depth. For this latter stage the depth was normalized to the depth midway through the slowest contraction to remove bias due to the variability in muscle depth between subjects. Root-mean-square (RMS) errors were calculated between the measured and predicted pennation and muscle depth. RMS errors were additionally calculated for models that used the mean parameters of *k* and *n* that had been calculated across all subjects (Table 2-1).

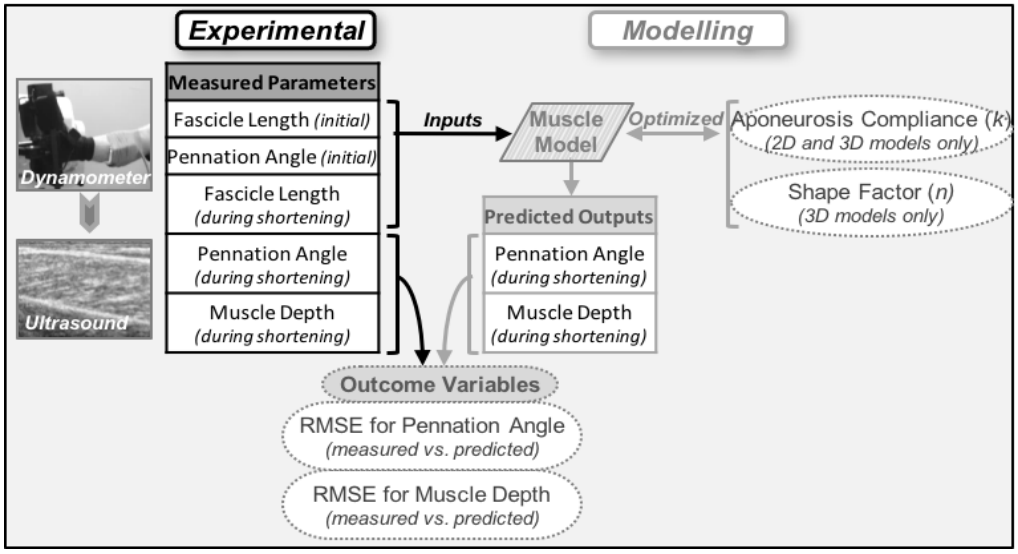

Figure 2-2. A block diagram showing the experimental (left panel/black arrow lines) and modelling (right panels/grey arrow lines) aspects of the study.

The effect of model type (1D, 2D and 3D), contraction type (isokinetic and isotonic), muscle type (MG and LG), coefficient type (subject-specific or mean *k* and *n*), and subject (random factor) on the RMS errors (for pennation and depth) were tested using ANOVA GLM (General Linear Model) with the maximum ankle torque and maximum ankle velocity for each trial as covariates. Tukey post-hoc comparisons were used to determine differences between the individual models. The interaction between model type and coefficient type was tested. All statistical tests were considered significant for $p < 0.05$. Values are reported as mean ± s.e.m..

2.3. Results

During plantarflexion for both the isokinetic and isotonic contractions of MG and LG, the muscle-tendon unit length, belly length and fascicle length decreased and the

pennation angle increased. The mean initial pennation was 19.17 ± 0.36 º for MG and 11.60 ± 0.28 º for LG, initial fascicle length was 77.84 ± 1.86 mm for MG and 53.66 ± 0.93 mm for LG, and the mean muscle depth was 16.71 ± 0.30 mm for MG and 14.08 ± 0.61 mm for LG (data as mean ± s.e.m. across all trials and subjects). During the ankle plantarflexions, depth of the muscle decreased for the MG by 3.8% but increased for the LG by 5.3%. The constant depth 1D model predicted the changes in pennation with a coefficient of determination r^2 of 0.990 ± 0.003 for the MG and 0.968 ± 0.005 for the LG. However, by definition, the constant depth model was unable to predict the changes in depth of the muscles. The 2D and 3D models had r^2 values similar to those of 1D model: 0.989 ± 0.003 and 0.989 ± 0.003 for MG, and 0.968 ± 0.005 and 0.968 ± 0.005 for LG, respectively.

Table 2-1. Shape factor n and compliance k from the muscle models optimized to the individual data.

Model	Coefficient	1D	2D	3D
MG	*k*	-	0.0241 ± 0.0018 † * ¥	0.0185 ± 0.0019 * ¥
	n	-	-	0.0246 ± 0.0091 † ¥
LG	*k*	-	0.0185 ± 0.0017 † ¥	0.0217 ± 0.0016 ¥
	n	-	-	-0.0522 ± 0.0175 †

Values are given as mean ± s.e.m. (N=10 subjects).
† denotes significant difference between MG and LG muscles. * denotes significant difference between 2D and 3D models. ¥ denotes significantly greater than 0.

When the models were optimized for each individual subject, the RMS error for the pennation angle with the 1D model was 1.070 ± 0.058 ° for the MG and 0.907 ± 0.055 ° for the LG. There was significant effect of model type, contraction type, muscle and coefficient type on muscle pennation RMS errors. Smaller errors occurred for isotonic contractions, at lower ankle torques and for the LG. There was a significant interaction between model type and coefficient type, with the smallest errors occurring for the 3D model when parameters were fitted for individual subjects.

RMS errors for muscle depth showed significant effect of model type, contraction type, muscle and coefficient type. Smaller errors occurred for isotonic contractions, at lower ankle torques, and for the MG. There was a significant interaction between model type and coefficient type, with the smallest errors occurring for the 3D model when parameters were fitted for individual subjects.

The modelled aponeurosis had significant compliance in 2D and 3D models for both MG and LG muscles (Table 2-1). The shape factor *n* was significantly different from zero for the MG indicating that the MG would show changes in width during plantarflexion even though the muscle belly depth does not increase during dynamic tasks. There was a small but significant *n* value of -0.052 for the LG (Table 2-1) indicating that the muscle would decrease by approximately 0.5% in width for a typical 10% increase in depth during plantarflexion (equation 15). A small but significant *n* value of 0.025 for the MG indicated that the muscle may increase by approximately 0.2% in width for a typical 10% decrease in depth during plantarflexion (equation 15).

The 1D model had constant depth. The 2D model was only able to predict decreases in depth as the load increased, however the 3D model was able to, and did predict decreases in depth for the MG and the increases in depth for the LG (Figure 2-3). When the models were optimized for each individual subject, the RMS error for the muscle depth with the 1D model was 0.59 ± 0.029 mm for the MG and 0.873 ± 0.049 mm for the LG. There was no significant difference in the RMS errors for depth between the 1D and 2D models, but the 3D models of both the MG and LG showed significantly less error than the 1D or 2D models (Figure 2-4). However, when the models used the mean values of *n* and *k* the RMS errors for the predicted depth, there were no significant differences between the three models.

2.4. Discussion

All three models used in this study gave very good predictions for the pennation angle from the fascicle length: the coefficient of determination or r^2 value was greater than 0.96 for the three muscle models. From a practical purpose, if the intent of a model is purely to establish a good relation between fascicle length and pennation then the more simple 1D model (equation 3) that assumes constant muscle depth appears a suitable choice for these muscles. This result is in contrast to a previous study (Herbert and Gandevia, 1995) that measured only pennation for the brachialis and suggested that it could not adequately fit a model with constant depth between the aponeuroses. They noted that the brachialis underwent substantial increases in depth during fixed-end contractions and, coupled with a speculated shortening of an intramuscular tendon, this could result in much larger increases in pennation than predicted by the model.

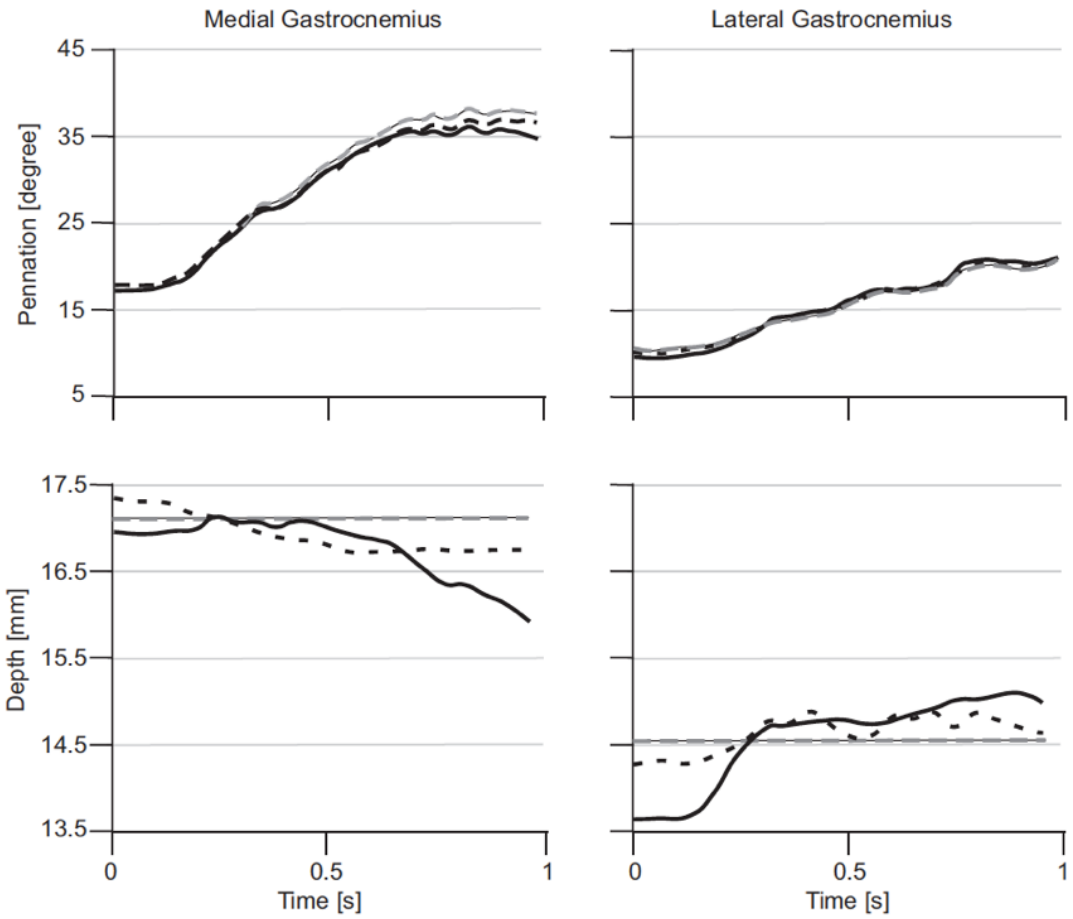

Figure 2-3. Pennation angle and muscle depth in the medial and lateral gastrocnemius during isokinetic plantarflexions for a representative contraction (45°/s).

Measured pennation angle and muscle depth are shown by the thick solid lines. Predicted pennation and depth are shown for the 1D (thin solid line), 2D (grey dashed line) and 3D (black dashed line) models. Note the paths for the 1D and 2D models are very similar. Data are shown for the mean, n=10 subjects.

The 1D model, by definition, was unable to account for changes in muscle depth. However, LG muscle belly depth has been shown to change during both isometric, and dynamic contractions (Azizi et al., 2008; Maganaris et al., 1998; Wakeling et al., 2011; Randhawa et al., 2012), and the MG and LG change in depth differently (Maganaris et al., 1998; Wakeling et al., 2011) with the MG decreasing in depth and the LG increasing in depth during ankle plantarflexions (Figure 3; Randhawa et al., 2012). The 2D and 3D models in this study differ in their ability to predict changes in muscle depth that occur during plantarflexion (Figure 2-3; Figure 2-4). 2D models can change in depth as the

aponeurosis is loaded (Zuurbier and Huijing, 1992), but can only allow a decrease in depth as the aponeurosis is stretched and this will not be sufficient to predict the increases in depth that occur in the LG during plantarflexion. The 3D model, on the other hand, has the ability to predict either increases or decreases in depth during the ankle plantarflexions. Indeed, the 3D model predicted the opposing changes in depth that occurred between the MG and LG, whilst simultaneously predicting the pennation more accurately than the 1D or 2D models (Figure 2-3). If the purpose of a model is to predict the change in muscle depth with greater accuracy in addition to the changes in pennation during contraction, then the 3D model would be the best choice from the models evaluated here. From a computational perspective, the fact that the 1D model is a specific case of the 3D model (with default values of n=0 and k=0) may make this single model (equation 19) attractive because it represents both the 1D and 3D situations. However, it should be noted that this 3D model comes with additional computational complexity, and its requirement for muscle-specific and subject-specific parameters n and k may negate its utility for general musculoskeletal simulations.

The 1D model does not need to consider the aponeurosis compliance to make good predictions of pennation. The 2D and 3D models allowed the aponeuroses to stretch when under load. The aponeurosis compliance k (Table 2-1) indicates that the aponeurosis could stretch 2% (longitudinally) at maximal ankle torque and this is a conservative estimate when compared to studies that have directly measured aponeurosis stretch of up to 5.9% (Arampatzis et al., 2005; Muramatsu et al., 2001). The models showed greatest errors at high levels of force, and this occurred for the high-torque plantarflexions and the isokinetic contractions that were at maximal effort: both these cases coincide with times when there should be large aponeurosis strains. It is possible that the inability of the models to predict and operate at large aponeurosis strains may be a factor influencing such errors. Recently, we have shown that the aponeurosis stiffness and stretch greatly influence the extent to which the muscle pennation changes during contraction and the magnitude of the whole muscle force (Rahemi et al., 2014). Understanding the role and contribution of the aponeurosis compliance is a necessary aspect of understanding the structure and dynamics of muscle contraction (Kawakami et al., 1998; Rahemi et al., 2014).

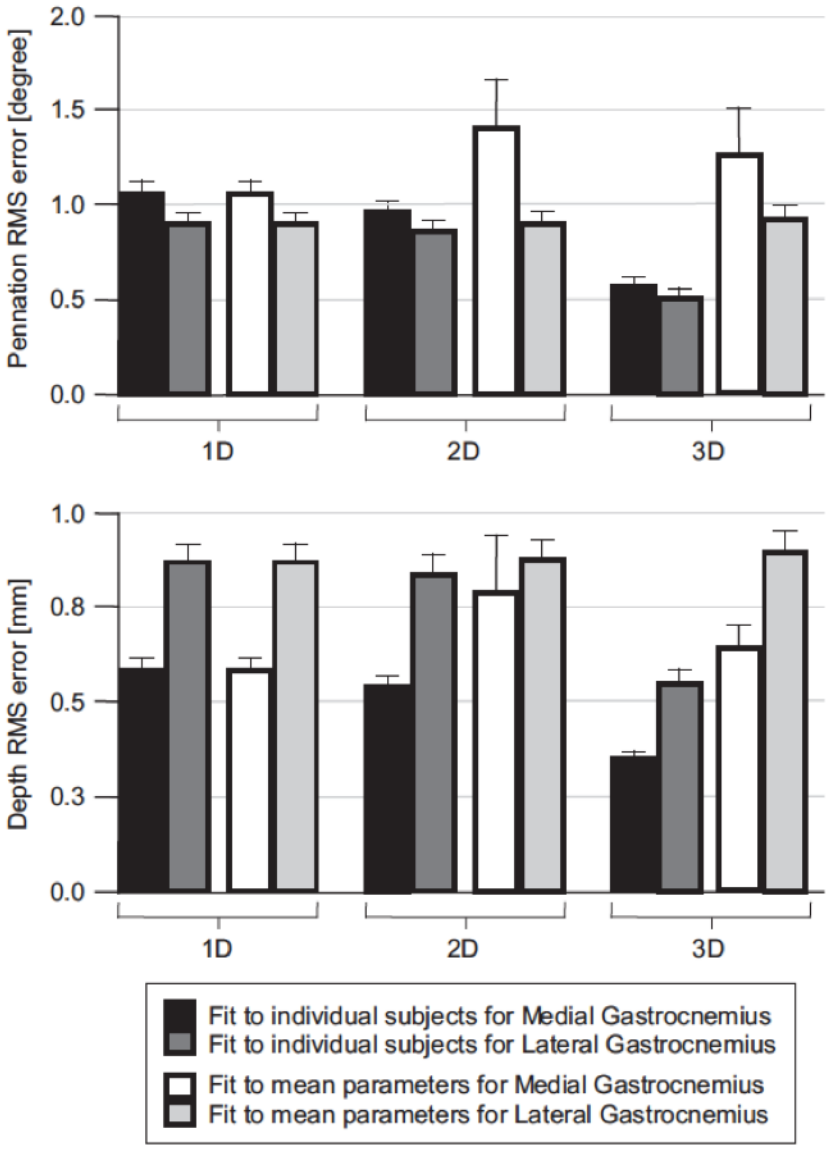

Figure 2-4. Root-mean-square (RMS) errors for the 1D, 2D and 3D models for the predicted pennation angle and muscle depth.
Medial gastrocnemius is shown with black bars and lateral gastrocnemius with dark-grey bars for models fitted to individual subjects. Medial gastrocnemius is shown with white bars and lateral gastrocnemius with light-grey bars for models fitted to mean parameters (n and k). Data are shown for the mean ± s.e.m., n=10 subjects.

The effect of different modes of bulging has previously been modelled for the axial muscle in the salamander during swimming (Brainerd and Azizi, 2005). The measured changes in dorsoventral height were compared to predictions from models that made different assumptions on dorsoventral and mediolateral bulging (similar to depth, and

width from this study, respectively). It was found that the measured pattern of dorsoventral bulging for the axial muscle fell between the assumptions of equal dorsoventral – mediolateral bulging and of all the bulging occurring in the mediolateral direction, and it was suggested that the muscle fibre rotations were impacted by bulging in the mediolateral and/or dorsoventral directions. Here we find a different result for the pennate MG and LG in man, in that the relation between fascicle length and pennation is much less sensitive to muscle depth and width, and that changes in muscle width may be very small.

It was initially expected that the opposing changes in the MG and LG depth during ankle plantarflexions would be balanced by opposing changes in width. This expectation motivated the use of the shape parameter *n* to relate the changes in width with the changes in depth of the individual muscle fascicles. For the case of the 10% fascicle shortening, the mean value of *n* for the 3D model (Table 2-1) would predict the fascicle depth to increase by 9.7% for the MG, and 10.5% for the LG. For this 10% shortening of the fascicles, the 3D model from this study (equations 14 and 15) would predict a 0.2% increase in width for the MG, and a 0.5% decrease in width for the LG. The direction of these changes in width are consistent with previous expectations based on measures of the whole muscle depth (Randhawa et al., 2012), however, the magnitudes are much smaller than expected. Additionally, recent imaging (Wakeling and Randhawa, 2014) and modelling (Hadi Rahemi, personal communication) studies indicate that the depth-wise expansion of the fascicles may be considerably less than decreases in fascicle length. Thus, the use of these 2D and 3D models does not adequately account for the changes in fascicle geometry that occur during contractions.

2.5. Limitations

The models tested in this study represent the muscle in a very abstract fashion, and there are many features of the muscle structure that were not considered. One assumption in the validation of the models was that the ankle joint torque could represent the muscle force. However, this assumption requires that each muscle of interest (MG or LG) maintained a constant moment arm about the ankle during plantarflexion, and that the proportion of the joint torque delivered by that muscle remained constant at different ankle angles and velocities. The moment arm of the Achilles tendon has been shown to increase during plantarflexion (Maganaris et al., 2006) and so the simulations were also evaluated using estimated muscle force based on varying Achilles tendon moment arms (Maganaris

et al., 2006). The estimates of *n* and *k*, when calculated for constant moment arm, or varying moment arm, were similar and none of the conclusions differed. Therefore, the conclusions from this study were not affected by the assumption of constant moment arm for these data.

An integral assumption for the models was that the muscle fascicles were considered as linear structures that lie in parallel “fascicle” planes. However, it has been shown that muscle fascicles are curvilinear (Maganaris et al., 2002; Muramatsu et al., 2002b; Wang et al., 2009; Namburete et al., 2011, Rana et al., 2013), with the curvature being necessary to maintain mechanical stability within the muscle (van Leeuwen and Spoor, 1992) and the curvature changing with contraction state (Kawakami et al., 1998; Maganaris et al., 2002; Muramatsu et al., 2002b; Namburete et al., 2011; Namburete and Wakeling, 2012). Measuring fascicles as linear rather than curvilinear structures in 2D ultrasound images can lead to errors of up to 6% in fascicle length (Muramatsu et al., 2002b). It has previously been noted that the assumption of fascicles lying in planar sheets hinders the modelling of muscle belly mechanics and it is expected that fascicles should follow 3D trajectories that move away from the fascicle planes (van Leeuwen and Spoor, 1992). Recent studies have used 3D imaging to confirm this is indeed the case (Rana and Wakeling, 2011). Nonetheless, in a 3D study, Rana and co-workers (2013) showed that pennation angles for the MG and LG during contraction calculated from 2D ultrasound images (as per the methods in this study) would be less than 1 ° in error when compared to their actual 3D values.

The models in this study were motivated by the macroscopic changes in structure that occur during muscle contraction. At the microscopic level, radial forces occur within the myofilament lattice (Maughan and Godt, 1981; Cecchi et al., 1990) that depend on the myofilament spacing (Williams et al., 2010, 2012) and so it is unlikely that the myofilaments expand or contract asymmetrically in radial directions. It is possible that muscle fibres could show asymmetric bulging in a radial direction even if this does not occur at the myofilament level, due to a non-uniform distribution of cytoskeletal elements (Neering et al., 1991) and the movement of intracellular fluid from the myofilament lattice into the intermyofilament space during contraction (Cecchi et al., 1990). Indeed, recent evidence indicates that fascicle bulging may be asymmetric during contraction (Wakeling and Randhawa, 2014). Furthermore, changes in the shape of a muscle belly can be dissociated from changes in the depth and width of its constituent fibres due to the

changes in its fascicle lengths, orientations and 3D trajectories. Despite the complexities of the shape changes to the fascicles, even the simplest 1D model that we tested here (equation 3) resulted in very good predictions of the pennation for the MG and LG based solely on the muscle fascicle length.

Chapter 3.

Transverse strains in muscle fascicles during voluntary contraction: a 2D frequency decomposition of B-mode ultrasound images

This paper was published as Wakeling, J. M., & Randhawa, A. (2014). Transverse strains in muscle fascicles during voluntary contraction: a 2D frequency decomposition of B-mode ultrasound images. *International Journal of Biomedical Imaging*, Volume 2014, Article ID 352910, 9 pages http://dx.doi.org/10.1155/2014/352910.

Author contributions: A.R. and J.M.W. conceived and designed the study. J.M.W. designed the analytic approach. A.R. collected and analyzed the experimental data. Both A.R. and J.M.W. interpreted the results of experiments and drafted the manuscript. Both authors approved the final version for publication.

3.1. Introduction

Muscle fibres are nearly incompressible (Baskin and Paolini, 1967), and so must increase in girth as they shorten. This transverse expansion requires that the fibres in pennate muscle rotate to greater pennation angles during shortening to ensure they still pack together in close proximity (Alexander, 1982; Maganaris et al., 1998). Due to these fibre rotations, the fibres shorten at a lower velocity than the muscle belly in a process known as muscle belly gearing (Brainerd and Azizi, 2005; Wakeling et al., 2011; Randhawa et al., 2013), promoting a greater force and power production from the muscle. Understanding how muscle fibres change shape during contraction will inform how structural mechanisms affect the functional output of muscle.

It is commonly assumed that whole muscles maintain a constant volume during contraction, in a similar manner to their constituent fibres. Many muscle models are one-dimensional and thus assume constant thickness of the muscle belly (Maganaris et al., 1998; Alexander and Vernon, 1975; Zajac, 1989; Delp and Loan, 1995; Van den Bogert, 2011). Some studies have modelled muscle as 2D structures, but have implemented a

constant area assumption (Randhawa et al., 2013; Zuurbier and Huijing, 1992; Epstein and Herzog, 1998; Van Leeuwen, 1992), and other studies of 3D properties implement constant or nearly incompressible volumes (Otten and Hullinger, 1995; Azizi et al., 2002; Oomens et al., 2003; Blemker et al., 2005). However, whole muscle may change volume to a greater extent than fibres, due to a variable amount of blood that may pool and be pumped out from the muscle, through the action of the muscle contraction (Sheriff and van Bibber, 1998). Additionally, recent imaging studies have shown that muscle varies in thickness in a complex and muscle-specific manner. Muscle thickness is not constant during contraction, and can vary for both isometric (Maganaris et al., 1998) and dynamic (Wakeling et al., 2011; Randhawa et al., 2013; Azizi et al., 2008) contractions.

The belly gearing within a muscle can vary according to the mechanical demands of the contraction (Wakeling et al., 2011; Randhawa et al., 2013; Azizi et al., 2008), and so the fibres may exist at a range of different pennation angles for a given fibre length: it has been suggested that this variability is related to the load and stretch of connective tissue such as aponeurosis (Randhawa et al., 2013; Azizi et al., 2002; Azizi et al., 2008). Currently we do not know how the changes in transverse fibre dimensions relate to dynamic changes in fibre geometry, belly gearing and thus the functional output of the muscle.

Recent developments in muscle imaging have allowed the longitudinal properties of muscle fibres to be determined. Diffusion-tensor MRI can identify the longitudinal direction of muscle fibres (Damon et al., 2002; Heemskerk et al., 2009; Kan et al., 2008; Lansdown et al., 2007; Levin et al., 2011) allowing fibres to be tracked and their length calculated. However, MRI imaging necessitates prolonged, isometric contractions and thus is not suitable for dynamic studies of gearing. B-mode ultrasound imaging of muscle allows the fascicles to be imaged at faster rates, and a range of automated approaches have been used to quantify the fascicle lengths and even curvatures during dynamic contractions (Rana et al., 2009; Namburete et al., 2011; Darby et al., 2011; Gillett et al., 2013). Neither these MRI nor ultrasound techniques have allowed the width of the fascicles, or a measure of their transverse expansion to be quantified. However, muscle fascicles appear as nearly parallel, repeating bands within B-mode ultrasound images and the width of these bands can potentially be extracted by frequency decomposition of the images. The purpose of this study was to develop a method to extract information on the spatial frequencies of the fascicular structure within the muscle belly from B-mode

ultrasound images, and to relate this information to the fascicle size, shape and orientations during muscle contraction.

3.2. Methods

Six male subjects took part in this study (age 28.8 ± 5.5 years; mass 78.3 ± 6.2 kg; height 178 ± 2.3 cm; mean ± s.d.). All subjects provided informed consent in accordance with requirements from the university Office of Research Ethics.

Images were acquired from the medial gastrocnemius (MG) and lateral gastrocnemius (LG) of the right leg during ankle plantarflexion contractions. Subjects were seated on a dynamometer (System 3, Biodex, New York, USA) with their knee held at 135 °, their shank horizontal and their foot secured to a footplate on the dynamometer. The central axis of the dynamometer was aligned to meet the axis through the medial and lateral maleoli. Subjects performed cyclic ankle extensions against isotonic loads, and in time to the beat of a metronome. The dorsiflexion torque was limited to 0.5 N m, and three plantarflexion conditions were presented (5@0.42, 25@0.35 and 5@16: torque [N m] @ cycle frequency [Hz]); each condition had a 15 ° range of motion from 5 to 20 ° plantarflexion. Each trial consisted of 10 cycles of contraction, from which the middle 5 were analyzed.

The MG and LG muscle bellies were imaged using 128-element (60 mm width) linear array B-mode ultrasound probes (Echoblaster 128, Telemed, Lithuania), scanning at 40 Hz. The probes were aligned to the fascicle planes to obtain nearly continuous lines for the fascicles in each image. The probes were secured to the leg using custom mounts with adhesive and elasticized bandages. The probes measured from the MG and LG simultaneously, and were synchronized to the position P and torque data T from the dynamometer (recorded at 1000 Hz: USB-6229, National Instruments, Austin, TX, USA).

Each ultrasound frame formed a square image $f(x, y)$ of $N = 512$ pixels per side with each greyscale pixel indexed by its x- and y-coordinate (Figure 3-1). Images were manually digitized (ImageJ software, NIH, Maryland, USA) to identify three coordinates on the superficial aponeurosis, three coordinates on the deep aponeurosis and two coordinates on a representative fascicle. Aponeuroses were described using second-order polynomials that were fit to both the superficial and the deep coordinates using least-

squares minimization, and the muscle belly thickness L_y was calculated as the mean distance between the aponeuroses. The fascicle inclination θ_d within the fascicle plane was given by the angle between the *x*-axis and the vector between the two digitized fascicle points. The fascicle length L_f was given by the length of the linear line passing through the fascicle coordinates that intersected the best-fit linear lines through the superficial and deep aponeuroses.

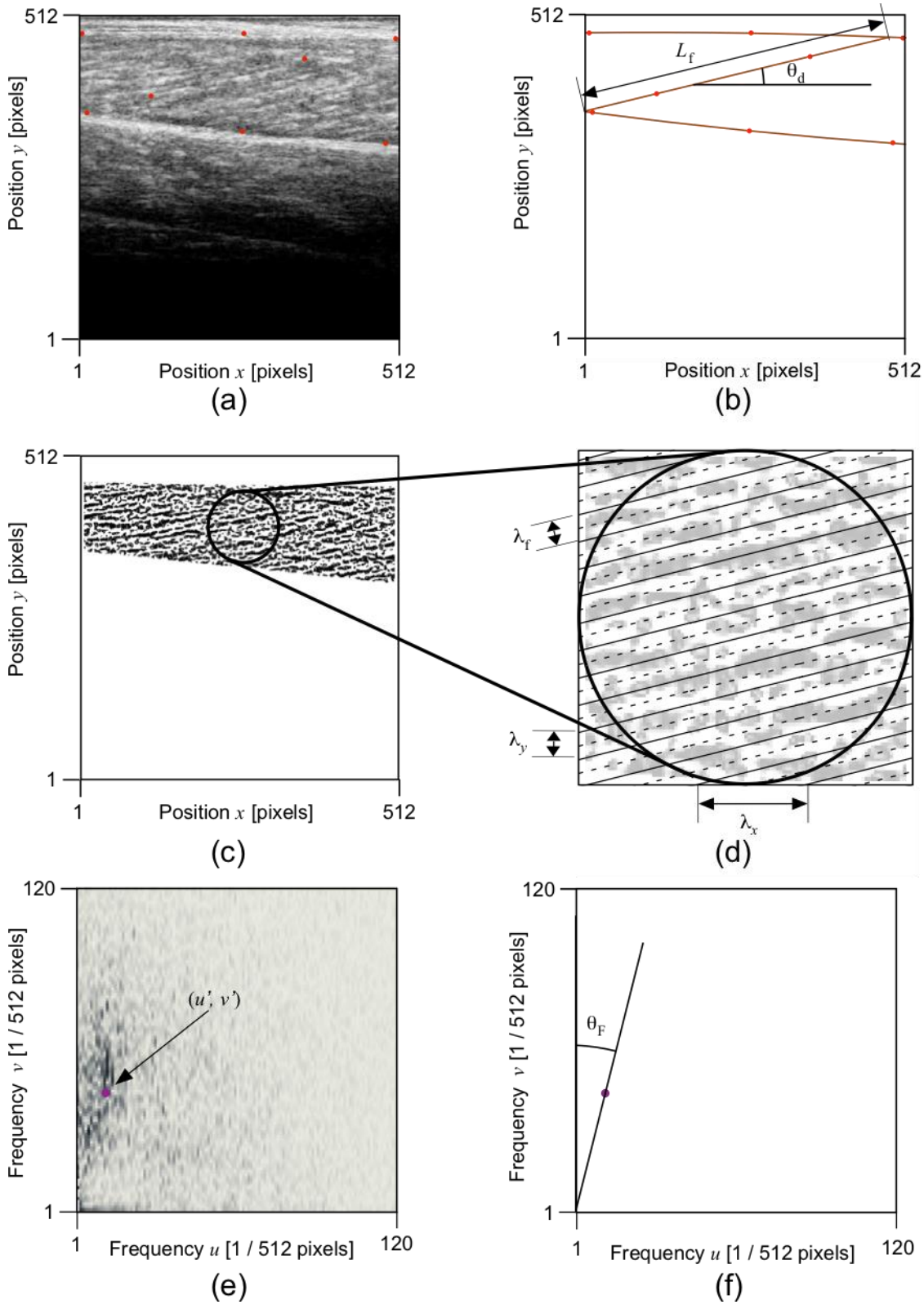

Figure 3-1. The analysis method.

Coordinates on the superficial and deep aponeuroses and a representative fascicle were manually digitized (red points) for each ultrasound image (A) and used to calculate the fascicle length L_f and inclination angle θ_d relative to the *x*-axis (B). Fascicles were enhanced using multi-scale vessel enhancement filters and the region of interest determined between the aponeuroses (C). The repeating fascicular nature is described by its transverse wavelength λ_f, that can be resolved into wavelengths λ_u and λ_v that are in the *x*- and *y*- directions, respectively (D). The spatial frequencies *u* and *v* were determined using a Discrete Fourier Transform, and the major spatial frequencies characterized by the moment of frequency (*u'*, *v'*) (E). The inclination angle θ_F was determined from the major spatial frequencies (F), and the wavelengths λ_u and λ_v calculated from these frequencies.

Each image was filtered using multiscale vessel-enhancement filtering. This method enhances the tubular structures in the image that are formed by the fascicles (Frangi et al., 1998), and is capable of resolving tubular structures of different radii, and has previously been applied to B-mode ultrasound images (Rana et al., 2009; Namburete et al., 2011; Rana et al., 2013). Here we followed Rana and co-workers (Rana et al., 2009) by using scales of 1.5, 2, 2.5 and 3. The region of interest was taken as the area of muscle tissue within the filtered image that was bounded by the aponeuroses, and a strip 10 pixels wide was removed inside the aponeuroses to ensure that the region of interest contained no features that were aligned with the aponeuroses.

Muscle fascicles appear as dark lines in the image and connective tissue between the fascicles appears as bright structures that parallel the fascicles (Rana et al., 2009). The striped nature of the fascicles is enhanced and retained within the filtered image and be characterized by the spatial frequency of the stripes. The spatial frequencies $F(u, v)$ of the filtered image $f(x, y)$ were determined by a 2D Discrete Fourier analysis of the region of interest, where:

$$F(u,v) = \frac{1}{N}\sum_{x=0}^{N-1}\sum_{y=0}^{N-1} f(x,y)\left[Cos\left(\frac{2\pi(ux+vy)}{N}\right) + jSin\left(\frac{2\pi(ux+vy)}{N}\right)\right]$$

and,

$$j = \sqrt{-1},$$

The amplitude spectra for the region of interest describe the amplitudes of the pixel intensities across a range of frequencies:

$$|F(u,v)| = \sqrt{\mathrm{Re}^2(u,v) + \mathrm{Im}^2(u,v)}$$

This is reduced to a single frequency value for each direction (*u′* and *v′*) using the m^{th} moment of frequency:

$$u' = \frac{\sum_{u=b_1}^{b_2}\sum_{v=b_1}^{b_2}\left[|F(u,v)|^m u\right]}{\sum_{u=b_1}^{b_2}\sum_{v=b_1}^{b_2}|F(u,v)|^m},$$

and

$$v' = \frac{\sum_{v=b_1}^{b_2}\sum_{u=b_1}^{b_2}\left[|F(u,v)|^m v\right]}{\sum_{v=b_1}^{b_2}\sum_{u=b_1}^{b_2}|F(u,v)|^m},$$

The moments of frequency were calculated across the frequency range of $b_1 = 4$ to $b_2 = 120$, and this contained more than 99% of the power of the amplitude spectra.

The wavelengths for the fascicle stripes λ_x and λ_y were given by:

$$\lambda_x = \frac{1}{u'} \qquad \text{and} \qquad \lambda_y = \frac{1}{v'}$$

The dominant repeating structure within the region of interest is given by the muscle fascicles. For large inclinations (≈ 90 °) λ_x would be small and λ_y would be large; conversely, for small inclinations (≈ 0 °) λ_x would be large and λ_y would be small. The fascicle inclination θ_F (relative to the *x*-direction) can be determined from the Fourier analysis as follows:

$$\theta_F = \mathrm{ArcTan}\left(\frac{\lambda_y}{\lambda_x}\right)$$

The best value for *m* was determined by comparing θ_d and θ_F for $1 \le m \le 8$ (see Statistics section below).

The wavelengths λ_x and λ_y reflect the dominant characteristics of the repeated fascicles in the region of interest. Not only do they provide information about the fascicle inclination, but also on the wavelength of the "fascicle stripes" λ_f, i.e. the wavelength of the stripes in a transverse direction across the fascicles:

$$\lambda_f = \lambda_x \mathrm{Sin}\,\theta_F$$

The muscle belly thickness L_y, fascicle length L_f and the wavelength λ_f were normalized by their respective means that occurred throughout the five contraction cycles to yield normalized terms $\hat{L}_y$, $\hat{L}_f$, and $\hat{\lambda}_f$, respectively.

Pixel brightness in each ultrasound image are a measure of the echogenicity of the material being scanned. It is possible that as the muscle expands in a transverse direction, there is an uneven expansion of fascicular and connective tissue. This would result in a change in the distribution of pixel brightness within the region of interest. This possibility was examined by quantifying the mean pixel brightness B_p within the region of interest.

The best value for m was determined from the correlation coefficient r and the root-mean-square error (RMSE) between θ_d and θ_F for each contraction sequence. The effect of m on r and RMSE was determined with ANOVA with subject (random), muscle and condition as factors (Minitab v16, Minitab Inc., State College, PA, USA).

For each condition the time ω was normalized to each contraction (0 to 360 °), with 0 ° occurring at the mid-point of each dorsiflexion movement. The parameters P, T, $\hat{L}_f$, $\hat{L}_y$, θ_d, θ_F, $\hat{\lambda}_f$, and B_p were each described by a Fourier series of the form:

$$c_1 + a_1 \mathrm{Sin}(\phi_1 + \omega) + a_2 \mathrm{Sin}(\phi_2 + 2\omega),$$

where the coefficients c_1, a_1, and ϕ_1 describe the mean value, the amplitude and the phase for the first harmonic. The effect of subject (random), muscle, condition, parameter and a muscle-by-parameter interaction on these Fourier coefficients was determined using ANOVA.

Statistical tests were considered significant at the $\alpha = 0.05$ level. Mean values are reported as mean ± standard error of the mean.

3.3. Results

Subjects performed a series of isotonic plantarflexions (Figure 3-2), with the ankle plantarflexion torque increasing during each plantarflexion. The fascicle length within the medial and lateral gastrocnemius shortened during each plantarflexion, and this coincided with an increase in the inclination angle of the fascicles. During fascicle shortening the thickness of the both the fascicles and muscle belly increased, with the relative increases in the muscle belly thickness being greater than those for the fascicles. During each contraction cycle, the pixel intensity within the region of interest varied, with the lowest intensities occurring when the fascicles were shortest but thickest.

The estimates of the inclination angle based on the Fourier transform, were dependent on the moment of frequency, *m*, selected. There was no significant effect of m on the correlation between the inclination angle determined by manual digitization, θ_d, and the inclination angle determined from the discrete Fourier transform, θ_F, however, there was a significant effect of *m* on the root-mean-square error between these values (Figure 3-3). A value of *m* = 5 resulted in close to the greatest correlation and lowest RMSE, and so was selected for further analysis. When considered across all subjects, muscles and contraction conditions, the RMSE for *m* = 5 was 3.4 º. The error between the two measures of inclination was partly due to the smaller amplitude of change in inclination for the θ_F than for θ_d.

The ANOVA showed there was a significant effect of the muscle, subject, parameter and muscle-by-parameter interaction on the amplitude of the cyclic changes, a_1. The main effects from the ANOVA (Figure 3-4) showed that the a_1 for MG was 0.41 greater than for LG. The interaction effect showed that a_1 for θ_d for the MG was greater than for the LG, however this effect was not seen for θ_F. The magnitude of the parameter effects on a_1 can be seen in Table 3-1 and Table 3-2.

The ANOVA showed there was a significant effect of the subject, parameter and muscle-by-parameter interaction on the phase of the cyclic changes, o_1. The interaction effect showed that o_1 for $\hat{\lambda}_f$ was slightly smaller, and for $\hat{L}_y$ was slightly larger for the MG than for the LG: in other words, there was a greater phase difference between the cycles of fascicle thickness and muscle belly thickness for the MG than for the LG. The magnitude of the parameter effects on a_1 can be seen in Table 3-1 and Table 3-2: there was no

significant difference in the phase difference between $\hat{L}_y$, θ_d and θ_F. When the phase for fascicle length was offset by 180 º (o_1 + 180 º) there was no significant difference between its phase and those for $\hat{L}_y$, θ_d and θ_F, and so the timing of fascicle length shortening exactly matches the increases in fascicle thickness.

Table 3-1. Fourier coefficients for the medial gastrocnemius.

Parameter	MG		
	c_1	a_1	o_1
P	−13.06 ± 0.20°	7.93 ± 0.19°	−1.4 ± 2.1°
T	7.59 ± 1.05 N m	21.30 ± 1.91 N m	252.7 ± 3.4°
$\hat{L}_f$	1.00 ± 0.00	0.22 ± 0.02	29.7 ± 2.9°
$\hat{\lambda}_f$	1.00 ± 0.00	0.017 ± 0.002	182.6 ± 9.2°
θ_d	17.10 ± 0.45°	5.34 ± 0.46°	215.0 ± 2.8°
θ_F	15.86 ± 0.27°	1.64 ± 0.14°	217.8 ± 3.6°
$\hat{L}_y$	1.00 ± 0.00	0.023 ± 0.003	286.7 ± 13.2°
B_p	146.27 ± 4.72	7.21 ± 0.48	38.4 ± 4.3°

Values are shown as mean ± s.e.m. (n = 6), and are for the first harmonic of the Fourier series.

Table 3-2. Fourier coefficients for the lateral gastrocnemius.

Parameter	LG		
	c_1	a_1	o_1
P	−13.06 ± 0.20°	7.93 ± 0.19°	−1.4 ± 2.1°
T	7.59 ± 1.05 N m	21.30 ± 1.91 N m	252.7 ± 3.4°
$\hat{L}_f$	1.00 ± 0.00	0.19 ± 0.02	36.2 ± 5.4°
$\hat{\lambda}_f$	1.00 ± 0.00	0.015 ± 0.001	209.3 ± 7.0°
θ_d	9.23 ± 0.57°	2.54 ± 0.34°	219.7 ± 5.4°
θ_F	11.40 ± 0.49°	1.62 ± 0.27°	216.6 ± 4.8°
$\hat{L}_y$	1.00 ± 0.00	0.027 ± 0.003	262.1 ± 16.4°
B_p	148.62 ± 4.17	7.22 ± 0.96	33.4 ± 5.5°

Values are shown as mean ± s.e.m. (n = 6), and are for the first harmonic of the Fourier series.

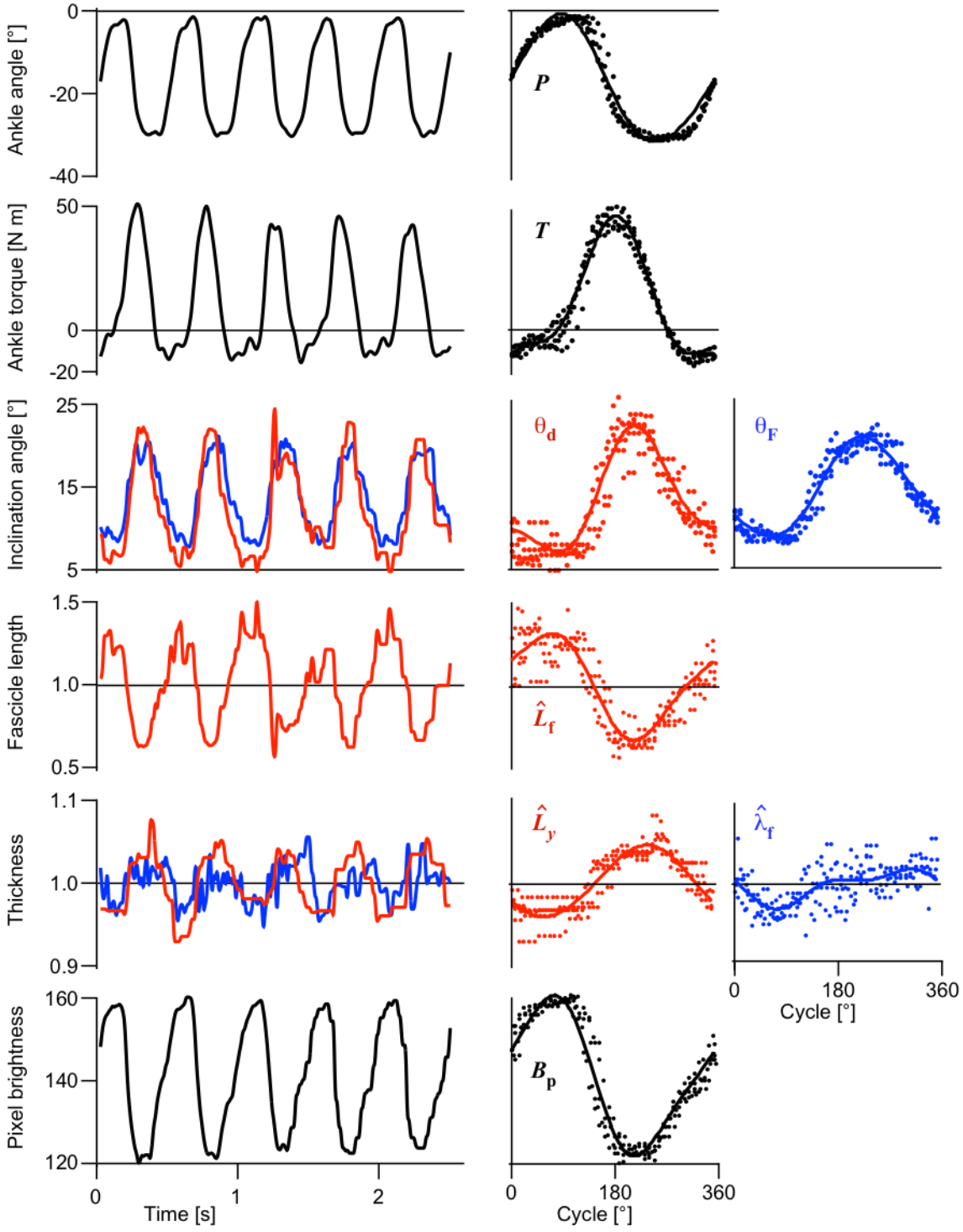

Figure 3-2. Muscle structural data for the lateral gastrocnemius during one set of ankle plantarflexions.

The first column shows the parameters changing over five contraction cycles. The middle and right columns show these data expressed as a percentage of the contraction cycle, and show individual points as well as the smooth model calculated from Fourier series. Parameters determined from manual digitization are shown in red, parameters determined following the Discrete Fourier Transform are shown in blue. $\hat{\boldsymbol{\lambda}}_{\mathbf{f}}$ was calculated with m = 5.

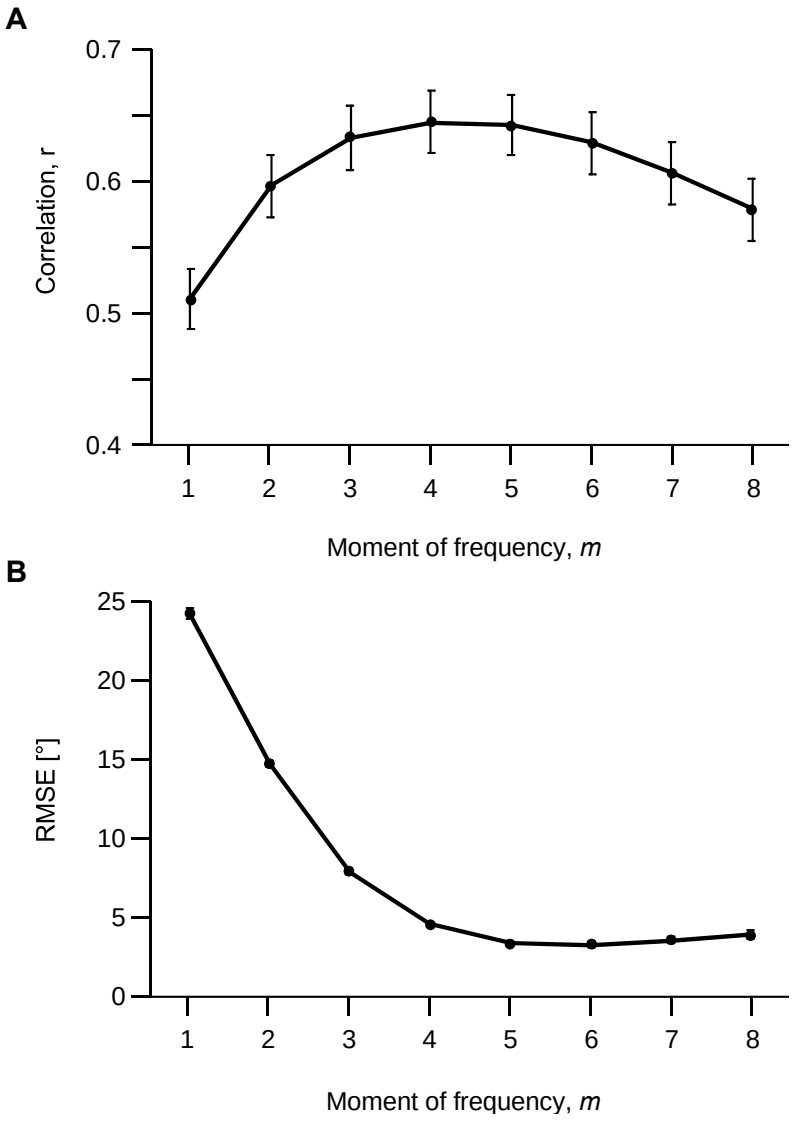

Figure 3-3. Error analysis for the selection of the moment of frequency, m. The correlation between the inclination angle determined by manual digitization, θ_{d}, and the inclination angle determined from the discrete Fourier transform, θ_{F} is shown for different values of m (A). The root-mean-square error between these terms is shown in (B). Points show the mean ± s.e.m. (n = 99).

3.4. Discussion

This study shows that there is information within B-mode images of the muscle bellies that has spatial frequencies that change in a cyclical manner during repeated contractions. These spatial frequencies are due to the fascicular (or vessel-like) structures within the muscle that were resolved by the multi-scale vessel enhancement filtering (Frangi et al., 1998). 2D information from the images was retained by the 2D Discrete Fourier Transform of the images, and allowed the inclination angle of the muscle fascicles to be determined, θ_F: this is a feature of the fascicles that could be validated against the manually determined inclination angles, θ_d (Figure 3-3).

A perfect match between θ_d and θ_F should not be expected. When ultrasound images are manually digitized, the inclination angles tend to reflect the dominant fascicle features within the image (Rana et al., 2009). However, there is variation of fascicle orientations across each image (Namburete et al., 2011), and sometimes non-fascicular features that may also occur in the image, and these features would influence the spatial frequencies determined by automated methods that consider the whole region of interest (Rana et al., 2009) such as the discrete Fourier transform as used in this study. The accuracy in these automated approaches can be maximized by careful selection of images that contain minimal non-fascicular structures (Rana et al., 2013) or by masking the undesired features within the region of interest. The inclinations θ_d and θ_F in this study measured the angles between the fascicles and the *x*-axis of the ultrasound images. By contrast, pennation angles measured in previous ultrasound studies are defined in different ways, eg. the angle between the fascicle and the superficial aponeurosis, or the deep aponeurosis or the mean direction of the superficial and deep aponeuroses (Maganaris et al., 1998; Kawakami et al., 1998; Narici et al., 1996; Wakeling et al., 2006). In this study, the θ_F was approximately 13 º and 8 º for the MG and LG, respectively, for an ankle plantarflexion angle of 5 º (calculated from data in Table 3-1 and Table 3-2), and these are approximately 5 º smaller than the pennations reported for seated subjects in the same dynamometer (Randhawa et al., 2013).

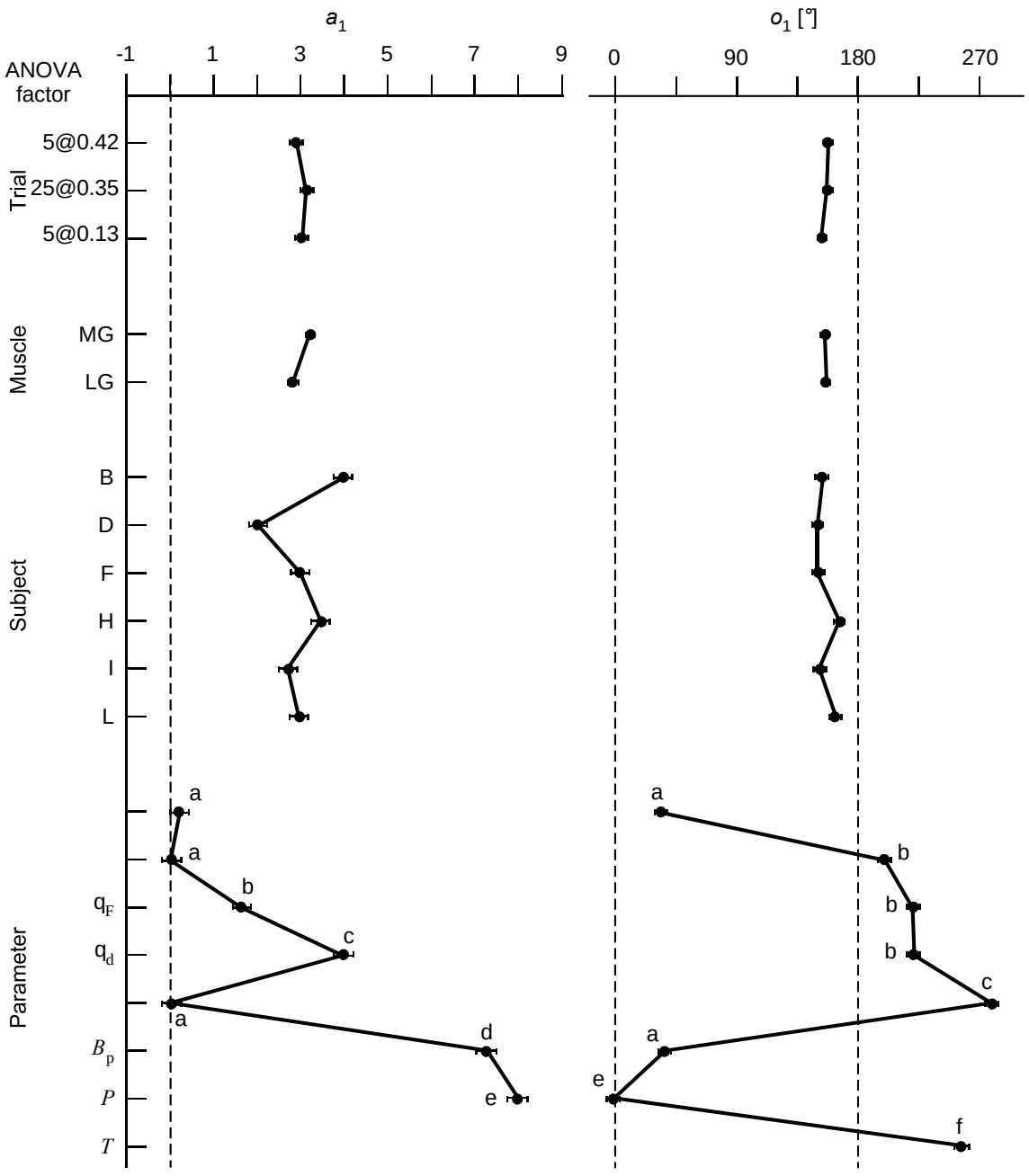

Figure 3-4. Main effects determined by ANOVA.
The effects of the experimental factors on the coefficients a_1 and o_1 for the first harmonic in the Fourier series are shown. Points show the least-square means ± s.e.m. as determined by the ANOVA. a_1 for torque was not tested due to its magnitude being much larger than the other variables. Letters next to the symbols indicate parameters that were not significantly different from each other, as calculated in a post-hoc Tukey analysis.

The transverse wavelength of the fascicle strains $\hat{\lambda}_f$ changed in a cyclical manner, in time with the fascicle shortening (Table 3-1; Table 3-2; Figure 3-4). As the fascicles shorten their transverse strain increased. The mean pixel brightness also decreased as the transverse strain increased (Table 3-1; Table 3-2; Figure 3-2; Figure 3-4), indicating a greater proportion of darker elements in the image for higher $\hat{\lambda}_f$. Within the muscle bellies, the fascicles and connective tissue have different echogenicities, with the fascicles appearing darker. It is possible that the increase in B_p with increased $\hat{\lambda}_f$ indicates that the transverse strain in the muscle fascicles is underestimated by $\hat{\lambda}_f$ (that includes elements from both fascicles and connective tissue).

The transverse strain was calculated by resolving λ_x and λ_y into the transverse direction. In theory, these values could be resolved into the longitudinal direction to provide a measure of longitudinal fascicle strain, however this is practically not possible. In an ideal ultrasound image, all the fascicles would appear as continuous lines between the two aponeuroses: these would have a longitudinal spatial frequency of less than 1 / 512 pixels, and therefore would be beyond the resolution of the technique. In reality, fascicles appear as partial lines between the aponeuroses, and the exact length of each line segment is very sensitive to the exact orientation of the fascicles relative to the scanning plane. During contraction the fascicles can change their orientation relative to the scanning plane (Rana et al., 2013), and thus fluctuations in line-length would reflect their 3D orientation as well as the fascicle length, and therefore preclude measurements of fascicle length using these methods.

Assuming that the muscle fibres (and presumably the fascicles) maintain a constant volume during contraction (Baskin and Paolini, 1967), then they must increase in girth as they shorten. If an additional assumption is made that the increase in girth for the muscle fascicles is radially symmetrical then the muscle fascicles should have a Poisson ratio of 0.43 for a longitudinal strain of 0.2, where the Poisson ratio is the ratio of the transverse strain/longitudinal strain. The Poisson ratio ν can be calculated from this study as the ratio of (a_1 for $\hat{\lambda}_f$)/ (a_1 for $\hat{L}_f$). The mean ν from this study was 0.09 $\pm$ 0.01, and was thus much smaller than expected. As discussed above, it is possible that $\hat{\lambda}_f$ is an underestimate, leading to low ν. An alternative estimate for the transverse strain for the fascicles can be calculated from the manually digitized parameters. If it is assumed that

the entire muscle belly consists of fascicles that are parallel to each other, then the distance between the aponeuroses must equal the width of the fascicles acting in parallel, adjusted by their inclination; thus the normalized fascicle thickness will equal $\hat{L}_y$ / Cos θ_d. This alternative estimate of fascicle thickness yields a mean ν of 0.20 $\pm$ 0.02 that is still less than expected. Data from this study thus indicate that increases in the transverse width of the fascicles does not meet that expected for isovolumetric muscle fibres that show radial symmetry in their expansion in girth. It will be necessary to investigate the fascicular expansion in the direction perpendicular to the scanning plane to identify the reasons for this discrepancy.

Changes to muscle belly thickness occur with both changes in fascicle thickness, and fascicle rotations to different pennation angles (Azizi et al., 2008), with the fascicle thickness and pennation angle being related to each other via intramuscular pressure, transverse forces and compliance in connective tissues (Azizi et al., 2002) such as aponeuroses and intramuscular connective tissue (Huijing, 2003). It is possible that the differences in whole-muscle bulging between MG and LG that have been reported in previous studies (Maganaris et al., 1998; Wakeling et al., 2011; Randhawa et al., 2013; Azizi et al., 2008; Narici et al., 1996) may reflect differences in the direction of the transverse or perpendicular (out of plane) bulging of the fascicles, or due to differences in connective tissue properties and the tendency for the fascicles to rotate. In this study we found similar transverse expansion and Poisson ratio of the fascicles occurring in both the MG and LG (Table 3-1; Table 3-2), thus indicating that differences in the bulging of the muscle belly are caused more by differences in connective tissue properties and the tendency for the fascicles to rotate than by differences in the fascicle bulging *per se*.

This study describes a method to determine the transverse strain in the muscle fascicles during contraction, and is the first study to describe these strains during dynamic and voluntary contractions. However, it should be noted that this methodological study has been constrained to a small set of contractions performed by male subjects: it will be important to understand how transverse bulging of the fascicles changes with both age and gender. Nonetheless, the results show that increases in transverse width are exactly timed with the reductions in the longitudinal length of the fascicles. Surprisingly, the magnitude of the transverse strains, as imaged within the ultrasound scanning planes, appears smaller than expected. However, the imaging methods preclude the measurement of strains perpendicular to the ultrasound scans. Fully 3D studies are

needed to explore the exact nature of shape changes to the fascicles during contraction, and to relate these to the mechanisms of muscle contraction.

Chapter 4.

Transverse anisotropy in the deformation of the muscle during dynamic contractions

This paper was published as Randhawa, A., & Wakeling, J. M. (2018). Transverse anisotropy in the deformation of the muscle during dynamic contractions. *Journal of Experimental Biology*, jeb-175794.

Author contributions: A.R. and J.M.W. conceived and designed the experiment. A.R. collected and analyzed the experimental data. Both A.R. and J.M.W. interpreted the results of experiments and drafted the manuscript. Both authors approved the final version for publication.

4.1. Introduction

Muscles are made up of fibre bundles called fascicles that actively generate force through their actin-myosin interactions. In pennate muscle, fascicles are oriented at an oblique angle to the line-of action of the muscle and run between sheets of connective tissue that form the aponeuroses. When pennate fascicles contract and shorten a component of their force acts to draw the aponeuroses together and decrease the belly thickness; however the fascicles will tend to increase in thickness to remain at a relatively constant volume leading to an increase in their pennation and a contrasting tendency to increase the aponeurosis separation (Millard et al., 2013; Zajac, 1989; Millard et al., 2013; Baskin and Paolini, 1967). The actual change in the overall transverse deformation depends on the balance of these effects plus additional factors that include the contribution of the stiffness of the extracellular matrix and compression from forces external to the muscle. Changes to the internal geometry of contracting muscle is thus a complex and multifactorial phenomenon.

In order to simplify the geometrical representation of muscle, many models assume that the belly thickness remains constant during contraction (Zajac, 1989; Delp et al., 2007; van den Bogert et al., 2011; Millard et al., 2013; Rajagopal et al., 2016; Randhawa and Wakeling, 2015). This allows a straightforward prediction of fascicle pennation given a fascicle length, however such models do not allow us to understand the

mechanisms by which shape changes influence muscle mechanics and the internal structure of muscles (Randhawa and Wakeling, 2015; Dick and Wakeling, 2018). Studying changes in the transverse belly deformation is functionally important as it can influence both fascicle strains (Azizi and Deslaurens, 2014) and tendon strains (Farris et al., 2013) and the resultant forces generated by the muscle. Understanding the interaction of the whole muscle shape to the fascicle deformations and geometry requires both 3D information of the deformations and a 3D mechanistic framework to describe the system.

Contracting muscles interact with adjacent muscles and surrounding tissues via both the myofascical connections between muscles (Huijing et al., 1998) and pressures exerted on surrounding tissues due to their tendency to bulge. For instance, connective tissues linking the aponeuroses of human soleus and gastrocnemii muscles (Kinugasa et al., 2013; Hodgson et al., 2006) may transmit force between these muscles (Bojsen-Møller et al., 2010) leading to a decrease in the relative displacement of *soleus* and *lateral gastrocnemius* (LG) with increased activity during knee flexion (Finni et al., 2017). Additionally, transverse load acting on muscles, which may be caused by transverse expansion of adjacent muscle bellies or externally applied forces, can cause substantial decreases in the longitudinal forces developed by a muscle belly (Siebert et al., 2017, 2014). Thus, understanding how muscles expand and impinge on each other is important to understanding muscle force development and function.

The *medial gastrocnemius* (MG) and the LG show contrasting changes in transverse deformation of the muscle belly during contraction (Maganaris et al., 1998; Randhawa et al., 2013; Randhawa and Wakeling, 2013), despite their anatomical and functional similarities. While the LG increases in thickness during plantarflexion, the belly of the MG thins as it shortens (Randhawa et al., 2013). As a muscle belly shortens in length, it should expand transversely in order to conserve volume (Zajac, 1989; Millard et al., 2013; Abbott and Baskin, 1962; Baskin and Paolini, 1967). Therefore, if the MG muscle belly shortens and decreases in thickness, it must increase in the width-wise direction that is orthogonal to length and thickness. Recent modelling studies that predicted asymmetry in the transverse belly deformations suggested that such asymmetries at the muscle belly level may be reflected by asymmetries in the transverse deformations of its constituent fascicles (Rahemi et al., 2015; Randhawa and Wakeling, 2015). To date there are no data to describe asymmetries in fascicle deformation during active contraction of skeletal

muscle, and so we hypothesized that such asymmetries would be observed during active contractions.

3D imaging of muscle and estimation of fascicle trajectories has been achieved in a number of MRI studies (Blemker and Delp, 2005; Heemskerk et al., 2009; Wokke et al., 2014; Mercuri et al., 2005), but these are largely limited to passive tissue due to the long scan times required for the image acquisition. Diagnostic ultrasound provides a more rapid scanning duration (Maganaris and Paul, 2000; Rana et al., 2013), allowing active muscle contractions to be tracked, and has recently been used to quantify transverse deformations in the fascicles during contraction from 2D ultrasound images (Wakeling and Randhawa, 2014). Combining this approach with 3D tracking of the ultrasound probe (Prager et al., 1998; Rana and Wakeling, 2011) should allow the 3D deformations in contracting muscle fascicles to be tracked.

The purpose of this study was to identify if asymmetries in the transverse deformations of muscle fascicles occur during active contractions of two pennate muscles, the LG and MG. We used a dual-probe ultrasound imaging technique to scan the contracting fascicles from orthogonal directions by tracking the position and orientation of the two probes. Using this technique, we quantified the 3D deformations of both the muscle belly and the fascicles during cyclic plantarflexion contractions.

4.2. Methods

4.2.1. Subjects

Six male and six female physically active university students participated in this study (age 28.8 ± 5.5 years; mass 78.3 ± 6.2 kg; height 178 ± 2.3 cm; mean ± s.d.). All subjects provided informed consent in accordance with requirements from the University Office of Research Ethics.

4.2.2. Dynamometer Tests

Subjects were seated on a dynamometer (System 3, Biodex, New York, USA) with a fixed knee angle of 163.8 ± 3.4 º determined using a goniometer, horizontal shank and foot secured to a footplate using Velcro straps (Figure 4-1 (A)). The central axis of the

dynamometer was aligned to the plantarflexion axis of the ankle, and the foot was held in a neutral position with respect to in/eversion and internal/external rotation. Subjects performed cyclic plantarflexion-dorsiflexion isokinetic contractions with the plantarflexion phase at maximal effort, and the dorsiflexion phase at minimal effort. Subjects began each series of contractions with their ankle at 15 ° dorsiflexion, each trial consisted of 8 cycles of plantarflexion, ending at a limit of 25 ° plantarflexion that was set on the dynamometer (Figure 4-1 (B)). Thus, the total ankle range of motion was 40 °. Dorsiflexion movements were velocity limited to 60 º s^{-1}. Five plantarflexion velocities were tested: 10, 45, 90, 150, 210 º s^{-1}, in a randomized order with one minute rest between trials. Ankle angle and ankle torque from the dynamometer were recorded at 1 kHz using a 16-bit data-acquisition system (USB-6229; National Instruments, Austin, TX, USA). The muscle bellies of the *medial gastrocnemius* (MG) and *lateral gastrocnemius* (LG) were imaged using B-mode ultrasound during these plantarflexion movements.

4.2.3. Bi-planar Ultrasound Imaging

Biplanar ultrasound imaging was performed on each of the two gastrocnemii muscles. This imaging involved simultaneous ultrasound scans from two linear array probes that scanned in orthogonal directions, and where the intersection of the scanning planes occurred within the muscle of interest (Figure 4-1 (B)). Each ultrasound probe was aligned to scan nearly continuous fascicles, and the scanning planes approximated the frontal and medial planes of the lower leg.

Ultrasound scans were acquired using 128-element (60 mm field-of-view, 50 mm depth and 7 MHz frequency) linear array B-mode ultrasound probes (Echoblaster 128, Telemed, Lithuania) scanning at 40 Hz. Each probe was fixed within a rigid body frame that was attached to a triad of LED markers (total of 6 LED markers). An optical motion capture system (Certus Optotrak, NDI) tracked the 3D positions of these LEDs at 100 Hz, and this was used to determine the relative orientations of the ultrasound scanning planes, and their line of intersection after prior calibration (Prager et al., 1998; Rana and Wakeling, 2011). Each probe and its marker triad was attached to a tripod. Tilting the tripod head allowed the probe to be aligned to the muscle of interest (Figure 4-1 (B)). The average angle between the two scanning planes was 88 º for the MG and 90 º for the LG, which was calculated from the angle between their normal vectors, and was averaged across all time-points for all trials. Pressure on the skin applied by the ultrasound probe can affect

muscle structure (Bolsterlee et al., 2015). This pressure artifact was minimized by using a water-filled latex balloon placed between each ultrasound probe and the skin (Figure 4-1 (B)). The balloon was secured on the probe using cable ties, and acoustic coupling ultrasound gel was placed between the balloon and both the skin and the probe surface. The balloon provided a continuous and deformable contact surface with the skin allowing for unrestricted skin motion and minimal contact pressure. The two ultrasound systems recorded simultaneously, and their trigger signals were used to synchronize all the data. The MG of the right leg was tested first followed by testing the LG of the left leg.

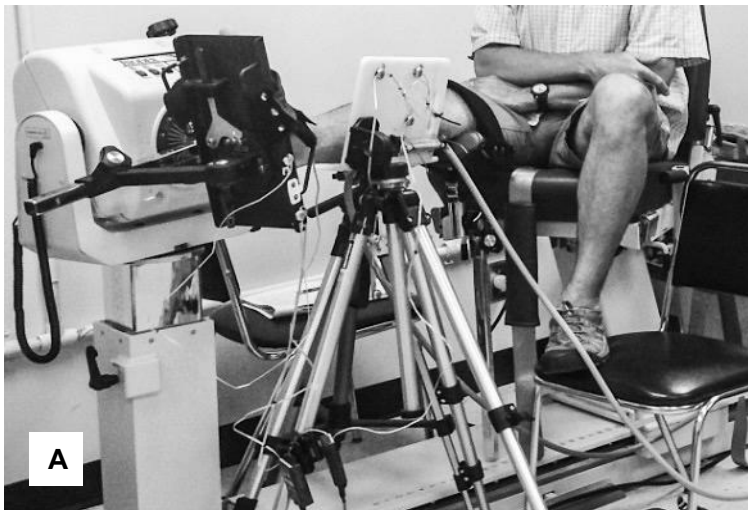
A

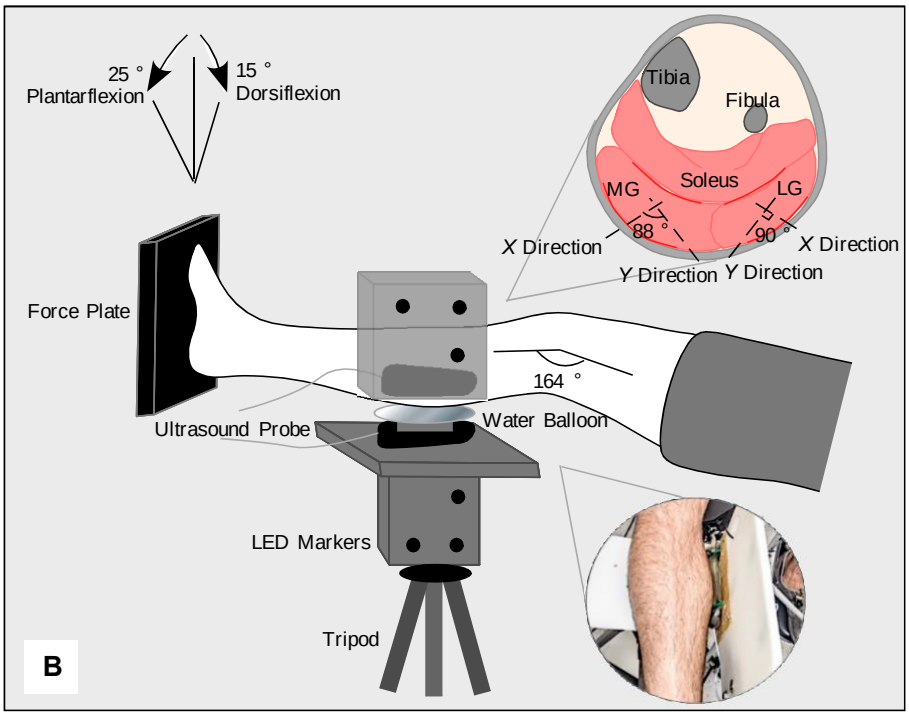
25 °
Plantarflexion
15 °
Dorsiflexion
Tibia
Fibula
Soleus
MG
LG
17 °
88 °
90 °
X Direction
X Direction
Y Direction
Y Direction
Force Plate
164 °
Ultrasound Probe
Water Balloon
LED Markers
Tripod
B

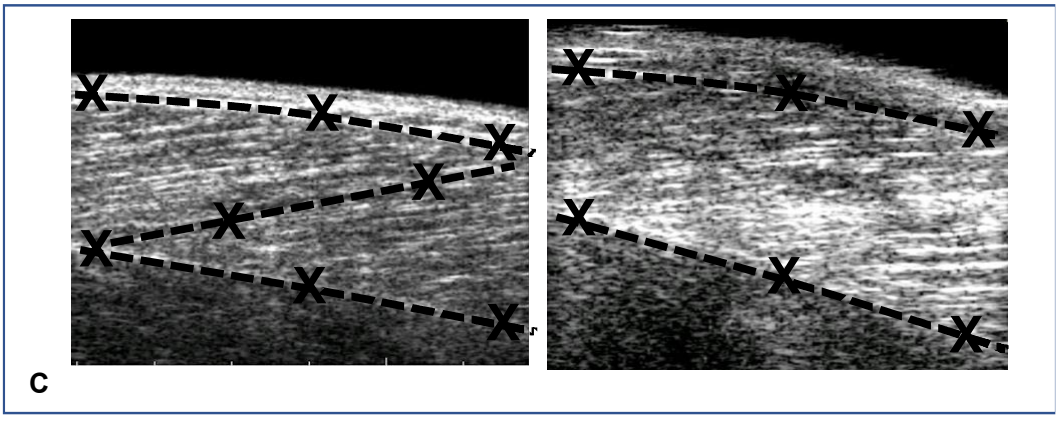
C

Figure 4-1. Procedure for quantifying muscle structural changes using dual-probe ultrasound technique during plantarflexions on a dynamometer.

(A) Experimental setup for measuring time varying *in vivo* changes in muscle structure during isokinetic plantarflexions on a dynamometer in the *medial gastrocnemius* of the right leg. Note: similar setup was used to test the *lateral gastrocnemius* of the left leg. (B) During each isokinetic condition, subjects generated eight cycles of maximal plantarflexion contractions from a dorsiflexed position. The dynamometer measured plantarflexion torques and ankle angles. Structural parameters were acquired using two ultrasound probes scanning the muscle from two orthogonal directions. A tripod was used to secure each probe in position. 3 LED markers attached rigidly to each ultrasound probe allowed their position and orientation to be measured using an optical motion capture system (Certus Optotrak, NDI, Waterloo, Canada) that is an integrated system containing 3 cameras that were tracking markers at 100 Hz. The optical motion capture system was positioned close to the dynamometer facing the left side of the subject's body. A water balloon between the skin surface and the ultrasound probe ensured minimal alteration of the skin and muscle by external pressure. All data were synchronized using triggers from the two ultrasound systems. (C) Ultrasound images from two orthogonal directions showing placement of coordinate points during manual digitization for the *medial gastrocnemius* muscle.

4.2.4. Ultrasound Image Processing

In each image the muscle belly off interest was segmented by identifying the region of interest. Three coordinates were manually digitized on each of the superficial and deep boundaries of the muscle (ImageJ software, NIH, Maryland, USA): these boundaries correspond to the aponeuroses for the slices that intersected the aponeurosis regions of the muscle (Figure 4-1 (C)). The probe orientation that most closely approximated the typical orientation used in two-dimensional ultrasound studies was considered to scan the *XZ* plane and was used to calculate the pennation; the images from this scanning view displayed the greatest changes in fascicle pennation. The second ultrasound probe scanned the muscle belly in an orthogonal *YZ* plane (Figure 4-1 (B)). The line of action of the muscle belly was considered the *Z* direction, and the longitudinal axis of the fascicles was considered the *z* direction.

Second-order polynomials were fit to the digitized points on the superficial and deep muscle boundaries using least-square minimization. Two further points were digitized on a prominent fascicle in each image: fascicle length was approximated from the linear line passing through the fascicle coordinates that intersected the polynomials on the muscle boundary (Figure 4-1 (C)). Pennation angle was the mean of the angles made by the intersection of the fascicle and the aponeuroses in the *XZ* plane. The

thickness of the muscle belly was the shortest distance from superficial to deep aponeurosis through the centre of the measured fascicle in the *XZ* plane.

Ultrasound images of the muscle bellies were further processed to calculate transverse fascicle deformations in the following manner. Multi-scale vessel enhancement filtering was used to enhance the vessel-like features in the muscle images that were depicted as alternating dark stripes (muscle fascicles) and light stripes (connective tissue), using scales of 1.5, 2, 2.5 and 3 pixels (Rana et al., 2009; Frangi et al., 1998). The region of interest of muscle tissue was segmented using the polynomials describing the muscle boundaries, and was eroded by 10 pixels to ensure features were of muscle fascicles and not the bright lines of the boundaries.

Spatial frequencies corresponding to the fascicular stripes were calculated for the regions of interest using 2D discrete Fourier transforms (Wakeling and Randhawa, 2014), with the frequency distributions being reduced to characteristic frequencies using their 5^{th} moments of area (Wakeling and Randhawa, 2014). These characteristic frequencies were converted to wavelengths in the *x-z* and *y-z* directions from the different scanning planes, and subsequently normalized to the mean transverse wavelength across all cycles for that muscle and subject. Image analysis was performed using custom-written code (Mathematica v. 7.0, Wolfram Research), and data were analyzed for the third to seventh plantarflexion cycles in each sequence of eight cycles.

4.2.5. Statistical Analysis

The kinematic parameters – ankle angle and ankle torque, and muscle parameters - pennation β, 'projected' belly length in *Z* direction $L_{b,Z}$, fascicle length in *z* direction $L_{f,z}$, belly transverse deformation in the *X* direction $L_{b,X}$, belly transverse deformation in the *Y* direction $L_{b,Y}$, fascicle transverse deformation in the *x* direction $L_{f,x}$, and fascicle transverse deformation in the *y* direction $L_{f,y}$; each changed in a cyclic manner over time and so were described by Fourier series (Wakeling and Randhawa, 2014). Fourier series is an effective way to extract the important features from cyclic data, whilst removing noise. Each contraction cycle was interpolated to an angle ω between 0 to 360 ° with 0 ° occurring at the midpoint of each dorsiflexion movement. Each parameter was described by a Fourier series of the form:

$$c_1 + a_1 Sin(o_1 + \omega) + a_2 Sin(o_2 + 2\omega)$$

where the coefficients c_1, a_1, and o_1 were the mean value, the amplitude of the cyclic changes, and the phase for the first harmonic, respectively. The first harmonic described the majority of the form of the cycles and was used for further statistical analysis, whereas the second harmonic values contain information on details of the waveforms and are included for future reference in Table 4-1. General linear model analyses of variance (ANOVA; Minitab v18, Minitab Inc., State College, PA, USA) were conducted for MG and LG to determine if differences in these Fourier coefficients for L_b and L_f differed between their *X-Y*, and *x-y* directions, respectively, or between isokinetic conditions, and subjects (random factor). The isokinetic velocity conditions were found to have no effect on the parameters tested, therefore all five conditions were pooled together. The parameters L_b and L_f were normalized to their mean value across all trials for each subject, and are denoted by $\hat{L}_b$ and $\hat{L}_f$, respectively. The 'projected' belly length was the component of L_f in the Z direction. This distance is shorter than the actual belly length, however, $\hat{L}_b$ is a close approximation to the normalized length of the muscle belly.

Differences were considered significant at the $p < 0.05$ level. Data are reported as mean ± standard error of the mean.

4.3. Results

During these series of isokinetic plantarflexions, the ankles of right and left leg moved through similar range of motion and generated similar ankle torque for both MG and LG during muscle shortening (Table 4-1). The ankle torque showed phasic increases during each plantarflexion, with the peak plantarflexion torque decreasing with angular velocity of the ankle.

During each series of contractions, the bellies of MG and LG muscles shortened during the plantarflexion phase in a similar manner (Table 4-1), and the MG and LG muscle fascicles shortened and rotated to greater pennation angles (Figure 4-2; Figure 4-3). The mean pennation for the MG (c_1) of 27 ° was greater than for the LG at 17 ° (Table 4-1) and this coincided with the MG showing a greater change in pennation (a_1), and change in fascicle length.

Table 4-1. Fourier coefficients for the medial gastrocnemius (MG) and the lateral gastrocnemius (LG).

Parameter	Ultrasound Probe	c_1	a_1	o_1	a_2	o_2
			MG muscle			
Ankle Angle (°)		-8.27 ± 0.69	18.42 ± 0.50	28.24 ± 2.86	7.07 ± 0.49	349.79 ± 4.40
Ankle Torque (N m)		23.87 ± 2.88	36.50 ± 2.93	301.35 ± 3.99	12.70 ± 1.29	274.18 ± 11.77
Pennation, β (°)	*XZ* Plane	27.42 ± 0.66	7.98 ± 0.44	264.90 ± 4.15	3.34 ± 0.304	217.21 ± 12.32
Belly Length, $\hat{L}_{b,Z}$	*Z* Direction	1.00 ± 0.011	0.394 ± 0.018	73.41 ± 3.14	0.151 ± 0.014	28.94 ± 9.26
Belly Deformation, $\hat{L}_{b,X}$	*X* Direction	1.00 ± 0.003	0.030 ± 0.002*****	10.09 ± 9.87*	0.017 ± 0.001*****	346.10 ± 11.55
Belly Deformation, $\hat{L}_{b,Y}$	*Y* Direction	1.00 ± 0.006	0.046 ± 0.005*****	58.62 ± 13.29*	0.025 ± 0.003*****	360.33 ± 16.82
Fascicle Length, $\hat{L}_{f,z}$	*z* Direction	1.00 ± 0.009	0.314 ± 0.016	73.21 ± 3.21	0.129 ± 0.013	31.82 ± 9.04
Fascicle Deformation, $\hat{L}_{f,x}$	*x* Direction	1.00 ± 0.002	0.029 ± 0.002*****	235.06 ± 11.32*	0.013 ± 0.001	189.81 ± 14.007
Fascicle Deformation, $\hat{L}_{f,y}$	*y* Direction	1.00 ± 0.001	0.021 ± 0.002*****	251.30 ± 9.79*	0.013 ± 0.001	227.87 ± 11.92
			LG muscle			
Ankle Angle (°)		-7.76 ± 0.86	18.18 ± 0.59	23.78 ± 3.45	6.24 ± 0.52	349.01 ± 5.32
Ankle Torque (N m)		24.89 ± 4.13	39.18 ± 2.91	306.99 ± 4.93	13.22 ± 1.60	246.89 ± 15.89
Pennation, β (°)	*XZ* Plane	17.03 ± 0.74	2.99 ± 0.29	265.58 ± 10.26	1.65 ± 0.17	217.94 ± 19.34
Belly Length, $\hat{L}_{b,Z}$	*Z* Direction	1.00 ± 0.026	0.275 ± 0.025	83.91 ± 9.01	0.124 ± 0.016	25.50 ± 17.20
Belly Deformation, $\hat{L}_{b,X}$	*X* Direction	1.00 ± 0.008	0.066 ± 0.007*****	309.71 ± 13.98	0.026 ± 0.004	297.03 ± 19.04
Belly Deformation, $\hat{L}_{b,Y}$	*Y* Direction	1.00 ± 0.005	0.034 ± 0.003*****	344.77 ± 18.04	0.020 ± 0.002	348.20 ± 18.66
Fascicle Length, $\hat{L}_{f,z}$	*z* Direction	1.00 ± 0.025	0.255 ± 0.023	83.65 ± 8.99	0.116 ± 0.015	25.90 ± 17.09
Fascicle Deformation, $\hat{L}_{f,x}$	*x* Direction	1.00 ± 0.001	0.012 ± 0.002*****	100.34 ± 10.32*	0.009 ± 0.002	158.11 ± 43.85
Fascicle Deformation, $\hat{L}_{f,y}$	*y* Direction	1.00 ± 0.001	0.021 ± 0.003*****	282.81 ± 13.38*	0.013 ± 0.002	219.33 ± 19.92

Values are shown as mean ± s.e.m. (n=12) and are for the first (o_1) and second harmonic (o_2) of the Fourier series.
*****Significant differences between *X* and *Y* directions for the belly, and *x* and *y* directions for the fascicle, as determined using ANOVA.

For the MG, the belly transverse deformation showed thinning in *X* and *Y* directions during plantarflexion while the fascicle expanded transversely in *x* and *y* directions (Figure 4-2; Figure 4-4 (B); Figure 4-4 (C)). In contrast, the LG belly expanded transversely in both *X* and *Y* directions whilst the LG fascicle decreased transversely in *x* direction and increased transversely in *y* direction during plantarflexion (Figure 4-3; Figure 4-4 (E); Figure 4-4 (F)).

There was a significant difference in the normalized amplitude of the cyclic changes, a_1, between the transverse deformation of the belly in *X* and *Y* directions, and between the transverse deformation of the fascicles in *x* and *y* directions for MG and LG (Figure 4-5; Table 4-1). In addition, for the LG the phase angle o_1 was significantly different between the two directions for the fascicle transverse deformation (by about 180 °) indicating that the transverse deformations were out-of-phase between the two *x* and *y* directions (Figure 4-5 (B)).

4.4. Discussion

4.4.1. Transverse anisotropy in muscle fascicles

The purpose of this study was to identify if transverse anisotropy in the muscle fascicles occurred during active contractions. Proving that asymmetries occur using data available from this imaging technique is an example of proof-by-contradiction. First, consider a fascicle with a circular cross-section that undergoes an asymmetrical deformation to become an ellipse with a strain of +10% along its major axis, and -5% along its minor axis. If the *x* and *y* scanning directions were aligned at 45 and 135 **°** to the major axis, respectively, then the measured strains would be $\varepsilon_x = \varepsilon_y = +2.8\%$. Thus it is possible that symmetrical strains could be calculated in the *x* and *y* directions even if the actual fascicle deformation was transversely anisotropic. However, if asymmetrical strains are calculated in orthogonal *x* and *y* directions at any alignment within a transverse section then this cannot have occurred from a transversely isotropic deformation, and this would be a proof-by-contradiction that asymmetrical fascicle expansion does occur. Whilst the data from this study do not allow us to be certain about the nature of the deformations in MG, the results from this study do, indeed, show asymmetries in the fascicle deformations for the LG, as seen by phase-relationship of their strains ε_x and ε_y differing by 180 **°** (Figure 4-4 (F); Figure 4-5 (B); Table 4-1). Thus, the data support the proof that fascicle deformations can be transversely anisotropic during active muscle contractions.

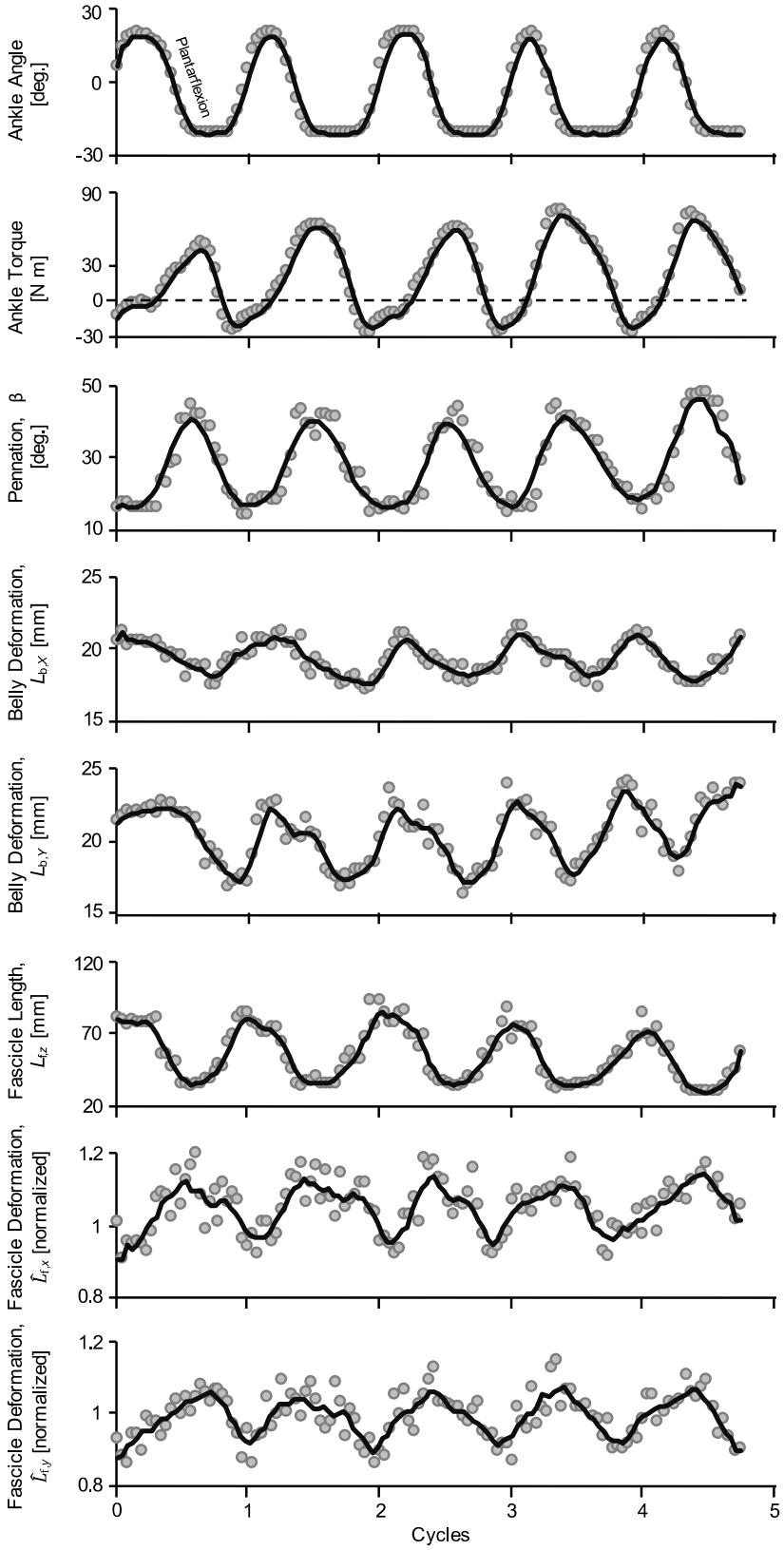
Ankle Angle [deg.]
30
0
-30
Plantarflexion
Ankle Torque [N m]
90
30
0
-30
Pennation, β [deg.]
50
30
10
Belly Deformation, $L_{b,X}$ [mm]
25
20
15
Belly Deformation, $L_{b,Y}$ [mm]
25
20
15
Fascicle Length, L_{fz} [mm]
120
70
20
Fascicle Deformation, $\tilde{L}_{f,x}$ [normalized]
1.2
1
0.8
Fascicle Deformation, $\tilde{L}_{f,y}$ [normalized]
1.2
1
0.8
0
1
2
3
4
5
Cycles

Figure 4-2. Muscle structural data for the Medial Gastrocnemius (MG) during 5 cycles of isokinetic ankle plantarflexions at 150 ° s-1.

Plots show the parameters changing over five contraction cycles for subject A. Raw traces of the ankle angle and ankle torque were acquired from the dynamometer. Structural parameters: β, $L_{f,z}$, $L_{b,X}$ and $L_{b,Y}$, were determined from manual digitization. $\hat{\boldsymbol{L}}_{f,x}$, and $\hat{\boldsymbol{L}}_{f,y}$ were determined following the discrete Fourier transform. Data are shown as individual points (grey) as well as a moving average (black).

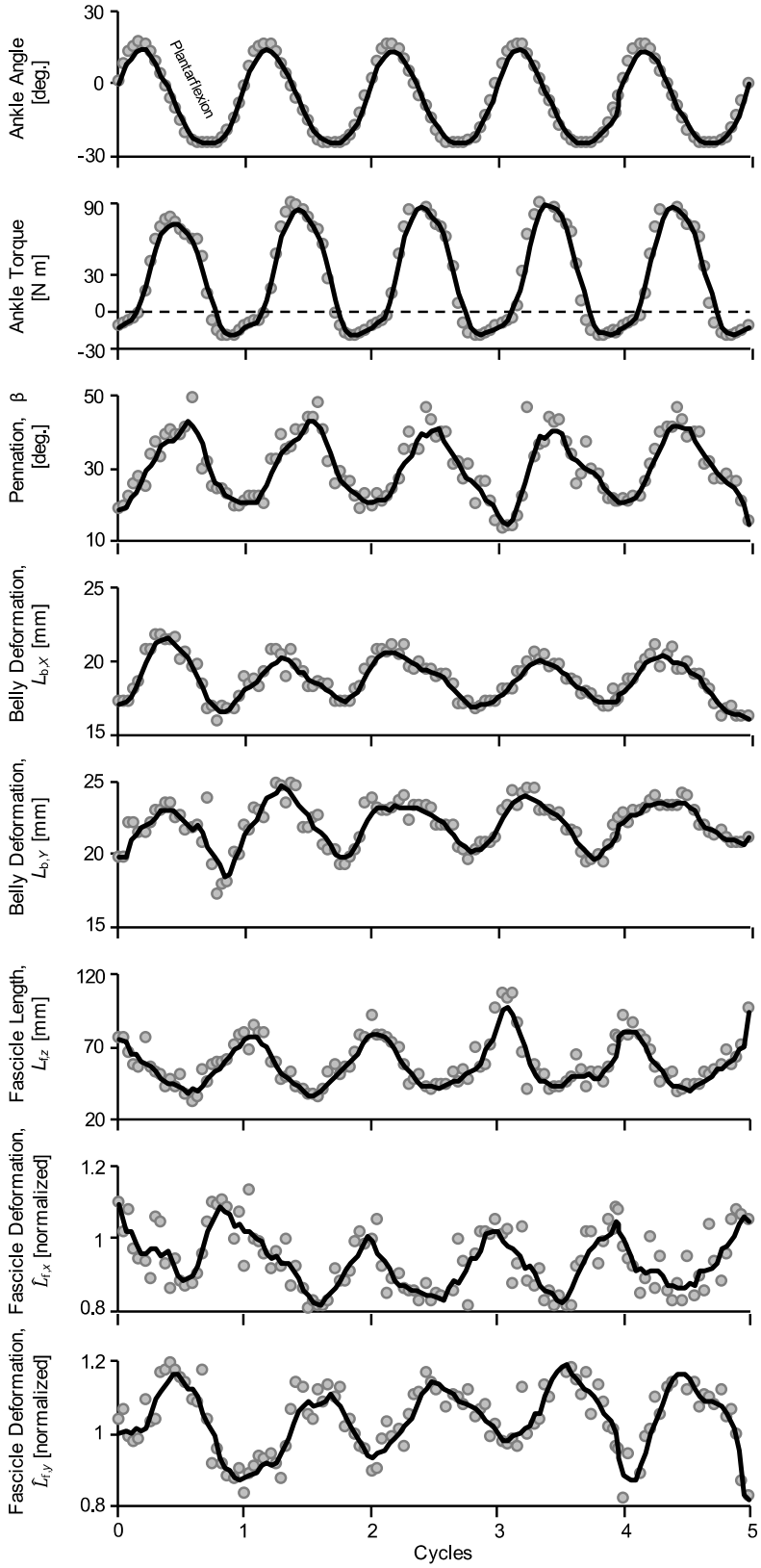
Ankle Angle [deg.]
30
0
-30
Plantarflexion
Ankle Torque [N m]
90
30
0
-30
Pennation, β [deg.]
50
30
10
Belly Deformation, $L_{b,X}$ [mm]
25
20
15
Belly Deformation, $L_{b,Y}$ [mm]
25
20
15
Fascicle Length, $L_{f,Z}$ [mm]
120
70
20
Fascicle Deformation, $\tilde{L}_{f,X}$ [normalized]
1.2
1
0.8
Fascicle Deformation, $\tilde{L}_{f,Y}$ [normalized]
1.2
1
0.8
0
1
2
3
4
5
Cycles

Figure 4-3. Muscle structural data for the Lateral Gastrocnemius (LG) during 5 cycles of isokinetic ankle plantarflexions at 90 ° s-1.

Plots show the parameters changing over five contraction cycles for subject B. Raw traces of the ankle angle and ankle torque were acquired from the dynamometer. Structural parameters: β, $L_{f,z}$, $L_{b,X}$ and $L_{b,Y}$, were determined from manual digitization. $\hat{\boldsymbol{L}}_{f,x}$, and $\hat{\boldsymbol{L}}_{f,y}$ were determined following the discrete Fourier transform. Data are shown as individual points (grey) as well as a moving average (black).

4.4.2. Factors causing transverse anisotropy within a muscle

During contraction, cross-bridge forces develop between the myosin and actin myofilaments: and these forces have a longitudinal component that acts to slide the filaments past each other and a transverse component that acts to squeeze the myofilament lattice together (Daniel et al., 2013; Williams et al., 2013). The muscle fibres are typically considered to be nearly isovolumetric (Abbott and Baskin, 1962), and so shortening caused by the longitudinal component of cross-bridge force is matched by a tendency of the muscle fibres to increase transversely in order to maintain their volume (Rahemi et al., 2014, 2015). This increase in girth is in a transverse or radial direction across the fibres, and is thus opposed by both the radial forces from the cross-bridges, and cytoskeletal structures within the muscle fibres. The cytoskeletal elements within the muscle fibres are additionally distributed in a non-uniform manner (Neering et al.,1991) and the intracellular fluid moves into the myofilament space from the myofilament lattice during contraction (Cecchi et al.,1990). Thus transverse anisotropy within the muscle fibres can even exceed transverse anisotropies that may occur in the myofilament lattice. The actual deformation of the fibres additionally depends on forces that are external to the fibres, and these external forces may derive from surrounding tissues or even be external to the body, and are transmitted through myofascial structures and the extracellular matrix. These external forces will often be directional, for instance the compressive force between sheets of aponeurosis due to the muscle fibres drawing them together (Rahemi et al., 2014; Azizi et al., 2008), or external forces where the body contacts the environment (Holt et al., 2016; Wakeling et al., 2013; Siebert et al., 2017). Thus there would be an asymmetry to the stress distribution through the muscle that would likely cause deformations in the fibres that are transversely anisotropic (Rahemi et al., 2014, 2015).

Muscle fascicles are bundles of fibres that create the striations seen in the ultrasound image. Fascicles additionally contain the extracellular matrix (ECM), blood vessels, nerves and intramuscular fat and are surrounded by the perimysium membrane.

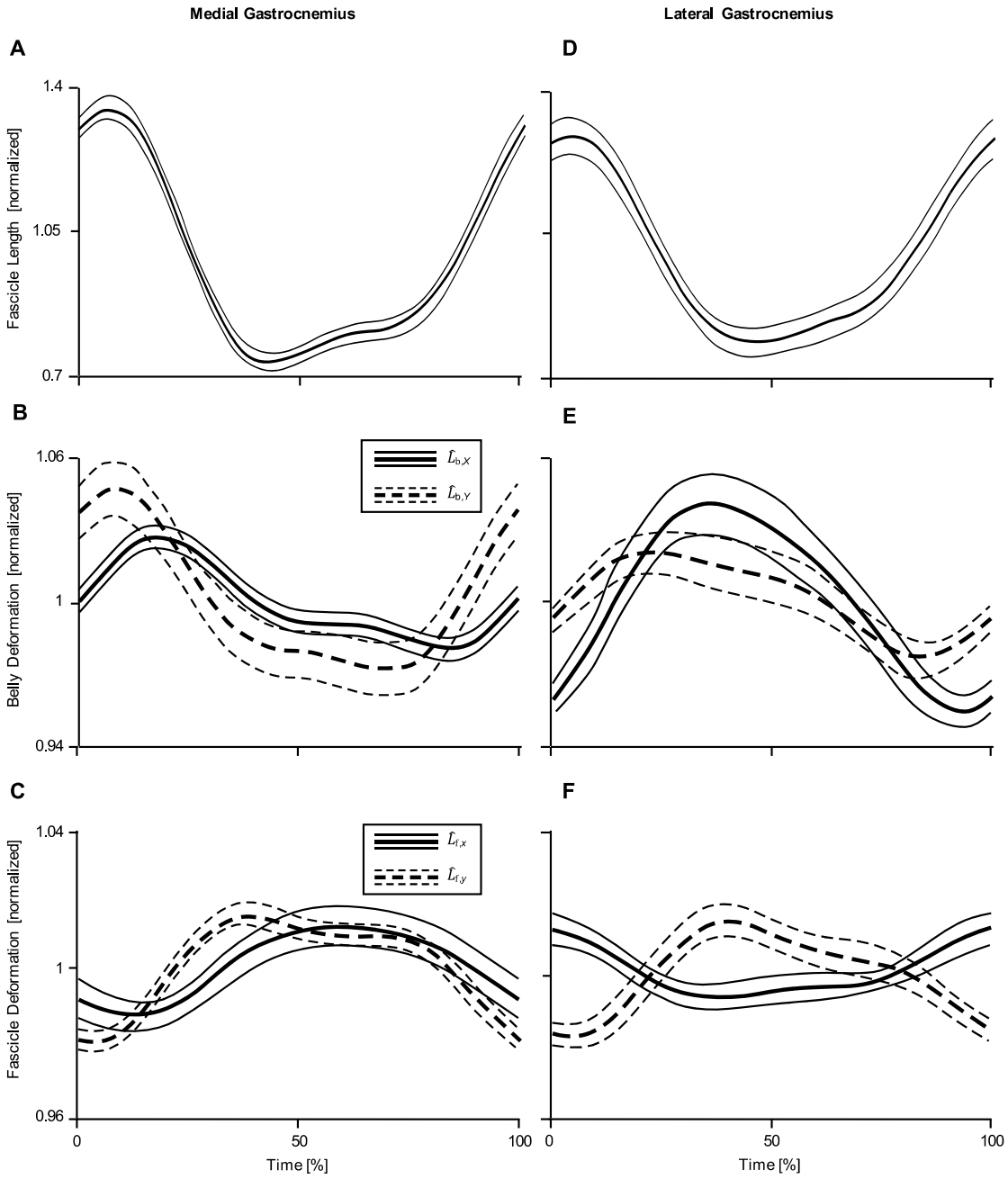

Figure 4-4. Comparison of orthogonal belly and fascicle changes from the two gastrocnemii muscles during plantarflexion.

Plots show time-varying comparisons for changes in $L_{f,z}$, $\hat{\boldsymbol{L}}_{b,X}$, $\hat{\boldsymbol{L}}_{b,Y}$, $\hat{\boldsymbol{L}}_{f,x}$, and $\hat{\boldsymbol{L}}_{f,y}$ from the MG (A,B,C) and the LG (C,D,E). Data are pooled across all subjects for all isokinetic plantarflexions and averaged over five contraction cycles. Data are shown as the mean ± s.e.m., n=12 subjects.

Thus, the material properties of the ECM and fluid movement within the fascicle can influence deformations in the fascicle that are additional to the deformations of their constituent fibres (Karakuzu et al., 2017; Yucesoy, 2010; Yucesoy and Huijing, 2007). A recent MRI study on muscle shape showed small decreases in volume as the muscle was passively stretched (Bolsterlee et al., 2017), although it was noted that these volume changes were within the realm of measurement error. However, this ratio of the changes in volume relative to longitudinal strain was of a similar magnitude to the changes in volume reported for the ECM, measured optically on the dissecting microscope, during passive stretch when larger magnitude displacements were used (Smith et al., 2011). When the muscle is active, increases in intramuscular pressure may additionally occlude blood flow in a process known as the skeletal muscle pump (Kagaya and Muraoka, 2005), and so it is not unreasonable to expect that changes to the fascicle volume may occur. Such changes in volume and fluid movement within the fascicle may again occur in a transversely anisotropic fashion due to similar stress asymmetries as discussed for the muscle fibres above.

The muscle belly encloses the space available for the muscle fascicles. As the fascicles shorten they act to draw the aponeuroses together, which tends to decrease the belly thickness. However, the fascicles increase in girth during shortening. The increase in girth may be in either the width or thickness direction, and indeed the relative deformations may vary between muscles (Randhawa and Wakeling, 2015). However, a general effect is for the muscles to increase in pennation to allow them to fit within the enclosed space (Zuurbier and Huijing, 1992; Fukunaga et al., 1997). This increase in pennation would tend to increase the distance of the muscle belly between the aponeuroses. Thus the actual change in transverse deformation of the muscle belly depends on the balance between fascicle shortening and rotation, on compliance within the connective tissues such as the aponeurosis itself (Rahemi et al., 2014; Holt et al., 2016; Azizi et al., 2008; Azizi and Roberts, 2009) and on forces external to the muscle (Siebert et al., 2017). Previous studies have shown that the MG and LG show opposing changes in thickness with the MG decreasing or maintaining a steady thickness (Maganaris, 1998; Randhawa et al., 2013; Randhawa and Wakeling, 2013) and the LG increasing in thickness (Maganaris et al., 1998; Wakeling et al., 2011; Azizi et al., 2008; Randhawa et al., 2013) during muscle belly or MTU shortening. This exemplifies the complexity that causes variations in the thickness of pennate muscle. Transverse

deformations of the muscle belly in other directions (Böl et al., 2013; Stark and Schilling, 2010) need to balance the changes in length, depth, width and maintenance of volume, and so deformations of the muscle belly may also be transversely anisotropic (Azizi et al., 2008; Randhawa et al., 2013; Rahemi, 2015).

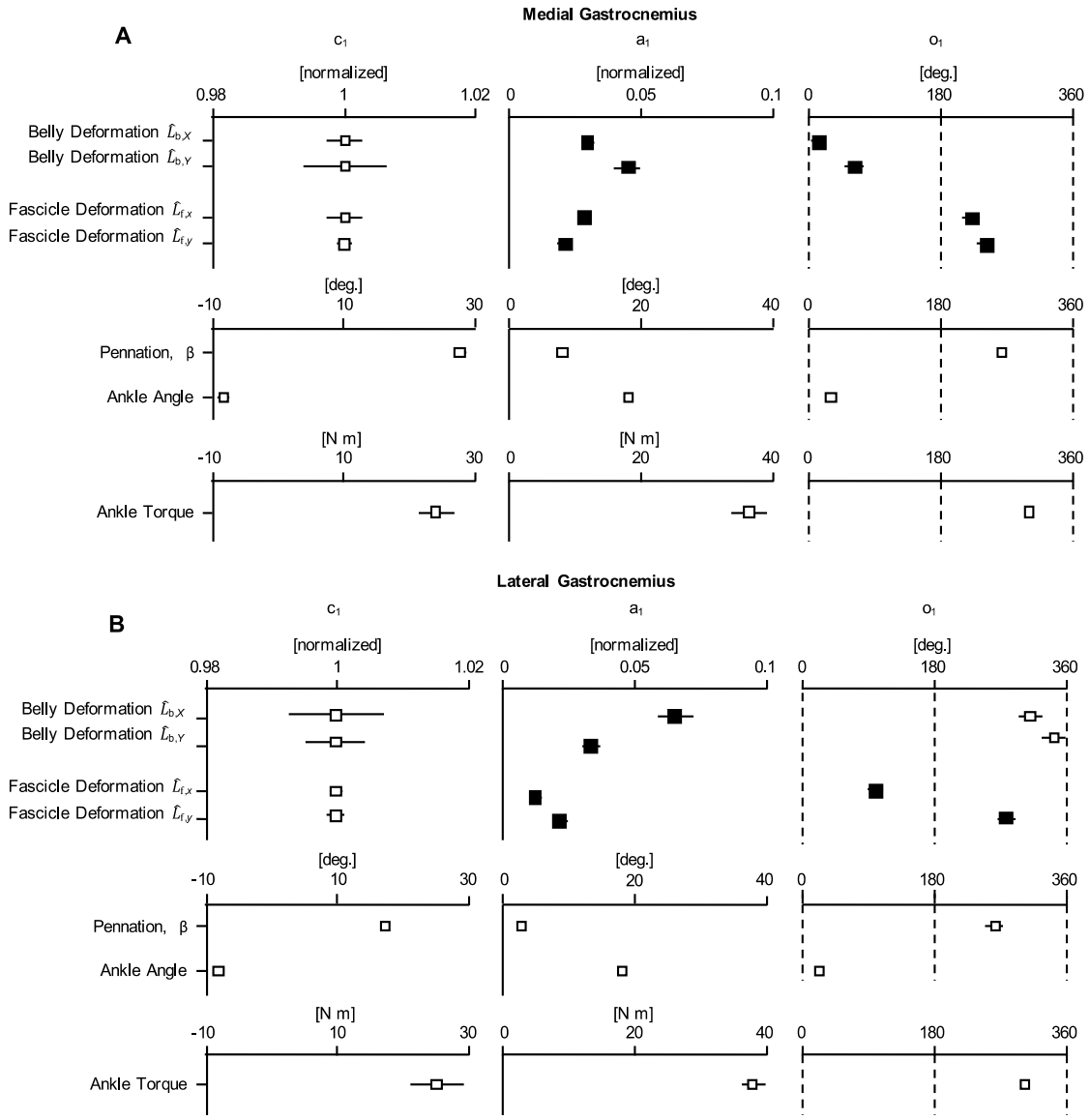

Figure 4-5. The effects of structural parameters on the coefficients c1, a1 and o1 for the first harmonic in the Fourier series are shown for the two gastrocnemii muscles.

Data points show the mean (boxes) ± s.e.m. (horizontal bars) from the MG (A) and the LG (B). For these parameters, solid symbols indicate coefficients that were significantly different between the two ultrasound views (ANOVA: $p<0.05$). *n* = 12 subjects.

4.4.3. Transverse anisotropy within the gastrocnemius muscles

This study showed transverse anisotropy for the contracting fascicles of the LG. The LG fascicles decreased in length by 36% on average and increased in pennation by 4.4 ± 0.45 ° during these contractions. The LG fascicles thinned in their *x* direction and expanded in their *y* direction (Figure 4-4 (E); Figure 4-4 (F)), with these transverse deformations being almost totally out-of-phase. By contrast, the MG fascicles decreased in length by 31% and increased in pennation by 8.0 ± 0.44 ° but the fascicles decreased in both their transverse *x* and *y* directions (Figure 4-4 (C); Figure 4-4 (D)). However, following the proof-by-contradiction arguments above, using these data we can not be sure whether transverse deformations in the MG fascicles were asymmetrical or not, however, the presence of transverse anisotropy in the LG fascicles demonstrates that this is clearly a feature that can occur during active muscle contraction. Studies in the past have predicted (Randhawa and Wakeling, 2015) and measured (Wakeling and Randhawa, 2014) transverse expansions of muscle fascicles, however, the extent of these changes in comparison to longitudinal shortening of fascicles were smaller than predicted. Here we found a similar result: a 33% decrease in fascicle length led to change in transverse deformation of 3% and 1.2% in *x* direction and 2.1% and 2.1% in *y* direction for the MG and LG, respectively. Similar discrepancies in fascicle length and transverse deformations were observed in muscle models during maximal and submaximal muscle contractions (Rahemi et al., 2014, Randhawa et al., 2013).

The theory described above relates stress asymmetries within the muscle to asymmetries in the transverse deformations of the fascicles. Muscle stresses and intramuscular pressures will be greatest during maximal contractions and lowest when the muscle is relaxed. Indeed, during passive muscle length changes the reduced or absent stress asymmetries may not be sufficient to cause transverse anisotropy in the muscle fascicles. Thus, these findings may not be evident in studies of passive muscle, and indeed pilot work from this study did not reveal transverse anisotropy at the fascicle level during passive muscle length changes.

In this current study, the LG belly showed transverse bulging between the aponeurosis (ε_X = +7%) whereas the MG belly decreased by ε_X = -3% during muscle shortening. These results are consistent with previous studies that have shown LG belly thickening transversely during isometric tasks, isotonic tasks and during cycling

(Maganaris et al., 1998; Wakeling et al., 2011; Azizi et al., 2008; Randhawa et al., 2013) and the MG belly thinning transversely during isokinetic and cycling tasks (Randhawa et al., 2013; Randhawa and Wakeling, 2013).

Deformations of the muscle belly in the *Y* direction were similar to those in *X* direction, with LG ε_Y = +3%, and MG ε_Y = -5%. The magnitude of the belly deformations in *X* and *Y* directions was significantly different (Figure 4-4; Table 4-1), although the phase was similar. These differences in magnitude support the hypothesis that transverse anisotropy occurs at the level of the muscle bellies of the LG and MG during *in vivo* active dynamic muscle contraction, although this effect is less pronounced than for their muscle fascicles.

The results for the MG are somewhat surprising, because the muscle belly within the scanning region of the ultrasound transducers appears to be shortening in all three directions. However, proximal movement of a muscle's volume during shortening can alter the shape of muscles by decreasing the cross-section in some regions of the muscle while simultaneously increasing the cross-section in adjacent regions as seen in both human and rabbit muscle (Raiteri et al., 2016; Böl et al., 2013). The ultrasound transducer used in this study had a linear field of 60 mm that may only be about one third of the length of the whole muscle belly. Thus proportional deformations in the three directions within the scanning region should not be extrapolated to predictions on changes in the whole muscle volume. Additionally, it should be noted that regional variations in factors such as the architecture (Rana et al., 2013; Rahemi et al., 2014; Azizi et al., 2008), intramuscular pressure (Sejersted et al., 1984) and externally applied forces may also affect regionalization of any transverse deformations in both the muscle fascicles and muscle belly.

Myofascial force transmission is a process by which forces can be transmitted laterally between muscles via connective tissues within and between the muscles (Siebert et al., 2014; Maas and Sandercock, 2010; Huijing, 1999; Bojsen-Moller et al., 2010). Within the triceps surae muscles, the LG and soleus can work in unison by decreasing the inter-aponeurosis shear, increasing the stiffness of connective tissue structures, and this unison may affect how muscles change shape during active dynamic tasks (Finni et al., 2017). However, asymmetries at the fascicle level can be additionally decoupled from belly level changes due to the additional contribution of dynamic factors such as change in

fascicle length, pennation angle, reorientation of fascicles and 3D trajectories of fascicles during contraction.

4.4.4. Methodological Approach and Limitations

A complete three-dimensional analysis of the whole muscle belly during active dynamic tasks remains challenging, particularly when relying on non-invasive techniques such as in humans. Ultrasound allows for direct imaging from the region of muscle belly being scanned by the ultrasound transducer, and can be used to quantify changes in muscles and fascicles during active contractions (Rana et al., 2013; Randhawa and Wakeling, 2013; Maganaris and Paul, 2000). Ultrasound has a high temporal resolution and can be used to study both passive and active muscle structure (Cronin and Lichtwark, 2013; Narici et al., 1996; Fukashiro et al., 1995b). The dual-probe imaging and processing approach described in this study provides a successful experimental framework for quantifying structural changes in a three-dimensional perspective. Unlike the 3D ultrasound probe that scans in a single direction at any given time and acquires data sequentially in the 3D space, and requires longer scan times (Lindop et al., 2006; Lopata et al., 2010; Lopata et al., 2007), the dual-probe technique used here employs two probes that scan a common region of the muscle from two orthogonal directions and acquire data simultaneously from the given directions.

The ultrasound scans in this study were aligned to maximize the line-like quality of the muscle fascicles in the images. For any straight section of fascicle, there are an infinite number of scanning orientations that can achieve this criterion, and here we have selected two orthogonal directions that were roughly in the anterior-posterior and the medial-lateral directions across the muscle. It should be noted that (a) misalignment of the scanning directions relative to the fascicles can underestimate fascicle length and produce errors of up to 6% (Muramatsu et al., 2002b), (b) the displacement of the fascicles relative to the probes during contraction can result in errors of up to 1 ° in pennation angle (Rana et al., 2013; Rana and Wakeling, 2011; van Leeuwen and Spoor, 1992), and (c) the fascicles typically curve during contraction so the quality of the probe alignment would vary along the length of each fascicle. Nonetheless, the main purpose of this study to identify asymmetries in fascicle deformation was achieved by observing totally opposite effects in the LG fascicle deformation during plantarflexion, and this finding would be robust relative to the smaller variabilities caused by probe misalignments.

Muscle aponeuroses are sheets of connective tissue to which muscle fascicles attach. Aponeurosis is an important feature that is digitized in an ultrasound image as it defines the muscle boundary and thus helps quantify fascicle length, fascicle pennation and muscle bulging. Due to the orthogonal probe alignment in this study, some ultrasound scans would likely miss the aponeuroses of the muscle belly (Figure 4-1), making automatic detection of these boundaries more challenging. Thus, the muscle regions of interest were manually segmented; manual digitization of ultrasound images is a well-documented technique with a strong inter-tester and intra-tester reliability (Kwah et al., 2013; Rana et al., 2009), therefore, this was our method of choice.

One potential limitation to the approach used here is that if the fascicles are asymmetric in cross-section (for instance, see Sharafi and Blemker, 2010) then rotations of the muscle belly relative to the probes may result in asymmetric deformations being ascribed to the fascicles as they contract, and this would be of particular concern for the LG where we are reporting asymmetric deformations (Figure 4-4). However, the fascicular features being analyzed here were larger than actual muscle fascicles, in a manner typical of ultrasound studies, and there was no significant difference in their absolute transverse wavelengths (1.58 ± 0.07 and 1.50 ± 0.05 mm for the *X* and *Y* directions of LG, respectively). If we were to speculate that the longitudinal rotations of the fascicles or muscle belly were as great as their changes in pennation, then they would need a pronounced asymmetry (a ratio of 1 : 0.32 for their lengths in the major : minor axes of their cross-section) in order for longitudinal rotations to explain the asymmetries shown in Figure 4-4. However, the actual ratio of the transverse wavelengths of these fascicular features was 1 : 0.95 and so this rotational movement is unlikely to be the cause of the asymmetrical deformations reported here.

4.4.5. Conclusion

Active muscles changes in length, pennation and belly thickness, and understanding the nature of these changes in important for understanding the length and velocity of the muscle fibres and thus the forces a muscle can produce. The results from this study reveal that during maximal plantarflexion contractions, the LG muscle shows transverse anisotropy at the level of the fascicles. This work provides the first three-dimensional description of fascicle deformations during active muscle contraction. Many structures and forces both internal and external to the muscle may cause this anisotropy,

and have been discussed, and regional variations in muscle structure, intramuscular pressure variations and myofascial force transmission may also influence the deformations and warrant further investigation. Future work should explore the structural properties of connective and elastic tissues that specifically connect the MG and LG muscle bellies, and the potential role these tissues may have on how muscles change shape and influence muscle mechanics. Experimental studies such as this study are necessary to quantify the 3D changes in muscle shape during active dynamic tasks and highlight the importance of studying muscle structure in all three dimensions.

Chapter 5.

Discussion

5.1. Summary of thesis

We currently lack research that quantifies the 3D changes in muscle shape during active dynamic tasks and highlights the role of studying muscle structure in all three dimensions. To understand how muscles function, scientists have explored various aspects of muscle structure and its mechanical properties yet these studies have been focused on isolated muscles, fixed-length contractions or unidimensional muscle models (Siebert et al., 2015; Böl et al., 2013; Stark and Schilling, 2010). This research provides a detailed 3D analysis of muscle and fascicle structure during dynamic tasks by combining ultrasound imaging with a motion tracking system, and utilizing muscle models and experimental techniques to quantify transverse expansion of the muscle belly and fascicles during concentric contractions in humans.

In **chapter 2**, I evaluated the accuracy with which fascicle pennation and changes in depth were predicted by 1D, 2D and 3D structural models of gastrocnemii muscles (MG and LG) during ankle plantarflexions in man. I showed that the constant depth 1D model established a very good relation between fascicle length and pennation angle, however, this model was unable to account for changes in depth but would not allow the muscle to bulge when under load. With increased load and aponeurosis stretch, the 2D model predicted decreases in depth. The decreases in depth in MG and increases in depth in LG were correctly predicted by the 3D model, however, when mean parameters were used, the 3D model performed no better than the 1D model. This study provided evidence that even this simplistic 3D model may not be sufficient to study the geometric effects of muscle fascicles during contraction, and the 1D model is sufficient if the purpose of a model is purely to predict changes in pennation during contraction.

Recent developments in muscle imaging have allowed us to quantify properties of muscle fascicles, however, neither MRI nor ultrasound techniques have been used to directly measure the transverse expansion of fascicles. In **chapter 3**, I developed a method to extract information on the spatial frequencies of the fascicular structure within the muscle belly. Fascicles appear as nearly parallel, repeating bands within B-mode

ultrasound images, and information on their transverse deformation was extracted by frequency decomposition. Although the magnitude of transverse fascicle strain was smaller than expected, I found that the increase in transverse width was exactly timed with the longitudinal shortening of the fascicles. This was the first study that described transverse fascicle strains during active dynamic tasks. When the modelling predictions from **chapter 2** were compared to the experimental findings from **chapter 3**, I found a consistent result that the extent of transverse fascicle strain were smaller than longitudinal shortening of fascicles, however the experimental findings suggested that fascicle bulging would be asymmetric during muscle contraction.

Muscle fascicles are enclosed within the muscle belly, and influence the overall shape changes that occur in a muscle during contraction. The overall change in transverse deformation of the muscle belly depends on the balance between longitudinal fascicle strain, and changes in pennation, on connective tissue compliance (Rahemi et al., 2014; Holt et al., 2016; Azizi and Roberts, 2009) and on forces external to the muscle (Siebert et al., 2017). The changes in length, depth and maintenance of volume are balanced by transverse deformations of the muscle belly in other directions (Böl et al., 2013; Stark and Schilling, 2010). Therefore, deformations of the muscle belly may also be transversely anisotropic (Azizi et al., 2008; Randhawa et al., 2013; Rahemi, 2015). However, how muscle fascicles change in transverse deformation and influence the muscle belly changes has never been explored.

In **chapter 4**, I provide the first three-dimensional description of fascicle deformations during active muscle contraction. The two gastrocnemii muscles (LG and MG) were tested, and the results from this study reveal that during maximal plantarflexion contractions, the LG muscle shows transverse anisotropy at the level of the fascicles, however, this anisotropy was not evident in the MG. To my knowledge, this is the first study to describe asymmetries in fascicle deformation during active contraction of skeletal muscle. Using experimental studies such as this study, we can quantify the 3D changes in muscle structure during active dynamic tasks and highlight the role of studying muscle structure in all three dimensions.

5.2. Quantification of transverse anisotropy in muscle fascicles

Multidimensional muscle models have been in place to investigate various dynamic muscle properties where muscle structure can be represented by a simple 1D model with series of line segments or a 2D or 3D model as a relatively more complex system with additional input parameters thus improving the accuracy of predicting muscle behavior (Chao et al., 1993; Delp et al., 1990; Hoy et al., 1990; Randhawa et al., 2013; Blemker and Delp, 2004). In **chapter 2**, the 1D model was unable to account for changes in muscle depth. However, studies have shown that LG muscle belly depth changes during both isometric, and dynamic contractions (Azizi et al., 2008; Maganaris et al., 1998; Wakeling et al., 2011; Randhawa et al., 2012), and the MG and LG change in depth differently (Maganaris et al., 1998; Wakeling et al., 2011) with the LG increasing in depth and the MG decreasing in depth during ankle plantarflexions (Randhawa et al., 2012).

I found that the 2D and 3D models differ in their ability to predict changes in muscle depth that occur during plantarflexion. 2D models can only allow a decrease in depth as the aponeurosis is stretched (Zuurbier and Huijing, 1992) and this was not sufficient to predict the increases in depth that occur in the LG during plantarflexion. The 3D model in **chapter 2** had the ability to predict increases or decreases in depth during the ankle plantarflexions, and it predicted the opposing changes in depth that occurred between the MG and LG, whilst simultaneously predicting the pennation more accurately than the 1D or 2D models. However, due to the assumptions we make when building these models, all models may have limitations and may not represent in vivo muscle behavior with accuracy. Based on the findings of this study, it can be suggested that 1D models are sufficient to predict the structural parameters of the muscle such as fascicle length and pennation angle, and this is consistent with previous studies (Dick and Wakeling, 2017; Dick and Wakeling, 2018). Similar to the findings of previous modelling studies, our results show that changes in fascicle transverse deformation occurs dominantly in the depth-wise direction than the width-wise direction (Rahemi et al., 2015; Dick and Wakeling, 2018).

Dynamic shape changes can be modulated by the mechanical properties of aponeurosis and due to stress asymmetries produced by compressive forces and connective tissue resistance (Rahemi et al., 2014; Rahemi et al., 2015; Dick and Wakeling, 2017). Active muscle features such as fascicle strains, changes to pennation angles,

muscle bulging and fascicle curvature determine how a muscle changes shape during activity and this shape change can be different for different force and velocity levels and during different tasks such as single-joint movements versus dynamic walking (Fukunaga et al., 1997; Kawakami et al., 1998). A complete three-dimensional analysis of the whole muscle belly during active dynamic tasks remains challenging, particularly when relying on non-invasive techniques such as in humans.

Magnetic Resonance Imaging (MRI) has emerged as a promising tool to study whole muscle structure (Wokke et al., 2014; Mercuri et al., 2005), tissue properties such as fascicle orientations and curvatures by taking multiple scans of the segment using diffusion tensor imaging (Blemker and Delp, 2005; Heemskerk et al., 2009; Heemskerk et al., 2005), and to quantify strain characteristics of muscles in vivo by using spatial-tagging MRI techniques (Englund et al., 2011; Zerhouni et al., 1988). However, MRI studies are limited to quantifying passive muscle structure or muscle activities with low contraction intensity (Shin et al., 2009; Sinha et al., 2004); and MRI is unable to quantify fascicle deformations when the muscles are actively shortening. While there is no doubt that static muscle structure is important, asymmetries would be expected to be most pronounced during active tasks.

Brightness mode (B-mode) ultrasound allows for imaging of dynamic muscle contractions to quantify muscle structural properties and observe structural changes due to an underlying muscle pathology (Cronin and Lichtwark, 2013; Rana et al., 2013; Narici et al., 2003; Morse et al., 2005). Using B-mode ultrasound imaging and image processing techniques, muscle bellies were imaged in 2D and information on the spatial frequencies of the fascicular structure within the belly was extracted (**chapter 3**). The results from the 2D study indicated that the differences in the bulging of the muscle belly are caused more by differences in connective tissue properties and the tendency for the fascicles to rotate than by differences in the fascicle bulging as I found similar transverse expansion occurring in both the MG and LG in 2D images.

2D ultrasound imaging when combined with motion capture allows for the projection of 2D images from the ultrasound in 3D space and muscles can be visualized as a 3D entity (Rana and Wakeling, 2011; Barber et al., 2009; Malaiya et al., 2007). Further, this thesis provides an experimental technique that combines image processing with dual-probe ultrasound to quantify 3D changes in the transverse deformation of muscle

fascicles for the first time in **chapter 4**. The experimental results on 3D transverse deformations presented in **chapter 4** were particularly interesting. I provided experimental evidence that transverse deformations in the fascicles for the LG can be asymmetric during active muscle contractions as seen by phase-relationship of their strains. The 3D ultrasound probe that acquires data sequentially in the 3D space is unable to provide 3D information for a common muscle region as it uses sweeping motion in a single direction at any given time (Lindop et al., 2006; Lopata et al., 2010; Lopata et al., 2007). The dual-probe technique presented here employs two probes that scan a common region of the muscle belly from two orthogonal directions and acquire data simultaneously from the given directions and can provide information for a common muscle region in a 3D perspective.

5.3. Significance of transverse deformations in muscle mechanics

Muscle fascicles are bundles of fibres enclosed in a 3D space within the muscle belly. Regional variations in factors such as the architecture (Rana et al., 2013; Rahemi et al., 2014; Azizi et al., 2008), intramuscular pressure (Sejersted et al., 1984) and externally applied forces can affect the transverse deformations in both the muscle fascicles and muscle belly (Böl et al., 2015; Siebert et al., 2014). Although the focus of this thesis is primarily on the structural changes occurring at the muscle fascicles and belly levels, the findings from this thesis allow us to understand changes internal and external to the muscle fascicles and muscle belly with greater depth while highlighting the complexity of in vivo muscle behavior.

Stress asymmetries within the muscle are related to asymmetries in the transverse deformations of the fascicles. In **chapter 4**: a 33% decrease in fascicle length led to change in transverse deformation of 3% and 1.2% in the x direction and 2.1% and 2.1% in the y direction for the MG and LG, respectively. The extent of the transverse changes in comparison to longitudinal shortening of fascicles were smaller than predicted. Similar discrepancies in fascicle length and transverse deformations were observed in muscle models during maximal and submaximal muscle contractions (Rahemi et al., 2014, Randhawa et al., 2013).

This relates to the stress asymmetries during maximal contractions when muscle stresses and intramuscular pressures will be greatest. Indeed, during passive muscle length changes, the reduced or absent stress asymmetries may not be sufficient to cause transverse anisotropy in the muscle fascicles. Thus, transverse anisotropy at the fascicle level may not be evident in studies of passive muscle or minimally active muscle, as may be case for MRI studies. Due to the additional contribution of dynamic factors such as change in fascicle length, pennation angle, reorientation of fascicles and 3D trajectories of fascicles during contraction, asymmetries at the fascicle level can be decoupled from belly level changes (Azizi et al., 2008; Dick and Wakeling, 2017).

For the MG muscle, the muscle belly within the scanning region of the ultrasound transducers appears to be shortening in all three directions. The ultrasound transducer used in this study had a linear field of 60 mm and may only be about one third of the length of the whole muscle belly. However, the shape of the muscle can be altered due to the proximal movement of a muscle's volume during shortening by decreasing the cross-section in some regions of the muscle while simultaneously increasing the cross-section in adjacent regions as seen in both human and rabbit muscle (Raiteri et al., 2016; Böl et al., 2013). Thus, the observations of proportional deformations in the three directions within the scanning region should not be extrapolated to predictions on changes in the whole muscle volume.

Fascicles are surrounded by the perimysium membrane and additionally contain the extracellular matrix (ECM), blood vessels, nerves and intramuscular fat. Thus, fluid movement within the fascicle and the material properties of the ECM can influence deformations in the fascicle that are additional to the deformations of their constituent fibres (Karakuzu et al., 2017; Yucesoy, 2010; Yucesoy and Huijing, 2007). During contraction, a longitudinal component to the cross-bridges that are formed between the myosin and actin filaments acts to pull them past each other (Huxley and Niedergerke, 1954; Gordon et al., 1966), but there is additionally a transverse component to the cross-bridge forces that acts to squeeze the myofilament lattice together (Daniel et al., 2013; Williams et al., 2013). Shortening caused by the longitudinal component of cross-bridge force is matched by a tendency of the muscle fibres to bulge transversely in order to maintain their volume (Abbott and Baskin, 1962; Rahemi et al., 2014, 2015). This increase in girth in a transverse direction across the fibres is opposed by both the cytoskeletal structures within the muscle fibres and the radial forces from the cross-bridges and

external constraints, e.g. ECM. The intracellular fluid moves into the myofilament space from the myofilament lattice during contraction (Cecchi et al.,1990) and the cytoskeletal elements within the muscle fibres are additionally distributed in a non-uniform manner (Neering et al.,1991). Thus transverse anisotropy that may occur in the myofilament lattice can be exceeded by transverse anisotropies within the muscle fibres.

Myofascial structures and the extracellular matrix transmit external forces that may be derived from surrounding tissues or even from sources external to the body. The forces external to the fibres can also influence the deformation of the fibres. These external forces will often be directional, for instance the external forces where the body contacts the environment (Siebert et al., 2017; Holt et al., 2016; Wakeling et al., 2013), or the compressive force between sheets of aponeurosis due to the muscle fibres drawing them together (Rahemi et al., 2014; Azizi et al., 2008). Thus there would be an asymmetry to the stress distribution through the muscle that would likely cause deformations in the fibres that are transversely anisotropic (Rahemi et al., 2014, 2015). Furthermore, due to the changes in its fascicle lengths, orientations and 3D trajectories; changes in the shape of a muscle belly can be dissociated from changes in the depth and width of its constituent fibres.

5.4. Application and future directions

This thesis provides a combination of modelling and experimental approach to quantify in vivo transverse deformations in the muscle belly and fascicles. The experimental and modelling approaches were motivated by the macroscopic changes in structure that occur during muscle contraction. Muscles can show anisotropic changes during contraction at both belly and fascicle levels (Rahemi et al., 2014; Dick and Wakeling, 2018) due to a variable fascicle arrangement and pennation angles, and internal constraints placed by a complex connective tissue structure (Siebert et al., 2018; Dick and Wakeling, 2017; Stark and Schilling, 2010). It may be beneficial to explore the effects of muscle deformation by expanding the existing muscle modelling and experimental technique as the structures surrounding a muscle can influence muscle force and joint torques (Siebert et al., 2018; Reinhardt et al., 2016; Wakeling et al., 2013).

Due to a high temporal resolution and the ability to directly image a region of muscle belly, ultrasound can be used to study both passive and active muscle structure

(Cronin and Lichtwark, 2013; Rana et al., 2013; Maganaris and Paul, 2000; Narici et al., 1996; Fukashiro et al., 1995b). Here I used ultrasound with image processing to quantify changes in muscles and fascicles during active contractions. The dual-probe imaging and processing approach described in this thesis provides a successful experimental framework for quantifying structural changes in a three-dimensional perspective. The dual-probe technique used here employs two probes that scan a common region of the muscle from two orthogonal directions to acquire data simultaneously from the given directions. This is not currently possible to accomplish with the 3D ultrasound probe that scans in a single direction at any given time and acquires data sequentially in the 3D space (Lindop et al., 2006; Lopata et al., 2010; Lopata et al., 2007).

Longitudinal changes in fascicles influence the geometrical changes of the muscle belly. When muscles are loaded transversally, the rate of force development in the longitudinal direction reduces in addition to the maximum isometric force (Siebert et al., 2014). This may be due to the balancing of external and internal forces, or due to the myofilament deformation inhibiting the cross-bridges (Siebert et al., 2018). This force reduction has clinical implications for patients in wheelchairs who can experience high pressures during long-term sitting (Gefen et al., 2005; Linder-Ganz et al., 2007) leading to decreased gluteus muscle function. Similar observation can be made for individuals who wear orthoses such as patients with cerebral palsy or stroke. With advances in imaging technologies, we can determine the how altered muscle and fascicle structure in atrophy or spasticity impairs the mechanical function of muscles.

5.5. Conclusions

To conclude, transverse deformation of muscles and fascicles determines the extent of length change in muscles and the direction and magnitude of force generated by muscles. The 2D and 3D muscle models developed in this thesis represent a general expression of muscle geometry and can be used as 1D, 2D or 3D models for multiple applications to predict muscle forces during various tasks. The novel imaging techniques that were developed, validated and used to measure transverse expansions of fascicles during dynamic movements and changes in the overall 3D muscle structure provide a better understanding of the muscle structure. This is an important contribution to the field of muscle mechanics as 3D quantification of the transverse deformations within muscles

will have important implications in understanding the fundamentals of muscle behavior in the third dimension.

Additionally, these techniques can be used to study and understand the 3D changes in muscle structure during dynamic activities such as walking and to better understand the interaction of muscle belly and fascicle structure during various activities and pathologies. The methods developed in this study may have clinical applications: to understand how pathological muscle insults can affect the dynamic muscle behavior, how muscle structure is affected by muscle injuries, and surgical repairs to tendon and aponeurosis.

References

Abbott, B. C., & Baskin, R. J. (1962). Volume changes in frog muscle during contraction. *The Journal of physiology*, *161*(3), 379-391.

Agur, A. M., Ng-Thow-Hing, V., Ball, K. A., Fiume, E., & McKee, N. H. (2003). Documentation and three-dimensional modelling of human soleus muscle architecture. *Clinical Anatomy: The Official Journal of the American Association of Clinical Anatomists and the British Association of Clinical Anatomists*, *16*(4), 285-293.

Alexander, R. M. (1969). The orientation of muscle fibres in the myomeres of fishes. *Journal of the Marine Biological Association of the United Kingdom*, *49*(2), 263-290.

Alexander, R. M. (1975). The dimensions of knee and ankle muscles and the forces they exert. *J. Hum. Move. Stud.*, *1*, 115-123.

Alexander, R. McN, *Animal Mechanics. (1982). 2nd ed.* Blackwell Scientific Publications, London.

Alexander, R. McN. (1968). *Animal mechanics*. London: Blackwell Scientific Publications 301pp..

Arampatzis, A., Stafilidis, S., DeMonte, G., Karamanidis, K., Morey-Klapsing, G., & Brüggemann, G. P. (2005). Strain and elongation of the human gastrocnemius tendon and aponeurosis during maximal plantarflexion effort. *Journal of biomechanics*, *38*(4), 833-841.

Arnold, E. M., Hamner, S. R., Seth, A., Millard, M., & Delp, S. L. (2013). How muscle fiber lengths and velocities affect muscle force generation as humans walk and run at different speeds. *Journal of Experimental Biology*, jeb-075697.

Azizi, E., & Brainerd, E. L. (2007). Architectural gear ratio and muscle fiber strain homogeneity in segmented musculature. *Journal of Experimental Zoology Part A: Ecological Genetics and Physiology*, *307*(3), 145-155.

Azizi, E., & Deslauriers, A. R. (2014). Regional heterogeneity in muscle fiber strain: the role of fiber architecture. *Frontiers in physiology*, *5*, 303.

Azizi, E., & Roberts, T. J. (2009). Biaxial strain and variable stiffness in aponeuroses. *The Journal of physiology*, *587*(17), 4309-4318.

Azizi, E., & Roberts, T. J. (2010). Muscle performance during frog jumping: influence of elasticity on muscle operating lengths. *Proceedings of the Royal Society of London B: Biological Sciences*, *277*(1687), 1523-1530.

Azizi, E., Brainerd, E. L., & Roberts, T. J. (2008). Variable gearing in pennate muscles. *Proceedings of the National Academy of Sciences*, *105*(5), 1745-1750.

Azizi, E., Gillis, G. B., & Brainerd, E. L. (2002). Morphology and mechanics of myosepta in a swimming salamander (Siren lacertina). *Comparative Biochemistry and Physiology Part A: Molecular & Integrative Physiology*, *133*(4), 967-978.

Barber, L., Barrett, R., & Lichtwark, G. (2009). Validation of a freehand 3D ultrasound system for morphological measures of the medial gastrocnemius muscle. *Journal of biomechanics*, *42*(9), 1313-1319.

Baskin, R. J., & Paolini, P. J. (1966). Muscle volume changes. *The Journal of general physiology*, *49*(3), 387-404.

Baskin, R. J., & Paolini, P. J. (1967). Volume change and pressure development in muscle during contraction. *American Journal of Physiology-Legacy Content*, *213*(4), 1025-1030.

Benard, M. R., Becher, J. G., Harlaar, J., Huijing, P. A., & Jaspers, R. T. (2009). Anatomical information is needed in ultrasound imaging of muscle to avoid potentially substantial errors in measurement of muscle geometry. *Muscle & Nerve: Official Journal of the American Association of Electrodiagnostic Medicine*, *39*(5), 652-665.

Benninghoff, A., & Rollhäuser, H. (1952). Zur inneren Mechanik des gefiederten Muskels. *Pflüger's Archiv für die gesamte Physiologie des Menschen und der Tiere*, *254*(6), 527-548.

Biewener, A. A. (1998). Muscle function in vivo: a comparison of muscles used for elastic energy savings versus muscles used to generate mechanical power1. *American Zoologist*, *38*(4), 703-717.

Bishop, M. J., Plank, G., Burton, R. A., Schneider, J. E., Gavaghan, D. J., Grau, V., & Kohl, P. (2009). Development of an anatomically detailed MRI-derived rabbit ventricular model and assessment of its impact on simulations of electrophysiological function. *American Journal of Physiology-Heart and Circulatory Physiology*, *298*(2), H699-H718.

Blemker, S. S., & Delp, S. L. (2005). Three-dimensional representation of complex muscle architectures and geometries. *Annals of biomedical engineering*, *33*(5), 661-673.

Blemker, S. S., Pinsky, P. M., & Delp, S. L. (2005). A 3D model of muscle reveals the causes of nonuniform strains in the biceps brachii. *Journal of biomechanics*, *38*(4), 657-665.

Bojsen-Moller, J., Schwartz, S., Finni, T., Kalliokoski, K., & Magnusson, S. P. (2009). Lateral force transmission between lower leg muscles. In *Proceedings of the 14th Annual Congress of the European College of Sport Science*.

Bojsen-Møller, J., Schwartz, S., Kalliokoski, K. K., Finni, T., & Magnusson, S. P. (2010). Intermuscular force transmission between human plantarflexor muscles in vivo. *Journal of Applied Physiology*, *109*(6), 1608-1618.

Böl, M., Leichsenring, K., Weichert, C., Sturmat, M., Schenk, P., Blickhan, R., & Siebert, T. (2013). Three-dimensional surface geometries of the rabbit soleus muscle during contraction: input for biomechanical modelling and its validation. *Biomechanics and modeling in mechanobiology*, *12*(6), 1205-1220.

Bolsterlee, B., D'Souza, A., Gandevia, S. C., & Herbert, R. D. (2017). How does passive lengthening change the architecture of the human medial gastrocnemius muscle?. *Journal of Applied Physiology*, *122*(4), 727-738.

Bolsterlee, B., Veeger, D. H., & Chadwick, E. K. (2013). Clinical applications of musculoskeletal modelling for the shoulder and upper limb. *Medical & biological engineering & computing*, *51*(9), 953-963.

Bolsterlee, B., Veeger, H. D., van der Helm, F. C., Gandevia, S. C., & Herbert, R. D. (2015). Comparison of measurements of medial gastrocnemius architectural parameters from ultrasound and diffusion tensor images. *Journal of biomechanics*, *48*(6), 1133-1140.

Brainerd, E. L., & Azizi, E. (2005). Muscle fiber angle, segment bulging and architectural gear ratio in segmented musculature. *Journal of Experimental Biology*, *208*(17), 3249-3261.

Burkholder, T. J., & Lieber, R. L. (2001). Sarcomere length operating range of vertebrate muscles during movement. *Journal of Experimental Biology*, *204*(9), 1529-1536.

Cecchi, G., Bagni, M. A., Griffiths, P. J., Ashley, C. C., & Maeda, Y. (1990). Detection of radial crossbridge force by lattice spacing changes in intact single muscle fibers. *Science*, *250*(4986), 1409-1411.

Cronin, N. J., & Lichtwark, G. (2013). The use of ultrasound to study muscle–tendon function in human posture and locomotion. *Gait & posture*, *37*(3), 305-312.

Daley, M. A., & Biewener, A. A. (2003). Muscle force-length dynamics during level versus incline locomotion: a comparison of in vivo performance of two guinea fowl ankle extensors. *Journal of Experimental Biology*, *206*(17), 2941-2958.

Damon, B. M., Ding, Z., Anderson, A. W., Freyer, A. S., & Gore, J. C. (2002). Validation of diffusion tensor MRI-based muscle fiber tracking. *Magnetic Resonance in Medicine: An Official Journal of the International Society for Magnetic Resonance in Medicine*, *48*(1), 97-104.

Daniel, T. L., George, N. T., Williams, C. D., & Irving, T. C. (2013). In vivo time resolved X-ray diffraction reveals radial motions of myofilaments in insect flight muscle. *Biophysical Journal*, *104*(2), 485a-486a.

Darby, J., Hodson-Tole, E. F., Costen, N., & Loram, I. D. (2011). Automated regional analysis of B-mode ultrasound images of skeletal muscle movement. *Journal of Applied Physiology*, *112*(2), 313-327.

Delp, S. L., Anderson, F. C., Arnold, A. S., Loan, P., Habib, A., John, C. T., ... & Thelen, D. G. (2007). OpenSim: open-source software to create and analyze dynamic simulations of movement. *IEEE transactions on biomedical engineering*, *54*(11), 1940-1950.

Delp, S. L., Loan, J. P., Hoy, M. G., Zajac, F. E., Topp, E. L., & Rosen, J. M. (1990). An interactive graphics-based model of the lower extremity to study orthopaedic surgical procedures. *IEEE Transactions on Biomedical engineering*, *37*(8), 757-767.

Delp, S., & Loan, J. P. (1995). A graphics-based software system to develop and analyze models of musculoskeletal structures. *Comput. Biol. Medl*, *25*, 21-34.

Dick, T. J., & Wakeling, J. M. (2018). Geometric models to explore mechanisms of dynamic shape change in skeletal muscle. *Royal Society open science*, *5*(5), 172371.

Dick, T. J., Biewener, A. A., & Wakeling, J. M. (2017). Comparison of human gastrocnemius forces predicted by Hill-type muscle models and estimated from ultrasound images. *Journal of Experimental Biology*, jeb-154807.

Dickinson, M. H., Farley, C. T., Full, R. J., Koehl, M. A. R., Kram, R., & Lehman, S. (2000). How animals move: an integrative view. *science*, *288*(5463), 100-106.

Englund, E. K., Elder, C. P., Xu, Q., Ding, Z., & Damon, B. M. (2011). Combined diffusion and strain tensor MRI reveals a heterogeneous, planar pattern of strain development during isometric muscle contraction. *American Journal of Physiology-Regulatory, Integrative and Comparative Physiology*, *300*(5), R1079-R1090.

Epstein, M. (1998). Theoretical models of skeletal muscle: biological and mathematical considerations. *John Wiley & Sons*, 52-53.

Epstein, M., & Herzog, W., (1998). *Theoretical models of skeletal muscle. Biological and mathematical considerations* , John Wiley & Sons, Chichester, UK.

Epstein, M., Wong, M., & Herzog, W. (2006). Should tendon and aponeurosis be considered in series?. *Journal of biomechanics*, *39*(11), 2020-2025.

Farris, D. J., & Sawicki, G. S. (2012). Human medial gastrocnemius force–velocity behavior shifts with locomotion speed and gait. *Proceedings of the National Academy of Sciences*, *109*(3), 977-982.

Farris, D. J., Robertson, B. D., & Sawicki, G. S. (2013). Elastic ankle exoskeletons reduce soleus muscle force but not work in human hopping. *Journal of Applied Physiology*, *115*(5), 579-585.

Finni, T., Cronin, N. J., Mayfield, D., Lichtwark, G. A., & Cresswell, A. G. (2017). Effects of muscle activation on shear between human soleus and gastrocnemius muscles. *Scandinavian journal of medicine & science in sports*, *27*(1), 26-34.

Frangi, A. F., Niessen, W. J., Vincken, K. L., & Viergever, M. A. (1998, October). Multiscale vessel enhancement filtering. In *International Conference on Medical Image Computing and Computer-Assisted Intervention* (pp. 130-137). Springer, Berlin, Heidelberg.

Friederich, J. A., & Brand, R. A. (1990). Muscle fiber architecture in the human lower limb. *Journal of biomechanics*, *23*(1), 91-95.

Fry, N. R., Gough, M., & Shortland, A. P. (2004). Three-dimensional realisation of muscle morphology and architecture using ultrasound. *Gait & posture*, *20*(2), 177-182.

Fukashiro, S., Komi, P. V., Järvinen, M., & Miyashita, M. (1995a). In vivo achilles tendon loading during jumping in humans. *European journal of applied physiology and occupational physiology*, *71*(5), 453-458.

Fukashiro, S., Rob, M., Ichinose, Y., Kawakami, Y., & Fukunaga, T. (1995b). Ultrasonography gives directly but noninvasively elastic characteristic of human tendon in vivo. *European journal of applied physiology and occupational physiology*, *71*(6), 555-557.

Fukunaga, T., Ichinose, Y., Ito, M., Kawakami, Y., & Fukashiro, S. (1997). Determination of fascicle length and pennation in a contracting human muscle in vivo. *Journal of applied physiology*, *82*(1), 354-358.

Fukunaga, T., Kubo, K., Kawakami, Y., Fukashiro, S., Kanehisa, H., & Maganaris, C. N. (2001). In vivo behaviour of human muscle tendon during walking. *Proceedings of the Royal Society of London B: Biological Sciences*, *268*(1464), 229-233.

Fukunaga, T., Roy, R. R., Shellock, F., Hodgson, J. A., & Edgerton, V. R. (1996). Specific tension of human plantar flexors and dorsiflexors. *Journal of Applied Physiology*, *80*(1), 158-165.

Gans, C. (1982). Fiber architecture and muscle function. *Exercise and sport sciences reviews*, *10*(1), 160-207.

Gans, C., & De Vree, F. (1987). Functional bases of fiber length and angulation in muscle. *journal of Morphology*, *192*(1), 63-85.

Gillett, J. G., Barrett, R. S., & Lichtwark, G. A. (2013). Reliability and accuracy of an automated tracking algorithm to measure controlled passive and active muscle fascicle length changes from ultrasound. *Computer Methods in Biomechanics and Biomedical Engineering*, *16*(6), 678-687.

Gordon, A. M., Huxley, A. F., & Julian, F. J. (1966). The variation in isometric tension with sarcomere length in vertebrate muscle fibres. *The Journal of physiology*, *184*(1), 170-192.

Hamner, S. R., Seth, A., & Delp, S. L. (2010). Muscle contributions to propulsion and support during running. *Journal of biomechanics*, *43*(14), 2709-2716.

Hatze, H. (1978). A general myocybernetic control model of skeletal muscle. *Biological cybernetics*, *28*(3), 143-157.

Haughton, S. (1873). *Principles of animal mechanics*. Longmans, Green.

Heemskerk, A. M., Sinha, T. K., Wilson, K. J., Ding, Z., & Damon, B. M. (2009). Quantitative assessment of DTI-based muscle fiber tracking and optimal tracking parameters. *Magnetic Resonance in Medicine: An Official Journal of the International Society for Magnetic Resonance in Medicine*, *61*(2), 467-472.

Heemskerk, A. M., Strijkers, G. J., Vilanova, A., Drost, M. R., & Nicolay, K. (2005). Determination of mouse skeletal muscle architecture using three-dimensional diffusion tensor imaging. *Magnetic Resonance in Medicine: An Official Journal of the International Society for Magnetic Resonance in Medicine*, *53*(6), 1333-1340.

Heidlauf, T., Klotz, T., Rode, C., Siebert, T., & Röhrle, O. (2017). A continuum-mechanical skeletal muscle model including actin-titin interaction predicts stable contractions on the descending limb of the force-length relation. *PLoS computational biology*, *13*(10), e1005773.

Herbert, R. D., & Gandevia, S. C. (1995). Changes in pennation with joint angle and muscle torque: in vivo measurements in human brachialis muscle. *The Journal of Physiology*, *484*(2), 523-532.

Herzog, W. (2017). Skeletal muscle mechanics: questions, problems and possible solutions. *Journal of neuroengineering and rehabilitation*, *14*(1), 98.

Herzog, W., Leonard, T. R., Renaud, J. M., Wallace, J., Chaki, G., & Bornemisza, S. (1992). Force-length properties and functional demands of cat gastrocnemius, soleus and plantaris muscles. *Journal of biomechanics*, *25*(11), 1329-1335.

Herzog, W., Duvall, M., & Leonard, T. R. (2012). Molecular mechanisms of muscle force regulation: a role for titin?. *Exercise and sport sciences reviews*, *40*(1), 50-57.

Hiblar, T., Bolson, E. L., Hubka, M., Sheehan, F. H., & Kushmerick, M. J. (2003). Three dimensional ultrasound analysis of fascicle orientation in human tibialis anterior muscle enables analysis of macroscopic torque at the cellular level. In *Molecular and Cellular Aspects of Muscle Contraction* (pp. 635-645). Springer, Boston, MA.

Hill, A. V. (1938). The heat of shortening and the dynamic constants of muscle. *Proc. R. Soc. Lond. B*, *126*(843), 136-195.

Hill, A. V. (1964). The efficiency of mechanical power development during muscular shortening and its relation to load. *Proc. R. Soc. Lond. B*, *159*(975), 319-324.

Hill, A. V. (1970). *First and last experiments in muscle mechanics*. Cambridge University Press.

Hodgson, J. A., Finni, T., Lai, A. M., Edgerton, V. R., & Sinha, S. (2006). Influence of structure on the tissue dynamics of the human soleus muscle observed in MRI studies during isometric contractions. *Journal of Morphology*, *267*(5), 584-601.

Holt, N. C., & Azizi, E. (2016). The effect of activation level on muscle function during locomotion: are optimal lengths and velocities always used?. *Proc. R. Soc. B*, *283*(1823), 20152832.

Holt, N. C., Danos, N., Roberts, T. J., & Azizi, E. (2016). Stuck in gear: age-related loss of variable gearing in skeletal muscle. *Journal of Experimental Biology*, *219*(7), 998-1003.

Holt, N. C., Wakeling, J. M., & Biewener, A. A. (2014). The effect of fast and slow motor unit activation on whole-muscle mechanical performance: the size principle may not pose a mechanical paradox. *Proceedings of the Royal Society of London B: Biological Sciences*, *281*(1783), 20140002.

Hoy, M. G., Zajac, F. E., & Gordon, M. E. (1990). A musculoskeletal model of the human lower extremity: the effect of muscle, tendon, and moment arm on the moment-angle relationship of musculotendon actuators at the hip, knee, and ankle. *Journal of biomechanics*, *23*(2), 157-169.

Huijing, P. A. (1999). Muscle as a collagen fiber reinforced composite: a review of force transmission in muscle and whole limb. *Journal of biomechanics*, *32*(4), 329-345.

Huijing, P. A. (2003). Muscular force transmission necessitates a multilevel integrative approach to the analysis of function of skeletal muscle. *Exercise and sport sciences reviews*, *31*(4), 167-175.

Huijing, P. A., Baan, G. C., & Rebel, G. T. (1998). Non-myotendinous force transmission in rat extensor digitorum longus muscle. *Journal of Experimental Biology*, *201*(5), 683-691.

Huxley, H. E. (1964). Evidence for continuity between the central elements of the triads and extracellular space in frog sartorius muscle. *Nature*, *202*(4937), 1067.

Huxley, H. E. (1969). The mechanism of muscular contraction. *Science*, *164*(3886), 1356-1365.

Jenkyn, T. R., Koopman, B., Huijing, P., Lieber, R. L., & Kaufman, K. R. (2002). Finite element model of intramuscular pressure during isometric contraction of skeletal muscle. *Physics in Medicine & Biology*, *47*(22), 4043.

Josephson, R. K., & Edman, K. A. P. (1988). The consequences of fibre heterogeneity on the force-velocity relation of skeletal muscle. *Acta physiologica scandinavica*, *132*(3), 341-352.

Kagaya, A., & Muraoka, Y. (2005). Muscle architecture and its relationship to muscle circulation. *International Journal of Sport and Health Science*, *3*(Special_Issue_2005), 171-180.

Kan, J. H., Hernanz-Schulman, M., Damon, B. M., Yu, C., & Connolly, S. A. (2008). MRI features of three paediatric intra-articular synovial lesions: a comparative study. *Clinical radiology*, *63*(7), 805-812.

Karakuzu, A., Pamuk, U., Ozturk, C., Acar, B., & Yucesoy, C. A. (2017). Magnetic resonance and diffusion tensor imaging analyses indicate heterogeneous strains along human medial gastrocnemius fascicles caused by submaximal plantar-flexion activity. *Journal of biomechanics*, *57*, 69-78.

Kawakami, Y., Abe, T., & Fukunaga, T. (1993). Muscle-fiber pennation angles are greater in hypertrophied than in normal muscles. *Journal of Applied Physiology*, *74*(6), 2740-2744.

Kawakami, Y., Ichinose, Y., & Fukunaga, T. (1998). Architectural and functional features of human triceps surae muscles during contraction. *Journal of applied physiology*, *85*(2), 398-404.

Ker, R. F. (1981). Dynamic tensile properties of the plantaris tendon of sheep (Ovis aries). *Journal of Experimental Biology*, *93*(1), 283-302.

Kinugasa, R., Oda, T., Komatsu, T., Edgerton, V. R., & Sinha, S. (2013). Interaponeurosis shear strain modulates behavior of myotendinous junction of the human triceps surae. *Physiological reports*, *1*(6).

Klimstra, M., Dowling, J., Durkin, J. L., & MacDonald, M. (2007). The effect of ultrasound probe orientation on muscle architecture measurement. *Journal of Electromyography and Kinesiology*, *17*(4), 504-514.

Koryak, Y. A. (2008). Functional and clinical significance of the architecture of human skeletal muscles. *Human Physiology*, *34*(4), 482.

Kuno, S. Y., & Fukunaga, T. (1995). Measurement of muscle fibre displacement during contraction by real-time ultrasonography in humans. *European journal of applied physiology and occupational physiology*, *70*(1), 45-48.

Kurihara, T., Oda, T., Chino, K., Kanehisa, H., Fukunaga, T., & Kawakami, Y. (2005). Use of three-dimensional ultrasonography for the analysis of the fascicle length of human gastrocnemius muscle during contractions. *International Journal of Sport and Health Science*, *3*(Special_Issue_2005), 226-234.

Kwah, L. K., Pinto, R. Z., Diong, J., & Herbert, R. D. (2013). Reliability and validity of ultrasound measurements of muscle fascicle length and pennation in humans: a systematic review. *Journal of Applied Physiology*, *114*(6), 761-769.

Lansdown, D. A., Ding, Z., Wadington, M., Hornberger, J. L., & Damon, B. M. (2007). Quantitative diffusion tensor MRI-based fiber tracking of human skeletal muscle. *Journal of Applied Physiology*, *103*(2), 673-681.

Lee, S. S., Arnold, A. S., de Boef Miara, M., Biewener, A. A., & Wakeling, J. M. (2013). Accuracy of gastrocnemius muscles forces in walking and running goats predicted by one-element and two-element Hill-type models. *Journal of biomechanics*, *46*(13), 2288-2295.

Levin, D. I., Gilles, B., Mädler, B., & Pai, D. K. (2011). Extracting skeletal muscle fiber fields from noisy diffusion tensor data. *Medical Image Analysis*, *15*(3), 340-353.

Li, L., Tong, K. Y., Hu, X. L., Hung, L. K., & Koo, T. K. K. (2009). Incorporating ultrasound-measured musculotendon parameters to subject-specific EMG-driven model to simulate voluntary elbow flexion for persons after stroke. *Clinical Biomechanics*, *24*(1), 101-109.

Lichtwark, G. A., Bougoulias, K., & Wilson, A. M. (2007). Muscle fascicle and series elastic element length changes along the length of the human gastrocnemius during walking and running. *Journal of biomechanics*, *40*(1), 157-164.

Lieber, R. L., & Fridén, J. (2000). Functional and clinical significance of skeletal muscle architecture. *Muscle & Nerve: Official Journal of the American Association of Electrodiagnostic Medicine*, *23*(11), 1647-1666.

Lieber, R. L., & Ward, S. R. (2011). Skeletal muscle design to meet functional demands. *Philosophical Transactions of the Royal Society of London B: Biological Sciences*, *366*(1570), 1466-1476.

Lieber, R. L., Roberts, T. J., Blemker, S. S., Lee, S. S., & Herzog, W. (2017). Skeletal muscle mechanics, energetics and plasticity. *Journal of neuroengineering and rehabilitation*, *14*(1), 108.

Lindop, J. E., Treece, G. M., Gee, A. H., & Prager, R. W. (2006). 3D elastography using freehand ultrasound. *Ultrasound in medicine & biology*, *32*(4), 529-545.

Lopata, R. G., Nillesen, M. M., Gerrits, I. H., Thijssen, J. M., Kapusta, L., & de Korte, C. L. (2007, October). 10B-4 4D Cardiac Strain Imaging: Methods and Initial Results. In *Ultrasonics Symposium, 2007. IEEE* (pp. 872-875). IEEE.

Lopata, R. G., van Dijk, J. P., Pillen, S., Nillesen, M. M., Maas, H., Thijssen, J. M., ... & de Korte, C. L. (2010). Dynamic imaging of skeletal muscle contraction in three orthogonal directions. *Journal of Applied Physiology*, *109*(3), 906-915.

Maas, H., & Sandercock, T. G. (2010). Force transmission between synergistic skeletal muscles through connective tissue linkages. *BioMed Research International*, *2010*.

Maas, H., Baan, G. C., & Huijing, P. A. (2001). Intermuscular interaction via myofascial force transmission: effects of tibialis anterior and extensor hallucis longus length on force transmission from rat extensor digitorum longus muscle. *Journal of biomechanics*, *34*(7), 927-940.

Maganaris, C. N. (2003). Force-length characteristics of the in vivo human gastrocnemius muscle. *Clinical Anatomy: The Official Journal of the American Association of Clinical Anatomists and the British Association of Clinical Anatomists*, *16*(3), 215-223.

Maganaris, C. N., & Paul, J. P. (2000). Load-elongation characteristics of in vivo human tendon and aponeurosis. *Journal of Experimental Biology*, *203*(4), 751-756.

Maganaris, C. N., Baltzopoulos, V., & Sargeant, A. J. (1998). In vivo measurements of the triceps surae complex architecture in man: implications for muscle function. *The Journal of physiology*, *512*(2), 603-614.

Maganaris, C. N., Baltzopoulos, V., & Sargeant, A. J. (2002). Repeated contractions alter the geometry of human skeletal muscle. *Journal of applied physiology*, *93*(6), 2089-2094.

Maganaris, C. N., Baltzopoulos, V., & Tsaopoulos, D. (2006). Muscle fibre length-to-moment arm ratios in the human lower limb determined in vivo. *Journal of biomechanics*, *39*(9), 1663-1668.

Maganaris, C. N., Kawakami, Y., & Fukunaga, T. (2001). Changes in aponeurotic dimensions upon muscle shortening: in vivo observations in man. *The Journal of Anatomy*, *199*(4), 449-456.

Malaiya, R., McNee, A. E., Fry, N. R., Eve, L. C., Gough, M., & Shortland, A. P. (2007). The morphology of the medial gastrocnemius in typically developing children and children with spastic hemiplegic cerebral palsy. *Journal of electromyography and Kinesiology*, *17*(6), 657-663.

Manal, K., Roberts, D. P., & Buchanan, T. S. (2006). Optimal pennation angle of the primary ankle plantar and dorsiflexors: variations with sex, contraction intensity, and limb. *Journal of applied biomechanics*, *22*(4), 255-263.

Martin, D. C., Medri, M. K., Chow, R. S., Oxorn, V., Leekam, R. N., Agur, A. M., & McKee, N. H. (2001). Comparing human skeletal muscle architectural parameters of cadavers with in vivo ultrasonographic measurements. *The Journal of Anatomy*, *199*(4), 429-434.

Matson, A., Konow, N., Miller, S., Konow, P. P., & Roberts, T. J. (2012). Tendon material properties vary and are interdependent among turkey hindlimb muscles. *Journal of Experimental Biology*, jeb-072728.

Maughan, D. W., & Godt, R. E. (1981). Radial forces within muscle fibers in rigor. *The Journal of general physiology*, *77*(1), 49-64.

Mercuri, E., Jungbluth, H., & Muntoni, F. (2005). Muscle imaging in clinical practice: diagnostic value of muscle magnetic resonance imaging in inherited neuromuscular disorders. *Current opinion in neurology*, *18*(5), 526-537.

Millard, M., Uchida, T., Seth, A., & Delp, S. L. (2013). Flexing computational muscle: modeling and simulation of musculotendon dynamics. *Journal of biomechanical engineering*, *135*(2), 021005.

Morse, C. I., Thom, J. M., Birch, K. M., & Narici, M. V. (2005). Changes in triceps surae muscle architecture with sarcopenia. *Acta physiologica Scandinavica*, *183*(3), 291-298.

Muramatsu, T., Muraoka, T., Kawakami, Y., & Fukunaga, T. (2002a). Superficial aponeurosis of human gastrocnemius is elongated during contraction: implications for modeling muscle-tendon unit. *Journal of biomechanics*, *35*(2), 217-223.

Muramatsu, T., Muraoka, T., Kawakami, Y., Shibayama, A., & Fukunaga, T. (2002b). In vivo determination of fascicle curvature in contracting human skeletal muscles. *Journal of Applied Physiology*, *92*(1), 129-134.

Muramatsu, T., Muraoka, T., Takeshita, D., Kawakami, Y., Hirano, Y., & Fukunaga, T. (2001). Mechanical properties of tendon and aponeurosis of human gastrocnemius muscle in vivo. *Journal of Applied Physiology*, *90*(5), 1671-1678.

Namburete, A. I., & Wakeling, J. M. (2012). Regional variations in fascicle curvatures within a muscle belly change during contraction. *Journal of biomechanics*, *45*(16), 2835-2840.

Namburete, A. I., Rana, M., & Wakeling, J. M. (2011). Computational methods for quantifying in vivo muscle fascicle curvature from ultrasound images. *Journal of biomechanics*, *44*(14), 2538-2543.

Narici, M. (1999). Human skeletal muscle architecture studied in vivo by non-invasive imaging techniques: functional significance and applications. *Journal of Electromyography and Kinesiology*, *9*(2), 97-103.

Narici, M. V., Binzoni, T., Hiltbrand, E., Fasel, J., Terrier, F., & Cerretelli, P. (1996). In vivo human gastrocnemius architecture with changing joint angle at rest and during graded isometric contraction. *The Journal of physiology*, *496*(1), 287-297.

Narici, M. V., Landoni, L., & Minetti, A. E. (1992). Assessment of human knee extensor muscles stress from in vivo physiological cross-sectional area and strength measurements. *European journal of applied physiology and occupational physiology*, *65*(5), 438-444.

Neering, I. R., Quesenberry, L. A., Morris, V. A., & Taylor, S. R. (1991). Nonuniform volume changes during muscle contraction. *Biophysical journal*, *59*(4), 926.

Neptune, R. R., Kautz, S. A., & Zajac, F. E. (2001). Contributions of the individual ankle plantar flexors to support, forward progression and swing initiation during walking. *Journal of biomechanics*, *34*(11), 1387-1398.

Nishikawa, K. C., Monroy, J. A., & Tahir, U. (2018). Muscle Function from Organisms to Molecules. *Integrative and comparative biology*.

Oomens, C. W. J., Maenhout, M., Van Oijen, C. H., Drost, M. R., & Baaijens, F. P. (2003). Finite element modelling of contracting skeletal muscle. *Philosophical Transactions of the Royal Society of London B: Biological Sciences*, *358*(1437), 1453-1460.

Otten, E. (1988). Concepts and models of functional architecture in skeletal muscle. *Exercise and sport sciences reviews*, *16*(1), 89-138.

Otten, E., & Hulliger, M. (1994). A finite-elements approach to the study of functional architecture in skeletal-muscle. *ZOOLOGY-ANALYSIS OF COMPLEX SYSTEMS*, *98*(4), 233-242.

Peterson, C. L., Hall, A. L., Kautz, S. A., & Neptune, R. R. (2010). Pre-swing deficits in forward propulsion, swing initiation and power generation by individual muscles during hemiparetic walking. *Journal of biomechanics*, *43*(12), 2348-2355.

Prager, R. W., Rohling, R. N., Gee, A. H., & Berman, L. (1998). Rapid calibration for 3-D freehand ultrasound. *Ultrasound in medicine & biology*, *24*(6), 855-869.

Rack, P. M., & Westbury, D. R. (1969). The effects of length and stimulus rate on tension in the isometric cat soleus muscle. *The Journal of physiology*, *204*(2), 443-460.

Radtka, S. A., Oliveira, G. B., Lindstrom, K. E., & Borders, M. D. (2006). The kinematic and kinetic effects of solid, hinged, and no ankle–foot orthoses on stair locomotion in healthy adults. *Gait & posture*, *24*(2), 211-218.

Rahemi, H., Nigam, N., & Wakeling, J. M. (2014). Regionalizing muscle activity causes changes to the magnitude and direction of the force from whole muscles—a modeling study. *Frontiers in physiology*, *5*, 298.

Rahemi, H., Nigam, N., & Wakeling, J. M. (2015). The effect of intramuscular fat on skeletal muscle mechanics: implications for the elderly and obese. *Journal of The Royal Society Interface*, *12*(109), 20150365.

Raiteri, B. J., Cresswell, A. G., & Lichtwark, G. A. (2016). Three-dimensional geometrical changes of the human tibialis anterior muscle and its central aponeurosis measured with three-dimensional ultrasound during isometric contractions. *PeerJ*, *4*, e2260.

Rajagopal, A., Dembia, C. L., DeMers, M. S., Delp, D. D., Hicks, J. L., & Delp, S. L. (2016). Full-Body Musculoskeletal Model for Muscle-Driven Simulation of Human Gait. *IEEE Trans. Biomed. Engineering*, *63*(10), 2068-2079.

Rana, M., & Wakeling, J. M. (2011). In-vivo determination of 3D muscle architecture of human muscle using free hand ultrasound. *Journal of biomechanics*, *44*(11), 2129-2135.

Rana, M., Hamarneh, G., & Wakeling, J. M. (2009). Automated tracking of muscle fascicle orientation in B-mode ultrasound images. *Journal of biomechanics*, *42*(13), 2068-2073.

Rana, M., Hamarneh, G., & Wakeling, J. M. (2013). 3D fascicle orientations in triceps surae. *Journal of Applied Physiology*, *115*(1), 116-125.

Randhawa, A., & Wakeling, J. M. (2013). Associations between muscle structure and contractile performance in seniors. *Clinical Biomechanics*, *28*(6), 705-711.

Randhawa, A., & Wakeling, J. M. (2015). Multidimensional models for predicting muscle structure and fascicle pennation. *Journal of theoretical biology*, *382*, 57-63.

Randhawa, A., Jackman, M. E., & Wakeling, J. M. (2013). Muscle gearing during isotonic and isokinetic movements in the ankle plantarflexors. *European journal of applied physiology*, *113*(2), 437-447.

Rassier, D. E., MacIntosh, B. R., & Herzog, W. (1999). Length dependence of active force production in skeletal muscle. *Journal of applied physiology*, *86*(5), 1445-1457.

Roberts, T. J., Marsh, R. L., Weyand, P. G., & Taylor, C. R. (1997). Muscular force in running turkeys: the economy of minimizing work. *Science*, *275*(5303), 1113-1115.

Rome, L. C., Funke, R. P., Alexander, R. M., Lutz, G., Aldridge, H., Scott, F., & Freadman, M. (1988). Why animals have different muscle fibre types. *Nature*, *335*(6193), 824-827.

Sandercock, T. G., & Heckman, C. J. (1997). Force from cat soleus muscle during imposed locomotor-like movements: experimental data versus Hill-type model predictions. *Journal of Neurophysiology*, *77*(3), 1538-1552.

Sejersted, O. M., Hargens, A. R., Kardel, K. R., Blom, P., Jensen, O., & Hermansen, L. A. R. S. (1984). Intramuscular fluid pressure during isometric contraction of human skeletal muscle. *Journal of Applied Physiology*, *56*(2), 287-295.

Sharafi, B., & Blemker, S. S. (2010). A micromechanical model of skeletal muscle to explore the effects of fiber and fascicle geometry. *Journal of biomechanics*, *43*(16), 3207-3213.

Sheriff, D. D., & Van Bibber, R. (1998). Flow-generating capability of the isolated skeletal muscle pump. *American Journal of Physiology-Heart and Circulatory Physiology*, *274*(5), H1502-H1508.

Shin, D. D., Hodgson, J. A., Edgerton, V. R., & Sinha, S. (2009). In vivo intramuscular fascicle-aponeuroses dynamics of the human medial gastrocnemius during plantarflexion and dorsiflexion of the foot. *Journal of Applied Physiology*, *107*(4), 1276-1284.

Siebert, T., Günther, M., & Blickhan, R. (2012). A 3D-geometric model for the deformation of a transversally loaded muscle. *Journal of theoretical biology*, *298*, 116-121.

Siebert, T., Stutzig, N., & Rode, C. (2018). A hill-type muscle model expansion accounting for effects of varying transverse muscle load. *Journal of biomechanics*, *66*, 57-62.

Siebert, T., Till, O., Stutzig, N., Günther, M., & Blickhan, R. (2014). Muscle force depends on the amount of transversal muscle loading. *Journal of biomechanics*, *47*(8), 1822-1828.

Siebert, T., Tomalka, A., Stutzig, N., Leichsenring, K., & Böl, M. (2017). Changes in three-dimensional muscle structure of rabbit gastrocnemius, flexor digitorum longus, and tibialis anterior during growth. *Journal of the mechanical behavior of biomedical materials*, *74*, 507-519.

Sinha, S., Hodgson, J. A., Finni, T., Lai, A. M., Grinstead, J., & Edgerton, V. R. (2004). Muscle kinematics during isometric contraction: development of phase contrast and spin tag techniques to study healthy and atrophied muscles. *Journal of Magnetic Resonance Imaging: An Official Journal of the International Society for Magnetic Resonance in Medicine*, *20*(6), 1008-1019.

Smith, L. R., Gerace-Fowler, L., & Lieber, R. L. (2011). Muscle extracellular matrix applies a transverse stress on fibers with axial strain. *Journal of biomechanics*, *44*(8), 1618-1620.

Stark, H., & Schilling, N. (2010). A novel method of studying fascicle architecture in relaxed and contracted muscles. *Journal of biomechanics*, *43*(15), 2897-2903.

Van Den Bogert, A. J., Blana, D., & Heinrich, D. (2011). Implicit methods for efficient musculoskeletal simulation and optimal control. *Procedia IUTAM*, *2*, 297-316.

Van Leeuwen, J. L. (1992). Mechanics of animal locomotion. *Adv. Comp. Environ. Physiol.*, *11*, 190-250.

Van Leeuwen, J. L., & Spoor, C. W. (1992). Modelling mechanically stable muscle architectures. *Phil. Trans. R. Soc. Lond. B*, *336*(1277), 275-292.

Wakeling, J. M., & Johnston, I. A. (1998). Muscle power output limits fast-start performance in fish. *Journal of Experimental Biology*, *201*(10), 1505-1526.

Wakeling, J. M., & Randhawa, A. (2014). Transverse strains in muscle fascicles during voluntary contraction: a 2D frequency decomposition of B-mode ultrasound images. *Journal of Biomedical Imaging*, *2014*, 4.

Wakeling, J. M., Blake, O. M., Wong, I., Rana, M., & Lee, S. S. (2011). Movement mechanics as a determinate of muscle structure, recruitment and coordination. *Philosophical Transactions of the Royal Society of London B: Biological Sciences*, *366*(1570), 1554-1564.

Wakeling, J. M., Jackman, M., & Namburete, A. I. (2013). The effect of external compression on the mechanics of muscle contraction. *Journal of applied biomechanics*, *29*(3), 360-364.

Wakeling, J. M., Uehli, K., & Rozitis, A. I. (2006). Muscle fibre recruitment can respond to the mechanics of the muscle contraction. *Journal of The Royal Society Interface*, *3*(9), 533-544.

Wang, H. K., Wu, Y. K., Lin, K. H., & Shiang, T. Y. (2009). Noninvasive analysis of fascicle curvature and mechanical hardness in calf muscle during contraction and relaxation. *Manual therapy*, *14*(3), 264-269.

Whiting, B. (1999). Theoretical models of skeletal muscle: biological and mathematical considerations. *Medicine & Science in Sports & Exercise*, *31*(7), 1084.

Wickiewicz, T. L., Roy, R. R., Powell, P. L., & Edgerton, V. R. (1983). Muscle architecture of the human lower limb. *Clinical orthopaedics and related research*, (179), 275-283.

Williams, C. D., Regnier, M., & Daniel, T. L. (2010). Axial and radial forces of cross-bridges depend on lattice spacing. *PLoS computational biology*, *6*(12), e1001018.

Williams, C. D., Regnier, M., & Daniel, T. L. (2012). Elastic energy storage and radial forces in the myofilament lattice depend on sarcomere length. *PLoS computational biology*, *8*(11), e1002770.

Williams, C. D., Salcedo, M. K., Irving, T. C., Regnier, M., & Daniel, T. L. (2013). The length–tension curve in muscle depends on lattice spacing. *Proceedings of the Royal Society of London B: Biological Sciences*, *280*(1766), 20130697.

Williams, P. E., & Goldspink, G. (1984). Connective tissue changes in immobilized muscle. *Journal of Anatomy*, *138*(Pt 2), 343.

Winters, T. F., Gage, J. R., & Hicks, R. (1987). Gait patterns in spastic hemiplegia in children and young adults. *J Bone Joint Surg Am*, *69*(3), 437-441.

Winters, T. M., Takahashi, M., Lieber, R. L., & Ward, S. R. (2011). Whole muscle length-tension relationships are accurately modeled as scaled sarcomeres in rabbit hindlimb muscles. *Journal of biomechanics*, *44*(1), 109-115.

Wokke, B. H., Van Den Bergen, J. C., Versluis, M. J., Niks, E. H., Milles, J., Webb, A. G., ... & Kan, H. E. (2014). Quantitative MRI and strength measurements in the assessment of muscle quality in Duchenne muscular dystrophy. *Neuromuscular Disorders*, *24*(5), 409-416.

Yucesoy, C. A. (2010). Epimuscular myofascial force transmission implies novel principles for muscular mechanics. *Exercise and sport sciences reviews*, *38*(3), 128-134.

Yucesoy, C. A., & Huijing, P. A. (2007). Substantial effects of epimuscular myofascial force transmission on muscular mechanics have major implications on spastic muscle and remedial surgery. *Journal of Electromyography and Kinesiology*, *17*(6), 664-679.

Yucesoy, C. A., Koopman, B. H., Huijing, P. A., & Grootenboer, H. J. (2002). Three-dimensional finite element modeling of skeletal muscle using a two-domain approach: linked fiber-matrix mesh model. *Journal of biomechanics*, *35*(9), 1253-1262.

Zajac, F. E. (1989). Muscle and tendon Properties models scaling and application to biomechanics and motor. *Critical reviews in biomedical engineering*, *17*(4), 359-411.

Zajac, F. E., Neptune, R. R., & Kautz, S. A. (2002). Biomechanics and muscle coordination of human walking: Part I: Introduction to concepts, power transfer, dynamics and simulations. *Gait & posture*, *16*(3), 215-232.

Zerhouni, E. A., Parish, D. M., Rogers, W. J., Yang, A., & Shapiro, E. P. (1988). Human heart: tagging with MR imaging--a method for noninvasive assessment of myocardial motion. *Radiology*, *169*(1), 59-63.

Zuurbier, C. J., & Huijing, P. A. (1992). Influence of muscle geometry on shortening speed of fibre, aponeurosis and muscle. *Journal of biomechanics*, *25*(9), 1017-1026.

Zuurbier, C. J., & Huijing, P. A. (1993). Changes in geometry of activily shortening unipennate rat gastrocnemius muscle. *Journal of Morphology*, *218*(2), 167-180.

Zuurbier, C. J., Everard, A. J., van der Wees, P., & Huijing, P. A. (1994). Length-force characteristics of the aponeurosis in the passive and active muscle condition and in the isolated condition. *Journal of biomechanics*, *27*(4), 445-453.